Microglial response to neuronal expression of aberrant TDP-43

A Thesis submitted to Indian Institute of Science Education and Research Pune in partial fulfilment of the requirements for the BS-MS Dual Degree Programme

by

Riddhi Sandeep Petkar

Indian Institute of Science Education and Research Pune

Dr. Homi Bhabha Road,

Pashan, Pune 411008, INDIA.

Date: April, 2023

Under the guidance of

Supervisor: Dr. med. Sabine Liebscher, PhD

Institute of Clinical Neuroimmunology, Ludwig Maximilians University of Munich, Munich

From May 2022 to Mar 2023

INDIAN INSTITUTE OF SCIENCE EDUCATION AND RESEARCH PUNE

Certificate

This is to certify that this dissertation entitled Microglial response to neuronal TDP-43 pathology. Here towards the partial fulfilment of the BS-MS dual degree programme at the Indian Institute of Science Education and Research, Pune represents study/work carried out by Riddhi Sandeep Petkar at Indian Institute of Science Education and Research under the supervision of Dr. med. Sabine Liebscher, PhD Institute of Clinical Neuroimmunology, during the academic year 2022-2023.

Dr. med. Sabine Liebscher, PhD.
Emmy noether group leader
Institute of Clinical Neuroimmunology
Klinikum der Universität München
Biomedical centre
Ludwig Maximilians University of Munich
Munich, Germany

Riddhi Sandeep Petkar
BS-MS student
Batch of 2018

Declaration

I hereby declare that the matter embodied in the report entitled Microglial response to neuronal TDP-43 pathology are the results of the work carried out by me at the Institute of Clinical Neuroimmunology, Klinikum der Universität München, Biomedical centre, Ludwig Maximilians University of Munich(LMU), Munich under the supervision of Dr. med. Sabine Liebscher, PhD and the same has not been submitted elsewhere for any other degree.

Riddhi Sandeep Petkar
08/04/2023

Table of contents

List of Figures

List of Tables

Abstract

The TAR DNA-binding protein (TDP-43) is a ubiquitous RNA/DNA binding protein encoded by the TARDBP gene. TDP-43 pathology, characterised by the mislocalization of TDP-43 from the nucleus to the cytoplasm and the formation of hyperphosphorylated and ubiquitinated cytoplasmic inclusions/aggregates, is observed in 97% of Amyotrophic lateral sclerosis (ALS) and 50% of frontotemporal dementia (FTD) cases as well as in many other neurodegenerative diseases. There is a growing body of literature suggesting TDP-43 abnormality could interfere with neuronal health through multiple routes. Meanwhile, several recent studies indicated an involvement of microglia in disease progression by taking up pathological TDP-43 from affected neurons. To date it remains open, the microglial response to neuronal TDP-43 pathology was investigated. Adeno-assosciated virus (AAV) transduction was used to express human wild type TDP-43 (hTDP-43) , cytoplasmic TDP-43 (hTDP-43 ΔNLS) with mutation in nuclear localization sequence and cytoplasmic TDP-43 with RNA binding deficient mutation (hTDP-43 ΔNLS-5FL) in the primary motor cortex (M1) of CX3CR1 and C57BL/6J mice. Microglia morphology analysis revealed that microglia are more amoeboid cell-like in hTDP-43 and hTDP-43 ΔNLS-5FL injected mice compared to control (mCherry) and hTDP-43 ΔNLS injected mice. Using *in vivo* imaging to assess microglia process motility, it was demonstrated that microglia in hTDP-43 ΔNLS-5FL injected mice are more motile compared to microglia in mCherry-expressing controls. Further, the effect of these injections on motor skills was also investigated employing the pole test and cylinder test. The results from the pole test suggested that hTDP-43 injected mice display some motor dysfunction compared to hTDP-43 ΔNLS injected mice after 4 weeks of neuronal expression. Overall, this study suggests that microglia strongly respond and becoming ‘active’ in the presence of nuclear overexpression of hTDP-43 and to cytoplasmic aggregates of TDP-43 by transforming into amoeboid cell and increasing their process motility. Interestingly, the mere cytoplasmic mislocalization per se seems to not drive microglia reactivity. We thus conclude that the TDP-43 forms, primarily toxic to neurons, are nuclear overexpression and cytoplasmic aggregation.

Acknowlegments

I would like to thank Dr. med. Sabine Liebscher, PhD for giving me the opportunity to work on this project and for her constant guidance and support throughout the project.

I would like to extend my gratitude towards Shenyi Jiang for being such an amazing mentor to me and for teaching me experimental skills. She not only helped me with a lot of experiments and data analysis but also lent me an ear when I needed her the most. Special mention to Cem Araz and Liliana Ziegler for keeping me company through my monotonous experiments and constantly encouraging me during failures! I would also like thank XiaoQian Ye, Christopher Douthwaite, Zeynep Gunes, Steffan Jones, Anastasia Cakmak for being such wonderful lab members.

I would also like to thank Kerschensteiner lab and Bareyre lab for help with reagents and equipments. I am also grateful to the Animal facility (Core Facility Animal Models - CAM) at Biomedical centre for taking care of my experimental mice.

I am also grateful to my expert, Dr. Raghav Rajan for his insights and support. I have been constantly trying to put in practice his approach towards experiments and his positive attitude.

Lastly, I am very grateful to my family and friends for their constant motivation and boosting my morale when I felt like giving up. Thanks for providing me your constant love, care and support and for putting up with my constant whining.

Contributions

Contributor name	Contributor role
Shenyi Jiang, Dr. med. Sabine Liebscher, PhD	Conceptualization ideas
Riddhi Sandeep Petkar, Shenyi Jiang, Dr. med. Sabine Liebscher, PhD	Methodology
Dr. med. Sabine Liebscher, PhD	Software
-	Validation
Riddhi Sandeep Petkar, Shenyi Jiang, Dr. med. Sabine Liebscher, PhD	Formal analysis
Riddhi Sandeep Petkar	Investigation
Dr. med. Sabine Liebscher, PhD	Resources
Riddhi Sandeep Petkar	Data curation
Riddhi Sandeep Petkar	Writing – original draft preparation
Dr. med. Sabine Liebscher, PhD	Writing – review and editing
Shenyi Jiang, Riddhi Sandeep Petkar	Visualization
Shenyi Jiang, Dr. med. Sabine Liebscher, PhD	Supervision
Dr. med. Sabine Liebscher, PhD	Project administration
Dr. med. Sabine Liebscher, PhD	Funding acquistion

1. Introduction

1.1. Neurodegenerative disorders

Neurodegenerative disorder is a term used for various diseases of the nervous system characterized by the progressive loss of neurons (Przedborski S. et al., 2003). These disorders can lead to a wide range of symptoms like cognitive impairment, motor dysfunction, autonomic, sleep and psychiatric disturbances. Neurodegenerative disorders affect the lives of millions of people worldwide every year (Zheng et al., 2022). The most commonly occurring neurodegenerative disorders are Alzheimer's disease (AD), Parkinson's disease (PD) and Amyotrophic lateral sclerosis (ALS).

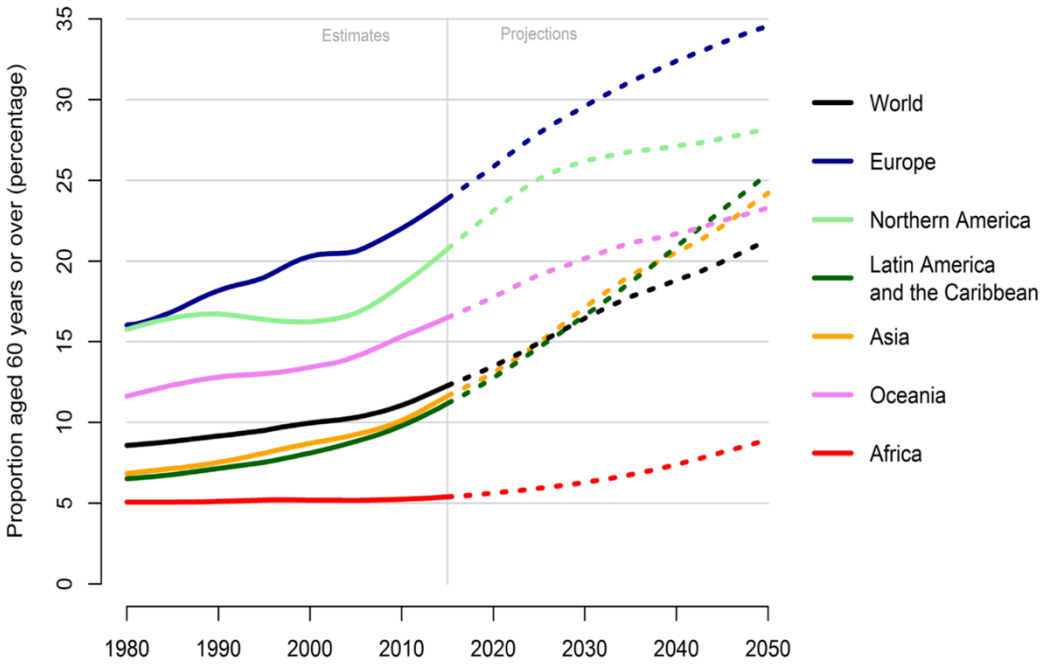

Data source: United Nations (2017). World Population Prospects: the 2017 Revision.

Figure 1. Percentage of people aged 60 or older in different parts of world. The percentage of people aged 60 or older is increasing gradually in all parts of the world. The increase is most prominent in European countries, and it is least prominent in African countries. (Adapted from United Nations (2017). World Population Prospects: the 2017 Revision, Creative Commons license CC BY 3.0 IGO)

The global prevalence of neurodegenerative disorders is on the rise, partly due to the ageing of the population. As per a report published by the United Nations, the proportion of the global population aged 65 years or older was 1 in 11 in 2019. The

report predicts that this proportion will nearly double to 1 in 6 by 2050 (Fig.1). This demographic shift will increase the prevalence of various neurodegenerative disorders even further, thus making it a global health concern. Neurodegenerative diseases can result in long-term disability, thus leading to decrease in quality of life and increase in healthcare expenses, which have a significant impact on individuals, families, and the community (Peng et al., 2020). The clinical management of this disease category is a significant challenge because, once the neurodegenerative process is initiated, it can only be delayed but not entirely stopped (Fu et. Al., 2018). As a result, there is an urgent need for effective treatment and prevention approaches to tackle this global health issue (Hampel et al., 2018).

1.2. Amyotrophic lateral sclerosis

1.2.1 Clinical manifestations and epidemiology of ALS

Amyotrophic lateral sclerosis (ALS), also known as Lou Gehrig's disease, is a neurodegenerative disorder that affects the motor neurons in the brain and spinal cord (Kiernan et al., 2011), leading to progressive muscle weakness, atrophy, and eventually paralysis.

Being one of the most common forms of adult motor neuron disease, ALS has an incidence of ~2/100,000 people per year, with uniform rates in Caucasian populations and lower rates in African, Asian and Hispanic populations (Cronin et al., 2007, Marin et al., 2017) and a prevalence of 2−5/100,000 people (Chiò et al., 2013). The total number of individuals with ALS is expected to grow from 80,162 in 2015 to 105,69 in 2040, representing an increase of >31% (Arthur et al., 2016., Fig. 2).

The disease can also affects speech, swallowing, and breathing, leading to significant disability and reduced quality of life (Hardiman et al., 2017). After diagnosis, patients live only up to 3-4 years, as they suffer from progressive paralysis and eventually die from respiratory failure (Cervenakova et al., 2000, Taylor et al., 2016).

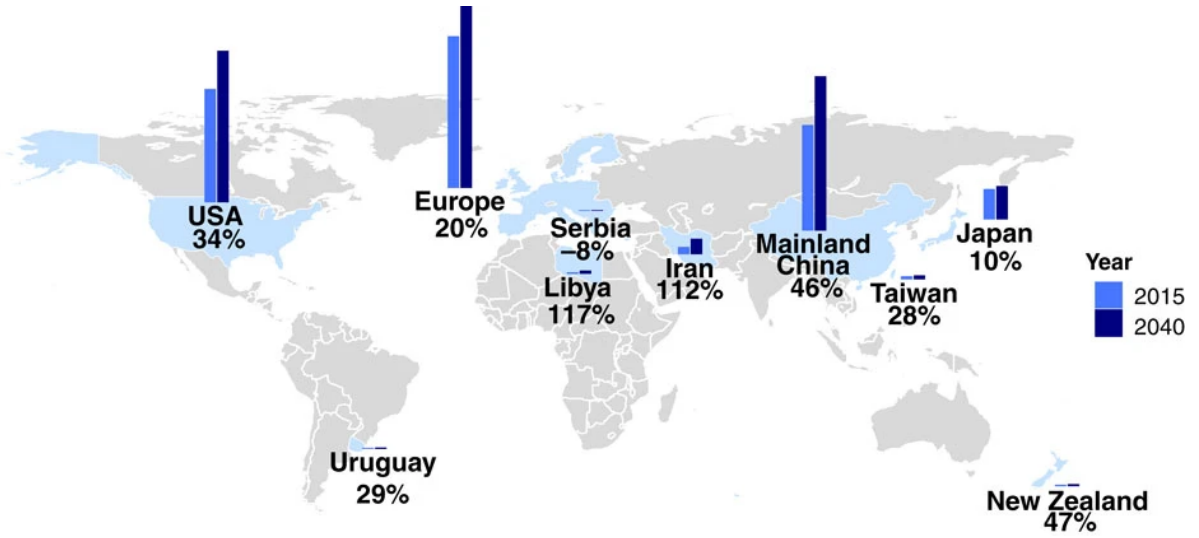

Figure 2. Projected increase in ALS incidences from 2015 to 2040. ALS cases will increase from 2015 to 2040. This increase in incidence of ALS cases will be most for Libya and Iran and the least for Japan among the countries that were studied (Reproduced from Arthur et al., 2016, Creative Commons Attribution 4.0 International License).

Despite significant advances in understanding the pathogenesis of ALS, the underlying mechanisms of motor neuron degeneration remain poorly understood, and there is currently no cure for the disease. However, several treatments and therapeutic strategies, including riluzole and edaravone, have been shown to slow disease progression and improve survival (Brooks et al., 2022).

The Food and Drug administration (FDA) has approved two drugs namely riluzole and edaravone for the treatment of ALS. However, both show only a slight improvement in ALS symptoms (Jaiswal et al., 2019). Riluzole blocks voltage-gated sodium channels, and it thus reduces the release of glutamate is believed to be casually involved in motor neuron degeneration in ALS (Schwartz et al., 2002). Edaravone works as an antioxidant, which reduces the oxidative injuries to neurons in ALS by scavenging free radicals (Hardiman et al., 2002). However, the exact mechanism of action of edaravone remains incompletely understood (Rothstein et al., 2017). However, currently existing medications can only extend survival by a few months (Jaiswal et al., 2019), thus, a greater understanding of the pathophysiology is urgently required to create more potent treatments and medications.

1.2.2 ALS genetics

ALS is categorized into two main types: sporadic and familial. Sporadic cases are more common, accounting for 90-95% of all cases, while familial cases, which result from genetic mutations inherited in an autosomal dominant pattern, account for the remaining 5-10% of cases (Ajroud-Driss et al., 2015). The two forms of ALS are clinically not distinguishable (Alsultan et al., 2016). Owing to the rapid development of molecular genetic techniques, genome-wide association studies and next-generation sequencing several ALS-linked genes were recently identified (Ghasemi et al., 2018). Although more than 50 potentially causative or disease-modifying genes have been found, mutations in the following genes are the most common - chromosome 9 open reading frame 72 (C9orf72), superoxide dismutase 1 (SOD1), fused in sarcoma (FUS), and TAR DNA-binding protein (TARDBP) (Ghasemi et al., 2018, Ngyuen et al., 2018) (Fig. 3).

C9orf72 is the most common genetic mutation linked to ALS, accounting for approximately 45-50% of familial cases and 9% of sporadic cases (DeJesus-Hernandez et al., 2011). The mutant C9orf72 gene is located on chromosome 9p21 and has a hexanucleotide repeat expansion in a non-coding intron (Renton et al., 2011, Starr et al., 2018). SOD1 is an important enzyme for the breakdown of superoxide radicals into oxygen and hydrogen peroxide. It was the first gene found to be associated with ALS and is responsible for about 10 – 20% of familial cases (Yun et al., 2020, Andersen et al., 2006, Rosen et al., 1993). FUS is a protein that binds to RNA and DNA and is involved in regulating RNA metabolism, including mRNA stability, transport, and splicing (Ishigaki et al., 2012, Masuda et al., 2015, Morlando et al., 2012). FUS mutations have been identified in less than 1% of sALS cases and around 4% of fALS cases (Deng et al., 2014, Ishigaki et al., 2018, Zou et al., 2017).

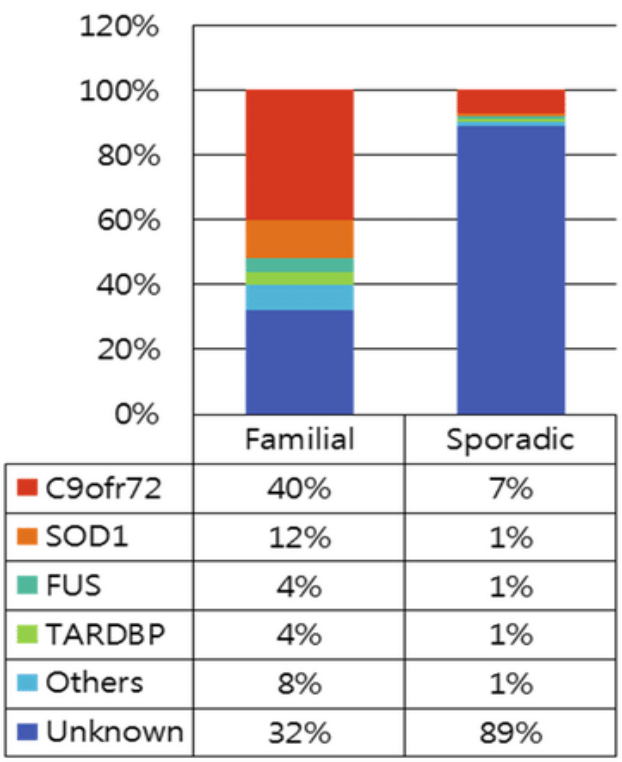

	Familial	Sporadic
C9ofr72	40%	7%
SOD1	12%	1%
FUS	4%	1%
TARDBP	4%	1%
Others	8%	1%
Unknown	32%	89%

Figure 3. Proportion of causative genes of familial and sporadic ALS. Each gene is represented in different colours. Mutations in C9orf72, SOD1, FUS and TARDBP are most common in ALS. C9of372 is the most common, followed by SOD1 gene. (Adapted from Yun et al., 2020, Creative Commons CC BY 4.0 license)

Mutations in the TARDBP gene have been found in approximately 5% of familial cases and 2% of sporadic cases (Ingre et al., 2015). The TARDP gene gives rise to the TDP-43 (Transactive response DNA binding protein 43 kDa) protein. TDP-43 protein inclusions have been observed in the cytoplasm of neurons in most cases of ALS and FTD, regardless of genetic mutations (Neumann et al., 2006). The pathology of the TDP-43 protein is complex and involves the mislocalization of the protein from the nucleus to the cytoplasm, as well as the formation of hyperphosphorylated and ubiquitinated cytoplasmic inclusions. There is a growing body of literature suggesting that TDP-43 abnormality could interfere with neuronal health through multiple routes (Keating et al., 2022). However, how exactly it is involved in the neurodegenerative process in vivo remains controversial.

1.3. TDP-43

1.3.1 Structure and function

TDP-43 is an RNA and DNA binding protein. In the nervous system, it binds to >6,000 pre-mRNAs (Polymenidou et al., 2011). Additionally, it also affects the levels of ~600 mRNAs and the splicing patterns of almost 950 mRNAs (Polymenidou et al., 2011). It is a 414-amino acid protein, and it contains RNA recognition motifs (RRM1 and RRM2, Fig. 4) (Buratti et al., 2001), a nuclear import and export signal (Winton et al., 2008), and a glycine-rich region, implicated in protein–protein interactions (Ayala et al., 2005) that include components of the RNA splicing machinery (Buratti et al., 2005). It plays an important role in various processes like - mRNA splicing, miRNA biogenesis, stress granule formation, transcription, translation etc. TDP-43 is also shuttled between cytoplasm and nucleus (Kawahara et al., 2012, Aulas et al., 2015).

TDP-43 is found in all cell types. It is primarily present in the nucleus; however, it is also located in mitochondria and cytoplasm (Wang et al., 2018, Winton et al., 2008). Using the autoregulation via cryptic exon suppression within the 3'UTR of TARDBP mRNA, TDP-43 expression is tightly regulated (White et al., 2018). Mice, that lack TDP-43, die already in the embryonic stage, while cultured cells that lack or overexpress the protein exhibit toxicity or cell death (Yang et al., 2014, Schmid et al., 2013, Herzog et al., 2017, Diaper et al., 2013, Kraemer et al., 2010, Sephton et al., 2010). TDP-43 was initially identified as a key component of cytoplasmic inclusions in motor neurons of individuals with ALS (Leigh et al., 1991). TDP-43 pathology has since been found in other neurodegenerative disorders, including Frontotemporal lobar degeneration (FTLD) and AD, as well as in limbic predominant age-related TDP-43 encephalopathy (LATE) (Mackenzie et al., 2010).

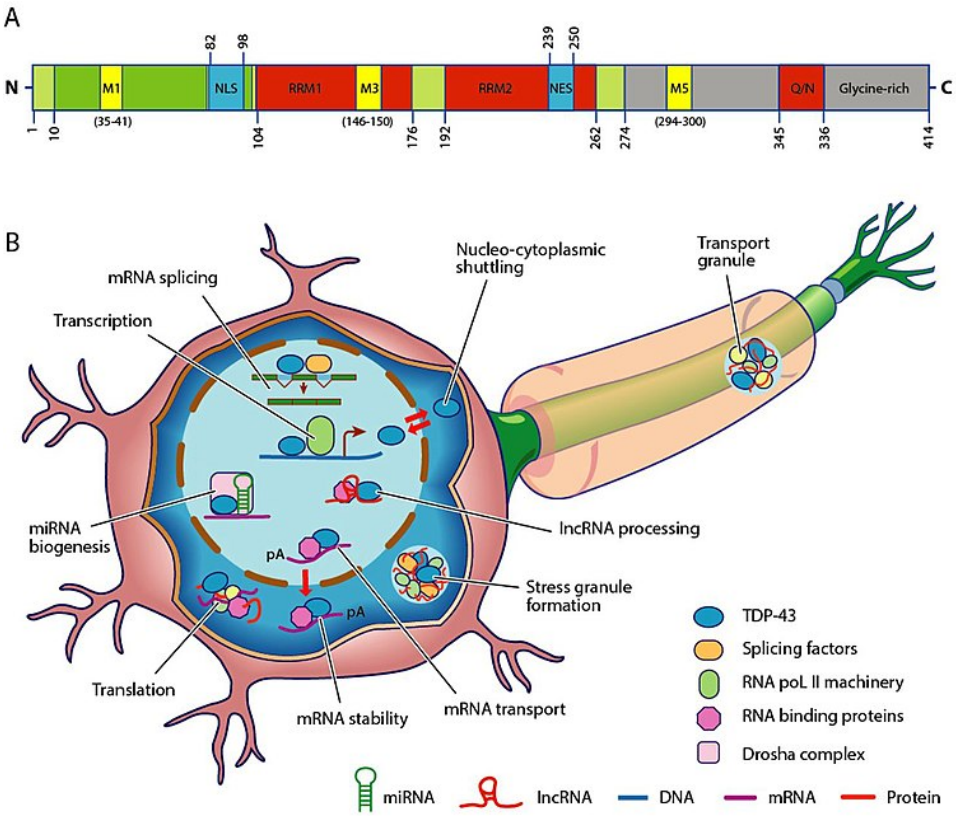

Figure 4. Structure and function of TDP-43. A) Structure of the TDP-43 protein. TDP-43 protein consists of 414 amino acids. The number denotes the number of amino acids. It has an N terminal and a C terminal. The N-terminal has a nuclear localization signal or sequence (NLS). The protein also has two RNA recognition motifs (RRM1 and RRM2), Mitochondrial localisation motifs (M1, M3 and M5) and a Nuclear Export Signal (NES). The C-terminal has Glutamine/asparagine(Q/N) and Glycine-rich domains, and it exhibits prion-like properties. The pathogenic mutations are primarily present in the C-terminal. B) In the nucleus, TDP-43 is involved in several important cellular functions like transcription, mRNA splicing, miRNA biogenesis, lncRNA processing and mRNA stability. In the cytoplasm, TDP-43 plays important role in translation, stress granule formation and mRNA stability. Although TDP-43 is predominantly present in the nucleus, it shuttles between the nucleus and cytoplasm. (Image reproduced from Boer et al., 2020, Creative Commons Attribution Non Commercial (CC BY-NC 4.0) license)

1.3.2 TDP43 pathology

TDP-43 pathology is characterised by the mislocalization of TDP-43 from the nucleus to the cytoplasm and the formation of hyperphosphorylated and ubiquitinated cytoplasmic inclusions/aggregates. During disease conditions, hyperphosphorylation, ubiquitination and cleavage of TDP43 takes place (Neumann et al., 2006, Arai et al.,

2006, Hasegawa et al., 2008). These changes to the protein can cause it to accumulate and aggregate in the cytoplasm (Fig. 6). In cases where TDP-43 is phosphorylated at specific sites such as serine 403/404 and 409/410, it can lead to the formation of abnormal protein inclusions commonly seen in TDP-43-related diseases (Zhang et al., 2009). The N terminal of TDP-43 plays a role in TDP-43 self-oligomerization which takes place in concentration-dependent ways (Chang et al., 2012). Mutations in the NLS within the N-terminal domain (NTD) region can cause TDP-43 to accumulate and aggregate in the cytoplasm (Fig. 5, Barmada et al., 2010).

The C-terminus plays an important role in the cellular localization of TDP–43, its solubility, and protein-protein interactions (Ayala et al., 2008). This domain resembles a prion-like domain. Prion-like domains, which are low-complexity sequences, play a key role in regulating protein folding and solubility, and proteins with prion-like domains can undergo phase separation (Liebman et al., 2012, McAlary et al., 2019). TDP-43's liquid-liquid phase separation is influenced by both hydrophilic and hydrophobic residues (Maharana et al., 2018). Mutations or abnormal post-translational modifications in this domain can cause irreversible aggregation via liquid-solid phase separation (Maharana et al., 2018). Most mutations associated with ALS and FTLD are found in the C-terminal domain of TDP-43 and can lead to intrinsic protein aggregation in several models (Ayala et al., 2008, Shin et al., 2017, Maharana et al., 2018).

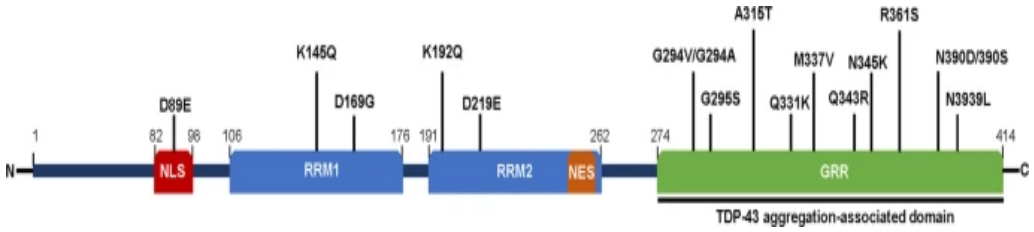

Figure 5. Structure and aggregation-associated domains of TDP-43. The TDP-43 mutations linked to a variety of diseases have been found in the Glycine-rich region (GRR). The majority of TDP-43 missense variants linked to the disease have been found to quicken TDP-43 aggregation. (Reproduced from Jo et al., 2020, Creative Commons Attribution 4.0 International License)

Several studies in yeast cells and in SH-SY5Y cells have demonstrated that TDP-43 mutations, including G294A, Q331K, M337V, Q343R, N345K, R361S, N390S and N390D, can enhance aggregation and cell toxicity (Johnson et al., 2009, Nonaka et al., 2009). Furthermore, in a Drosophila study, it was shown that the expression of the TDP-43 A315T mutant leads to neurotoxicity and protein aggregation (Guo et al., 2011). Moreover, it has been discovered that several peptides with pathogenic TDP-43 mutations, including G294V, G294A, and G295S, can form amyloid-like fibres which are twisted (Sun et al., 2014). Hence, we can conclude that the C-terminal domain of TDP-43 is the most important region of the protein when it comes to aggregation.

TDP-43 shuttles back and forth between the nucleus and the cytoplasm (Ayala et al., 2011). A negative-feedback mechanism is used to tightly regulates the amount and localization of TDP-43 (Ayala et al., 2011, Polymenidou et al., 2011). The nuclear import of TDP-43, however, is compromised under stress conditions such as heat shock, oxidative stress, and exposure to arsenite, and cytoplasmic TDP-43 accumulates within stress granules (SGs) with several other proteins and RNAs (Dewey et al., 2011, Colombrita et al., 2009, Barmada et al., 2014). TDP-43 is released from SGs harbouring TDP-43 when stress is relieved, and it then translocates into the nucleus (Udan-Johns et al., 2014). Nevertheless, persistent SG formation brought on by chronic stress results in a persistent build-up of cytoplasmic TDP-43 aggregates.

Apart from the dysregulation of these stress granules, malfunction of the nuclear pore complex (NPC) can also lead to aggregation and cytoplasmic mislocalization of TDP-43 (Chou et al., 2018). Studies have shown that the expression of (G4C2)30 RNA reduces the cytoplasm-nucleus gradient of Ran, a major regulator of TDP-43 nuclear localization, and disrupts the nuclear membrane structure (Ward et al., 2014). Additionally, the cytoplasmic accumulation of TDP-43 is also linked to other nuclear membrane proteins such as Nup62 and Kpnb1 (Nishimura et al., 2010). TDP-43 aggregates can also directly impair nucleocytoplasmic transport and nuclear pore complex function, leading to the mislocalization and aggregation of nucleoporins and transport factors (Chou et al., 2018, Gasset-Rosa et al., 2019). These events accelerate the cytoplasmic accumulation of TDP-43, contributing to neuronal dysfunction and toxicity (Jo et al., 2020).

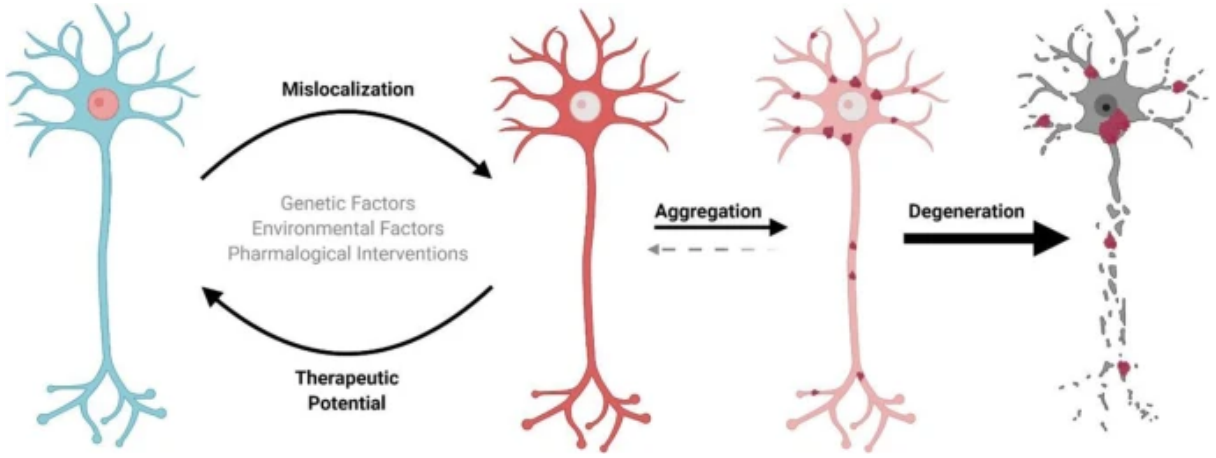

Figure 6. TDP-43 pathology Due to genetic and/or environmental causes, TDP-43 (red) mislocalizes (completely or partially) from the nucleus to the cytoplasm, thus causing negative effects on the cell. Long-term mislocalization leads to aggregation. Small TDP-43 aggregates can be eliminated by the cell under physiological conditions through proteasomal, endosomal, or autophagic degradation. Prolonged TDP-43 aggregate accumulation impairs physiological processes (e.g., SQSTM1 sequestration), thus aggravating disease pathology and accelerating neuronal death. Early interventions targeting TDP-43 mislocalization might be useful to stop cellular death. (Taken from Suk et al., 2020, Creative Commons Attribution 4.0 International License)

TDP-43 mislocalization may be increased by some missense variants (Winton et al., 2008). An ALS-linked A90V mutation in the NLS enhances the cytoplasmic aggregation of TDP-4355 (Winton et al., 2008).

1.3.3 TDP-43 neuronal propagation in ALS and FTD

The initial symptoms of ALS vary among people and can occur asymmetrically (Walling et al., 1999). Progressive muscle weakness and paralysis are common symptoms of ALS, even though not everyone with the disease experiences the same progression or sequence. The symptoms typically extend from one side of the body to the other as the condition worsens. The location of the disease's onset is also related to how severely motor neurons are lost in the corresponding part of the central nervous system (CNS) innervating the muscles within the affected body region. Thus, the spread of clinical

features points towards cell-to-cell propagation of TDP-43 pathology in ALS (Ravits et al., 2009).

ALS neuropathology can be roughly classified into the following four stages – Stage 1 - pathogenic TDP-43 (pTDP-43) inclusions are more prevalent in somatomotor neurons of the brainstem and spinal cord and agranular motor cortex's projection neurons (Braak et al., 2013, Brettschneider et al., 2013). Stage 2 - The prefrontal cortex, reticular formation, precerebellar brainstem nuclei, and parvocellular regions of the red nucleus also exhibit pTDP-43 aggregates. Stage 3 – is characterized by pTDP-43 pathology in the striatum, basal ganglia, and prefrontal cortex. Stage 4 - pTDP-43 pathology substantially develops into the hippocampus and dentate fascia and anteromedial portions of the temporal lobe and entorhinal cortex (Braak et al., 2013, Brettschneider et al., 2013).

According to clinical studies of ALS patients, pTDP-43 lesions and motor neuron degeneration both increase as the disease progresses (Braak et al., 2013). Some studies also show that pTDP-43 aggregates are further propagating in the somatomotor neurons' axons via axonal transport (Braak et al., 2013). Hence, it is believed that axonal transport plays a crucial role in the spread of p-TDP-43 in ALS. More studies are needed to understand the underlying molecular mechanisms of TDP-43 propagation and pathophysiology.

Patients with FTLD have a distinctive histopathology that includes aggregated TDP-43 or tau protein in cytoplasmic inclusions in neurons and glial cells (Jo et al., 2020). The pathogenic subtypes of FTLD include those with tau-positive inclusions (FTLD-tau), FUS-positive inclusions (FTLD-FUS), and TDP-43 and ubiquitin inclusions (FTLD-TDP-43). TDP-43-positive cytoplasmic inclusions are found in up to 50% of FTLD patients despite the fact that TDP-43 mutations are only present in a very small fraction of FTLD cases (Hasegawa et al., 2008, Cairns et al., 2007, Weihl et al., 2008). Patients with behavioural variation FTD (bvFTD) show particularly severe and pervasive TDP-43 pathology (Jo et al., 2020). Based on the results of a clinical cohort study, the progression of pTDP-43 pathology was also categorized into four stages. Stage 1 of FTLD - The orbital gyri, gyrus rectus, and inferior frontal gyrus of the prefrontal neocortex, as well as the amygdala, have widespread pTDP-43 inclusions.

Stage 2 - The superior and middle temporal gyri, striatum, and medial and lateral regions of the thalamus exhibit an elevated p-TDP-43 burden (Mackenzie et al., 2011). Stage 3 – pTDP-43 inclusions are observed in the anterior horn of the spinal cord, motor cortex and neocortical areas as well. Stage 4 - p-TDP43 inclusions are also observed in the occipital neocortex. Previous studies have linked p-TDP-43 lesions in FTD with changes in behaviour, language, and functional abilities. p-TDP-43 pathology travels to other areas of the brain through the axonal connections via cell-to-cell transmission (McKhann et al., 2001, Mioshi et al., 2010). The mechanism of propagation of TDP-43 pathology is similar in ALS and FTD, thus indicating a common molecular mechanism among p-TDP-43 proteinopathies (Geser et al., 2009, Mioshi et al., 2010). But what is the role of glial cells in TDP-43 pathology?

1.4 Role of non- neuronal glial cells in TDP-43 pathology

Several studies point towards a potential role of the three types of glial cells of the central nervous system (CNS)- astrocytes, microglial and oligodendrocytes in the onset and/or progression of ALS. In my project, I am specifically interested in the response of microglia to neurons expressing aberrant TDP-43.

1.4.1 Microglia

The word microglia come from two Greek words - the word micro means small, and the word glia refers to glue. Microglial cells are the resident macrophages of the central nervous system that act as the first line of defence. They constantly scour the cerebral milieu for infections and damage (Fig. 7, Soulet et al., 2008). Although some areas of the CNS, notably the spinal cord, are more densely populated than others like the white matter that typically contains less microglia than grey matter, these cells are more or less prevalent throughout the CNS. Microglia originate from the early erythroid myeloid progenitors of the yolk sac. Even before the blood-brain barrier has developed to its full maturity, they enter the developing brain (Lannes et al., 2017, Muzio et al., 2021).

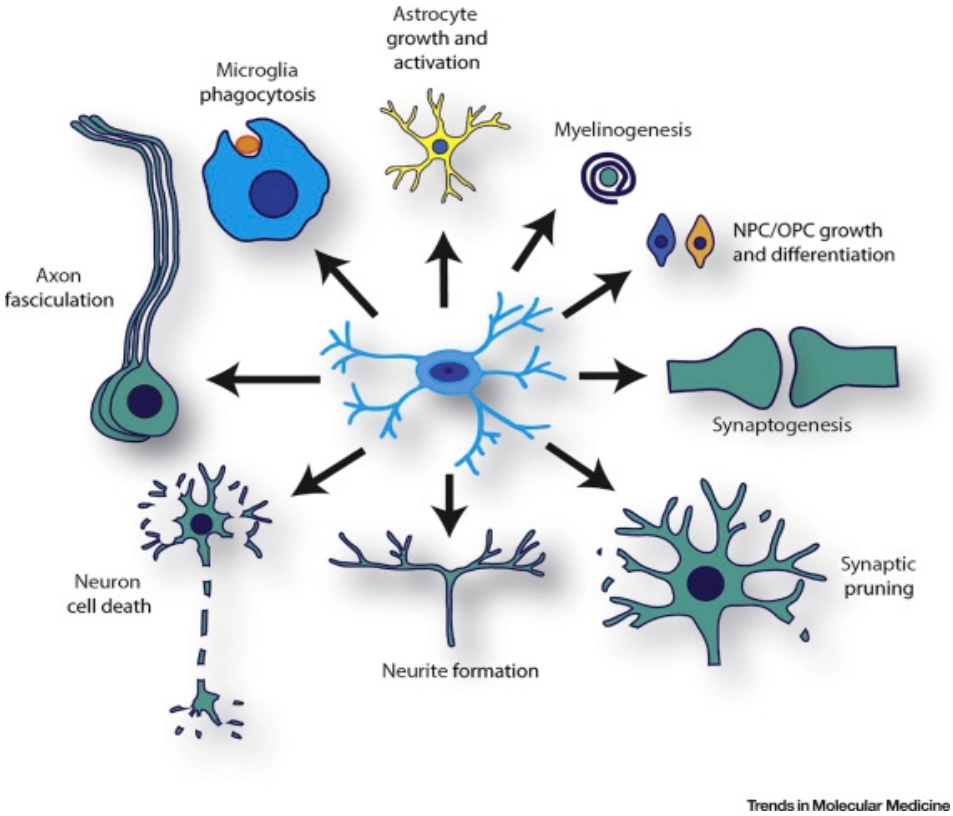

Figure 7. Microglia functions. Microglia are involved in several important functions in the brain such as axon fasciculation, programmed cell death, neurite formation and synaptogenesis. They also play an important role in specifying the fate of oligodendrocyte progenitor cell (OPC) and neural progenitor cell (NPC) and engulfing cellular debris(phagocytosis) (reproduced from Wright-Jin et al., 2019, License number - 5534060628337)

During physiological conditions, microglial morphology is characterized by very fine and highly ramified processes emanating from a small cell body. This morphology fosters the surveillance of the local microenvironment for potential cell damage or pathogens (Tremblay et al., 2011, Nimmerjahn et al., 2005). Upon cell damage or pathological conditions secreted molecules, so-called damage-associated molecular patterns (DAMPs), released by damaged cells, initiate a microglial inflammatory response, characterized by morphological changes such as an increase in cell body size and a gradual retraction of processes (Huang et al., 2018). This morphological transformation leads from a ramified morphology to a reactivated cell morphology and finally to an amoeboid cell form (Huang et al., 2018, Colonna and Butovsky, 2017). Swollen cell soma and completely retracted processes are characteristics of amoeboid shaped microglia cells. This morphological transformation aids in the microglial migration to the

pathological site or site of injury and also facilitates phagocytosis of cell debris (Davalos et al., 2005, Tremblay et al., 2011, Nimmerjahn et al., 2005). Thus, microglial morphology is an important indicator of diseased or pathological conditions.

Another important feature of microglia is microglial process motility. The processes of microglia undergo continuous extension and retraction (Nimmerjahn et al., 2005, Davalos et al., 2005). Process motility of microglia is important for execution of several functions like the surveillance of the local environment for potential pathogens or injury (Shibata et al., 2017). It also facilitates the regulation of synaptic excitability, synaptic pruning and thus the maintenance of synapses (Hong et al., 2016, Badimon et al., 2020). Microglial process motility can be affected in neurodegenerative disorders, during aging and systemic inflammation (Bolmont et al., 2008, Gyoneva et al., 2014, Hefendehl et al., 2014). Microglial migration is another important feature. In the healthy brain, although microglia continuously retract and extend their processes for the surveillance of the local microenvironment, there is almost no overall cell displacement. However, there are studies that show that after injury microglia travel long distances and accumulate at the damage sites (Kettenmann et al., 2011, Carbonell et al., 2005).

Microglia play an important role in the cell proliferation of neural precursors during brain development, thus contributing to CNS homeostasis under physiological conditions (Muzio et al., 2021). During postnatal life, microglia play an important role in synaptic pruning thus helping to establish and refine neural circuits (Muzio et al., 2021). Following a CNS injury, the morphology of microglia is altered, accompanied by an altered transcriptomic profile, characterized e.g., the downregulation of certain genes that are responsible for maintaining homeostasis in CNS, such as TMEM119 and an upregulation of genes like ccl2, ccl3, etc (Muzio et al., 2021). Despite extensive transcriptomic studies pointing towards alterations of the genetic makeup in activated microglia, it is still not fully understood how microglia serve a protective/harmful role in various neurological and neurodegenerative disorders (Liu et al., 2021, Lannes et al., 2017).

1.4.2 Microglia in Neurodegenerative disorders

There is lot of evidence from several studies suggesting potential therapies targeting microglial functions during disease pathology to halt the brain degeneration in these disorders (Muzio et al., 2021). There are also various ongoing clinical trials which use microglia as a therapeutic target in neurodegenerative disorders (Muzio et al., 2021).

Various studies suggest a pathogenic role of microglia in these neurodegenerative disorders. As such microglial activation has been observed through PET analysis in ALS patients (Turner et al., 2004). This study also showed that in both the motor and extra-motor brain areas, there exists diffuse microglial activation in ALS patients through the PET analysis (Turner et al., 2004) and in mouse models of the disease (Spiller et al., 2018). A very big limitation of all these studies, however, is the small number of ALS patient cases that have been investigated in these studies (Turner et al., 2004).

As a person ages, the gene expression in glial cells changes (Soreq et al., 2017), thus the varying ages of the patients included in this research may make it difficult to interpret the findings from these different studies. There is a consensus regarding the existence of non-cell autonomous factors that play an important role in ALS pathophysiology like non-neuronal cells like microglia and astrocytes (Nagai et al., 2007). In chimeric mice that had a mixture of wild type SOD1 gene expressing non neuronal cells and mutant form of SOD1 expressing cells, this concept was first demonstrated (Rosen et al., 1993). Wild-type non-neuronal cells like microglia and astrocytes prevented axonal degeneration and MN loss, thus considerably extending mouse survival The survival of mice was also increased by reducing the expression of the mutant SOD1 gene (SOD1G37R) in microglia (Clement et al., 2003). Despite having a longer lifespan, these mice eventually developed illness, indicating that pathogenic pathways that cause cell death are still present in MNs (Boillee et al., 2006).

Protein aggregation and misfolding are key hallmarks of ALS (Rubinsztein, 2006). Misfolded mutant SOD1 that is released in extracellular environment commonly found in ALS can lead to microgliosis (Urushitani et al., 2006). It is true that CD14 on

microglia interacts with extracellular SOD1G93A and SOD1G85R to cause the generation of pro-inflammatory mediators (Zhao et al., 2010). Using TLR2, CD14 and TLR4 blocking antibodies, as well as microglia lacking CD14 expression, this activation can be reduced in vitro (Zhao et al., 2018). Prolonged pharmacological suppression of TLR4 in SOD1G93A mice leads to a slight attenuation of MNs degeneration but does not result in a 2-week extension of survival, unlike TLR4 deletion in the SOD1G93A genetic background (Lee et al., 2010). These results show that microglia activation in SOD transgenic ALS animal models may serve as a target for the creation of novel therapeutic approaches (Fellner et al., 2013).

Several studies in other neurodegenerative disorders also show involvement of microglia. For example, in Alzheimer's disease, several of variations that increases the susceptibility to Alzheimer's disease are either found in or close to genes that microglia express (Muzio et al. 2021). Studies in Parkinson's disease also suggest a potential role of microglia. For example, a study showed that microglia engulf alpha-synuclein and then use tunnelling nanotubes to transfer these protein aggregates are transferred between various microglia. Healthy microglia also share mitochondria with the alpha-synuclein-overloaded microglia (Scheiblich et al., 2021, Fig. 8).

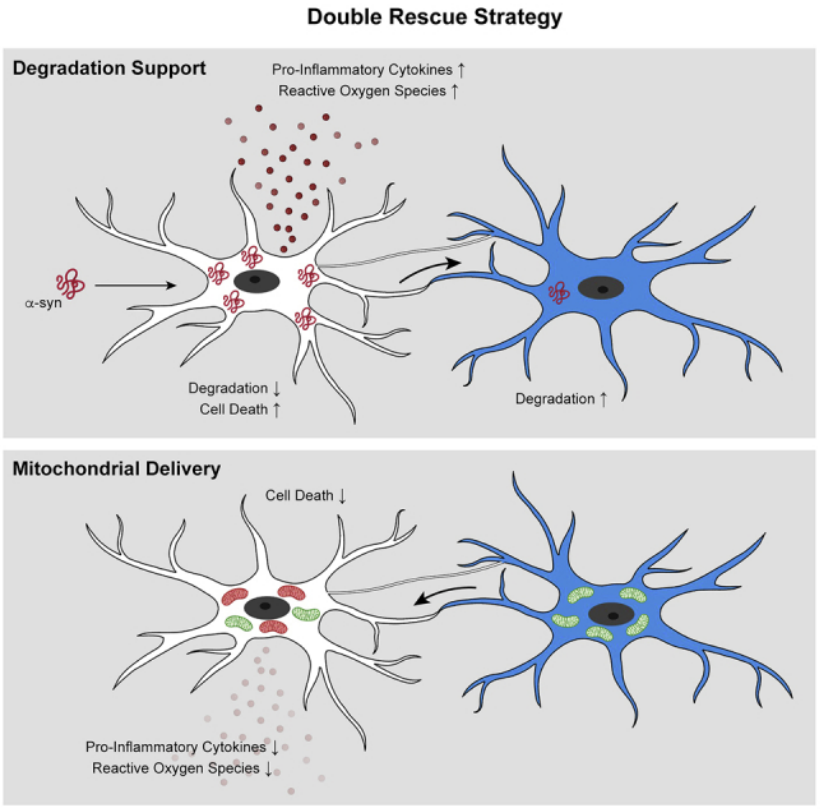

Figure 8. Alpha synuclein cargo clearance by microglia. Microglia engulf alpha synuclein and then using tunneling nanotubes they are transferred between various microglia. Healthy microglia also shares mitochondria with the alpha synuclein overloaded microglia.(Taken from Scheiblich et al., 2021, Creative Commons CC-BY license)

1.4.3 Role of microglia in TDP-43 pathology

A study by Xie et al, 2022 shows that the TREM2 deficit increased neuronal injury and motor impairments by impairing microglia's ability to phagocytically remove pathogenic TDP-43 (Xie et al., 2022). Their findings show that TDP-43 is a possible ligand to TREM2, and this interaction mediates the neuroprotective effects of microglia related to TDP-43 related neurodegeneration. Moreover, they also demonstrate that TDP-43 interacts with TREM2 in vitro, in vivo, and in silico. There are also studies that show that ALS monocyte-derived microglia-like cells (MDMi) recapitulate key pathological features like cytokine alterations, activated microglial morphology, cytoplasmic TDP-43 accumulation, DNA damage etc (Quek et al., 2022).

2 Objectives

The goal of my project was to investigate the effect of neuronal expressing aberrant TDP-43 on microglia, by addressing the following main aims -

a) To examine the effect of neuronal TDP-43 pathology on the morphology of microglia.
b) To characterize the effect of diverse forms of neuronal TDP-43 pathology on the motor skills of the mice.
c) To investigate the effect of neuronal TDP-43 pathology on the motility of microglial processes *in vivo.*

3. Materials and methods

3.1 Mice

All experiments were approved by the Government of Upper Bavaria. CX3CR1- GFP transgenic mice (a mouse line in which microglia express GFP) and C57BL/6J animals were used. All mice had ad libitum access to food and water. At our animal facility,

three to five littermates that were age and sex matched were housed together and kept on a 12-hour day/night cycle. All the experiments included both males and females.

3.2 Viral constructs

AAV-mediated viral constructs were injected in mouse primary motor cortex (M1). For these viral constructs, Adeno-associated virus (AAV), serotype 2/9 mediated transduction was used to express different proteins and this was conjugated with mCherry which served as fluorescent protein for this construct. Human synapsin (hsyn) is used as a promoter for these viral constructs (Fig. 9).

The following four viral constructs were used -

1. **AAV2/9-hSyn-mCherry-myc-his -** This construct was used as control as it facilitates the AAV-mediated expression of mCherry only.
2. **AAV2/9–hSyn-mCherry-myc-TDP43-his –** This has human full length TDP-43 protein. It results in nuclear overexpression in neurons. This is mentioned as hTDP43 in the text hereafter.
3. **AAV2/9–hSyn-mCherry-myc-hTDP43 (∆NLS1)-his -** This construct has 3 point mutations in nuclear localisation sequence (NLS) of TDP43. Thus, this results in cytoplasmic expression of TDP-43 protein.
4. **AAV2/9–hSyn-mCherry-myc-hTDP43(∆NLS1-5FL)-his**, includes 5 point mutations in RNA recognition motifs (RRM) which results in RNA binding deficit and it also has mutation in nuclear localisation sequence (NLS) results in cytoplasmic expression of TDP-43.

The structure of these constructs is shown in figure 9 . All of these constructs and AAVs were stored at -80°C. They were generated by Shenyi Jiang in the Liebscher lab.

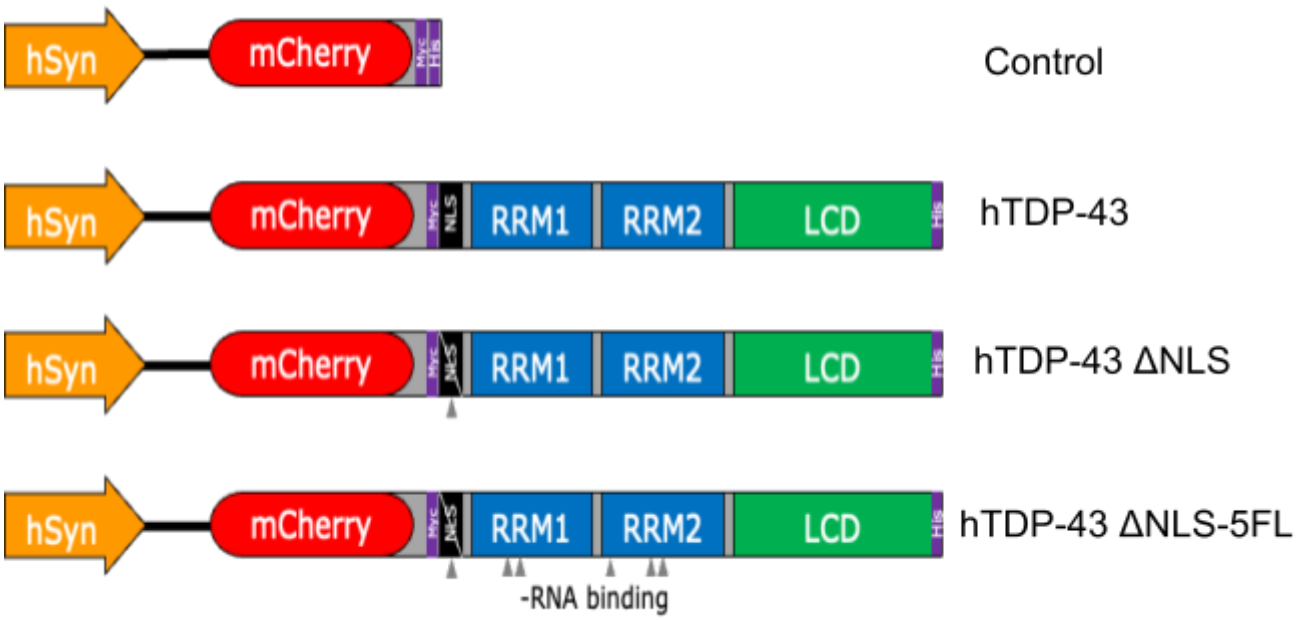

Figure 9. Structure of viral constructs. Structure of mCherry, hTDP-43, hTDP-43 ΔNLS and hTDP-43 ΔNLS-5FL construct (image generated by Shenyi Jiang).

3.3 Surgical procedure

All surgeries were performed when the mice reached 2.5 to 3 months of age. All the surgical instruments used like forceps, scissors etc. were sterilised using 70% ethanol.

Meloxicam (2mg/kg, Meloxidyl, Ceva Animal Health) was used as analgesic and was injected subcutaneously in all mice 30 mins before the surgery. Mice were deeply anaesthetised by injecting a combination of Medetomidine (0.5 mg/kg, Dormitor, Orion Pharma), Midazolam (5 mg/kg, Dormicum, Roche) and Fentanyl (0.05 mg/kg, Hexal) intraperitoneally. The absence of a toe-pinch reflex and a steady and slow respiratory rate was used to determine the depth of anaesthesia.

Following this, the mice were kept on a heating pad at 37°C . It was carefully positioned and fixed in the stereotaxic instrument. The fur above the skull is wiped with iodine and 70% ethanol. Lidocaine (local anaesthesia) is applied on the skin above the skull. To access the skull, the fur above it was excised using sterile scissors. The midline bony landmark which is located between the frontal and parietal bones is the place where sagittal and coronal sutures meet was spotted on skull. This was taken as reference to locate other brain areas. The right M1 was located on the skull and it was consequently

marked based on stereotactic coordinates from the mouse brain atlas (M-L - 1.5 to 1.6mm, A-P - 0.5 mm anterior). The above mentioned steps were the same for two types of surgical procedures performed in this project. One of them were the mice on which further *in vivo* imaging was performed and the other surgical procedures were done on the mice whose brain sections were used for confocal imaging following perfusion.

1. Surgery for *In vivo* imaging – Following the above steps, using a high-speed surgical drill, a circular craniotomy (4 mm diameter) was performed above M1. Precautions were taken to avoid potential bleeding due to damage of the vasculature during drilling. But, if bleeding occurs during drilling, sterile saline (B. Braun, Melsungen, Germany) and gelfoam (Medline) were applied to stop the same. As the bone flap covering the right M1 became loose, it was carefully raised and removed by inserting a pair of small forceps into the space between the bone flap and the dura. The dura was left intact during this step. The viral vectors mentioned earlier were injected, such that each mouse was injected with one viral vector. A micropipette with a siphon pump was used to do injections such that each injection site had 300 µl of the viral construct. Three such injections were performed on the motor cortex (coordinates: M-L - 1.5 to 1.6mm, A-P - 0.5 mm anterior). Sterile saline was intermittently used to prevent the cortex from drying. The bleeding was stopped using wet gelfoam and saline. Following this, a glass coverslip (4mm in diameter, Warner Instruments) was properly adjusted and implanted to fit into the cranial window and. Sterile saline was soaked up using sterile surgical sponges to create a dry surface to aid the initial seal between the skull and coverslip. Following this, UV curable dental cement (Venus Diamond Flow), histoacryl tissue glue (B. Braun, Melsungen, Germany), and dental acrylic (Paladur) were used to fix the aluminium head post. This custom-designed aluminium head post is used for head fixation under the objective during the imaging sessions (Fig. 10).

2. Surgery for confocal imaging - For the mice whose brains were later used for confocal imaging, the following procedure was used after giving analgesic and anaesthesia and placing the mouse in stereotaxic instrument as mentioned earlier. After locating M1 using stereotaxic coordinates, four holes were drilled in skull above M1 in both right and left hemisphere using a high-speed surgical drill (coordinates: M-L - 1.5 to 1.6mm, A-P - 0.5 mm anterior). Precautions were taken to avoid potential

bleeding due to damage of the vasculature during drilling. But, if bleeding occurs during drilling, sterile saline (B. Braun, Melsungen, Germany) and gelfoam (Medline) were applied to stop the same. The skin above the skull was stitched back.

Both types of surgeries were followed by injecting antagonist (Nalaxone 1.2 mg/kg, Flumazenil 0.5 mg/kg, Atipamezol 2.5 mg/kg) to wake the mouse from anaesthesia. The dosage of antagonist was roughly 80% of the anesthesia given to the mouse. Analgesia (Metacam, 10mg/kg) was administered every 12h post-surgery till 72h according to the animal license. Animals were kept back in their cages for 2 weeks post-surgery, to help them recover from surgery, before the in vivo imaging was started. For animals whose brain sections were later used for confocal imaging, they were also returned to their cages post-surgeries based on the time cohort they belonged to.

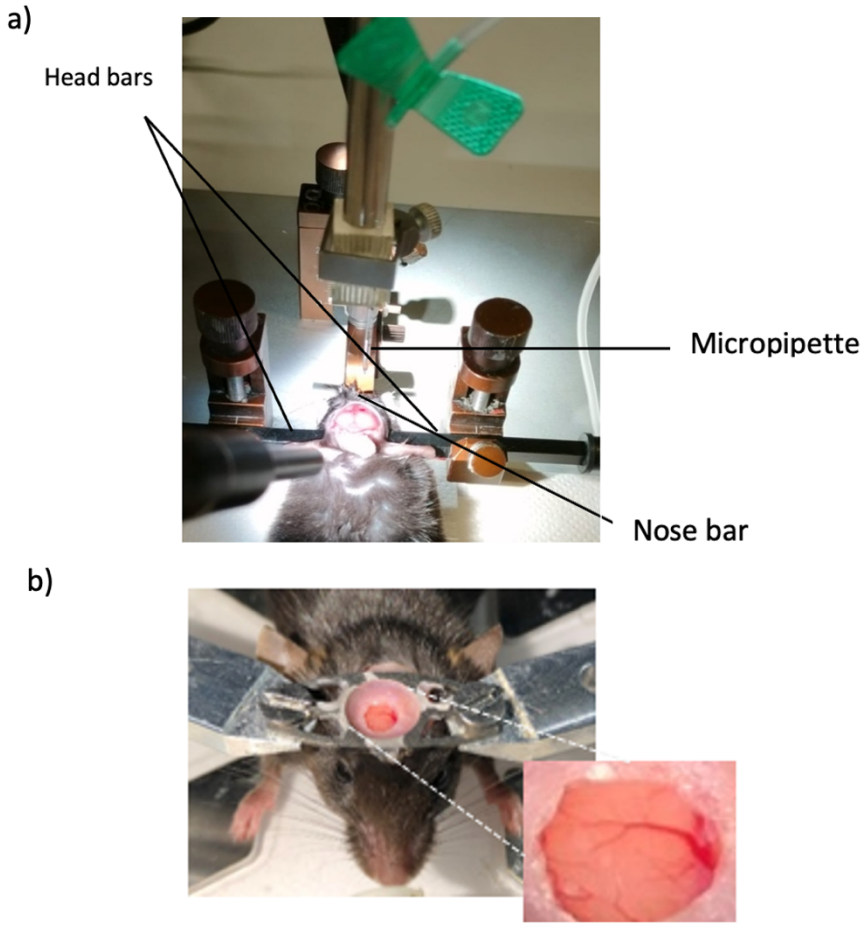

Figure 10. Surgical procedure. a) Micropipette is used to inject virus particles in the mouse primary motor cortex(M1) during stereotactic injection surgery. The mouse is fixed in a

stereotaxic apparatus using ear bars and a nose bar. b) For the cranial window, a glass coverslip is implanted on M1. A custom-made aluminium head bar is also fixed on the skull.

3.4 Chronic *in vivo* imaging

Chronic in vivo imaging was started two weeks post-surgery. The mouse was anesthetized with 3 vol% isoflurane in pure O_2 for 2-3min and after this mice were continuously under anaesthesia with 1-1.5 vol% isoflurane in pure O_2 using the isoflurane set-up (Abbott, Chicago, Illinois, USA). The absence of a toe-pinch reflex and a steady and slow respiratory rate was used to determine the depth of anaesthesia. Following this, the mouse was mounted under a two-photon microscope (Scientifica, Hyperscope) and images were acquired using a 16x, 0.8 numerical aperture objective (Nikon). This two-photon microscope is equipped with a mode-locked Ti: sapphire laser (Mai Tai eHP, Spectra-Physics) and it was tuned to 980nm for simultaneous excitation of GFP (microglia) and mCherry positive neurons. However as the mCherry signal was very faint at this excitation wavelength, we in addition recorded the same field of view at 1040 nm excitation. The mouse was kept on heating pad to maintain body temperature. Vascular patterns were used as landmarks for the identification and relocation of imaging sites in each imaging session. The mice are imaged every 4 days for the next 2 weeks. Timelapse imaging is performed at every 10 mins time interval for 3 timepoints during each imaging session. These scans taken at 8x zoom (512 x 512 pixels, covering an area of 85µm x 85µm) and for 1000 frames per plane for one single plane.

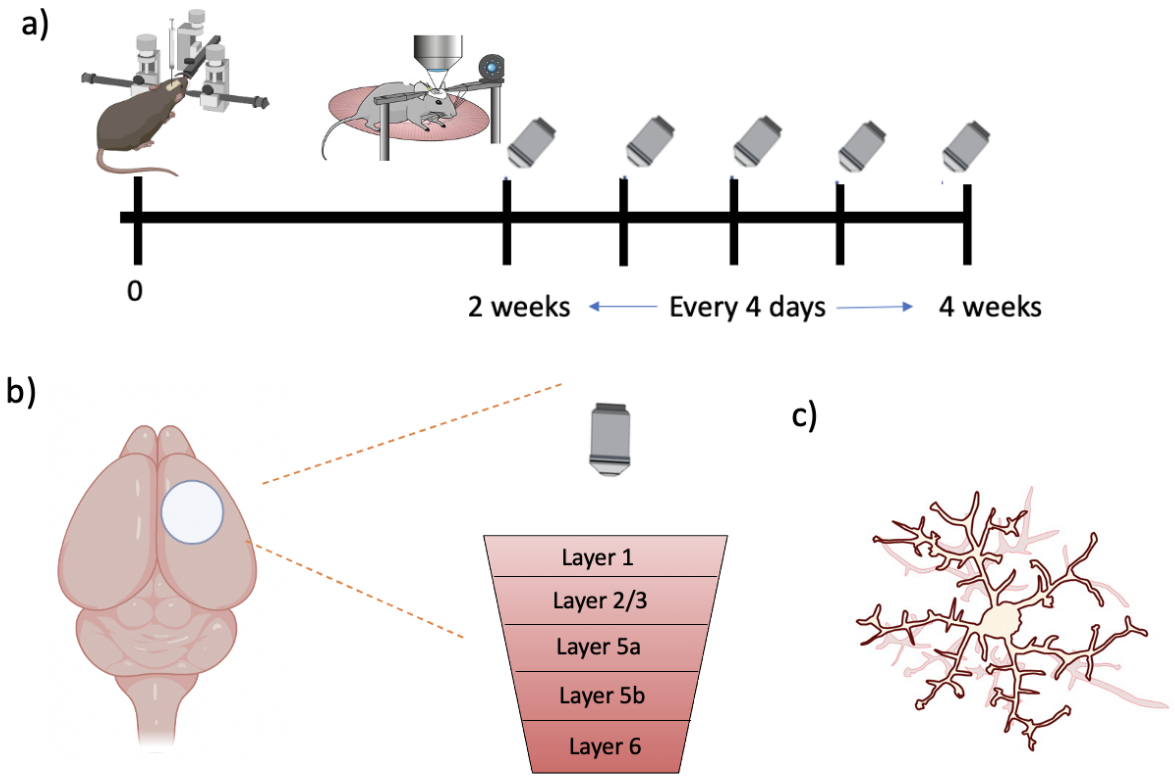

Figure 11. *In vivo* imaging. a) Schematic representation of timeline of *in vivo* imaging – timepoint 0 represents the surgery, 2 weeks post-surgery imaging is started and it's done for every 4 days for 5 timepoints till 4 weeks post-surgery b) Schematic representation of window and imaged brain area – primary motor cortex. The primary motor cortex consists of layers 1, 2/3, 5a, 5b and 6. c) Motility of microglial processes is assessed through *in vivo* imaging. (image made using Biorender.com and modified from Thorlabs Inc., methods- x.com, Tremblay et al. 2011, Commons Attribution 4.0 International License (CC-BY))

3.4 Perfusion

The mice were sacrificed with a lethal dose of ketamine and xylazine (KX). The concentration of KX given was double the concentration typically used for anaesthesia `(Ketamine – 130 mg/kg and xylazine – 10 mg/kg). Using scissors and forceps, a small slit was made over the abdominal cavity. This was cut open using scissors and the connective tissue was cut using forceps and scissors. The heart was located. A tiny incision was made over its right atrium. A needle containing PBS + heparin (1:500) was injected in its left ventricle so that the mouse is perfused intracardially by replacing the blood with PBS. The blood started flowing out of the right atrium and once the saline

started flowing out of the right atrium, this was stopped. After this, 4% PFA was injected in the left ventricle using a needle to fix the tissue. A vertical cut is made in the skin until the neck. Left and right cervical nodes were collected from the back and sides of the neck. A vertical cut was made into the skull along the midline to remove the skull from the surface of the brain. The brain was separated from the skull and it is kept in 4% PFA for 1 day. After this, the brain was kept in 30%w/v sucrose solution for a few days.

3.5 Sectioning, Immunostaining, mounting

The brain was sectioned using a vibratome into 100µm thick coronal sections. These brain sections were stored in PBS solution + 0.05% NaN3 (sodium azide). The sections were washed in PBS once for 10 mins and they were washed three times in PBST (1% TritonX-100) for 15 mins. They were incubated with blocking buffer - (1) 7 % Normal Goat Serum (Abcam), (2) 0.5% Bovine Serum Albumin (Sigma-Aldrich) and (3) 1% Triton (Sigma-Aldrich) for 1 hour. They were incubated with the following primary antibodies - Rabbit anti-TMEM119 (Abcam, Cat no.-ab209064, 1:250) and Goat anti-Iba1 (Wako chemicals, Cat no.- 011-27991, 1:300) at 4°C for 2 days on a shaker. Brain sections from C57BL/6J were stained with both IBA1 and TMEM119 antibodies. Brain sections from CX3CR1 mice were just stained with TMEM119 as they had microglia expressing GFP. After this step, the sections were washed three times with PBST (0.5% TritonX-100) for 15 minutes each. Later, the sections were incubated with secondary antibodies (AF647 and AF488, Invitrogen Thermo Fisher, Cat. No - A21244 and A32731, 1:500) overnight at 4°C on a shaker. Later, the sections are incubated with PBST for 15 minutes once and then twice with PBS for 10 minutes. They were incubated with DAPI (1:2000) for 20 minutes and then incubated with PBS for 10 minutes before mounting. The sections were placed on mounted on slides. Mounting media (Sigma-Aldrich) was added and a coverslip was placed carefully so as to avoid any bubbles and sealed with nail paint.

3.5 Confocal microscope

Brain sections containing M1 were scanned using a Confocal Laser Scanning Microscope (Leica SP8X WLL). HC PL APO 40x/1.30 Oil CS2 objective was used to

capture the images. The following settings were used for imaging - Resolution (1024x1024 pixel, 107.59 µm x 107.59 µm), Speed (400 Hz per line), Z-step size (0.4um), and zoom(1.4x)

3.6 Disease symptom screening

Since we injected TDP-43 viral vectors into mouse primary motor cortex, we wanted to see if the neuropathology would cause any motor deficits. I used the following tests to assess disease symptoms every two weeks.

Parameter	Grade	Score
Hind limb tremor	Not present	0
	Present	1
Hind limb extension	Complete extension	0
	Partial extension	1
	No extension	2
Tail elevation test	At or above the level of the body	0
	Tail drops frequently	1
	No elevation	2
Rearing behaviour test	Rearing at least twice in 5 min	0
	Rearing at least once in 5 min	1
	No rearing	2

Table 1. Screening Test. List of parameters with their scores based on the severity for disease screening.

3.6 Cylinder test

More subtle means to assess in particular supraspinal centers controlling motor function as the Cylinder test and the Pole test. The cylinder test is used to assess locomotor asymmetry for mouse models of various CNS diseases (Fig. 12a, Schallert et al., 2000). This test was performed on mice that got AAV injections only into one hemisphere. The animal moves inside a plastic cylinder, and the movement of its forelimbs as it rears up against the arena wall is monitored using a camera (GoPro

Hero8) and recorded. When the entire palm is on the arena wall, this shows that the forelimb is being used to support the body. As a fraction of all contacts, the number of impaired and unimpaired forelimb contacts is determined. With the help of this test, the motor abnormalities can be phenotyped. For the cylinder test, the total number of rearings was manually counted from the video. The first paw used (left or right) was noted. Further, the percentage of left paw usage first while rearing was calculated.

3.6 Pole test

The pole test was used to assess a mouse's ability to grab and navigate on a pole (Fig. 12b). It is mainly used to evaluate locomotor function and balance of mouse (Ogawa et al., 1985). Throughout the course of two training trials, mice are taught to perform the pole test. Mice are positioned on top of the pole (which is 50 cm long) with their heads facing upward. Animals typically spontaneously turn around on the tip of the pole and descend the entire length of the pole in order to return to their home cage. It is timed how long it takes the animals to turn so they are looking downhill (time to turn) and how long it takes them to descend to the base of the pole (total time).

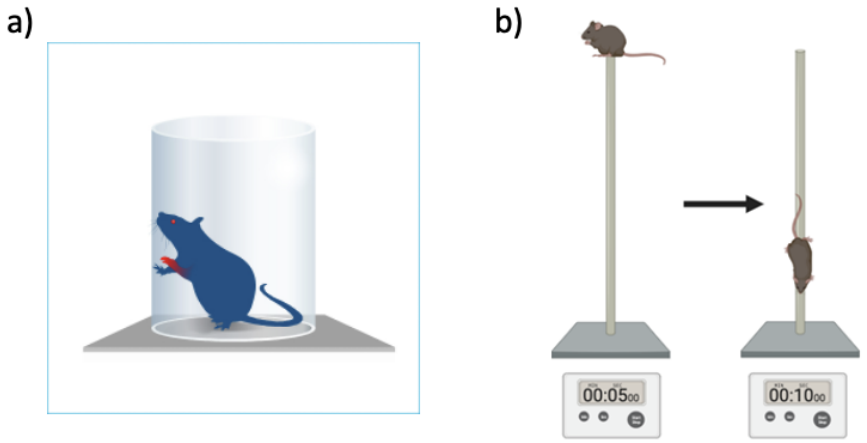

Figure 12. Behaviour test a) Schematic representation of cylinder test. The mouse is rearing with its forelimbs. b) Schematic representation of pole test. The time required for the mouse to turn and face downward and the time required to climb down the pole is assessed (Image taken from National Ataxia foundation and Neurofit)

3.7 Data analysis and Statistics

For the microglia process motility, a custom-made MATLAB code was used to register the images and to compute the differences in pixels between the 3 time points spaced by 10 min to obtain the fraction of the image that is constantly populated by processes of the microglia cell, termed ‘stable fraction’, the fraction of the image area where processes are retracted (‘area lost’) and the fraction of the image area where processes extent to (‘ area gained’). GraphPad Prism was used for statistical comparison and for plotting the computed data. Repeated measures 2 way ANOVA was used to perform the analysis. For the post-hoc analysis, Sidak’s multiple comparisons test was performed. To assess the microglia morphology, a MATLAB script was implemented for automated morphological analysis (Heindl et al., 2018). A Kruskal Wallis test was used for statistical comparison. For the post-hoc analysis, Dunn’s multiple comparisons test was performed. For the cylinder test data, 2 way ANOVA was used. For the pole test data, the Kruskal Wallis test was performed. For post-hoc analysis, Dunn’s multiple comparisons test was used.

4. Results

4.1 Neuronal TDP-43 pathology and consecutive microglial reactivity

a)

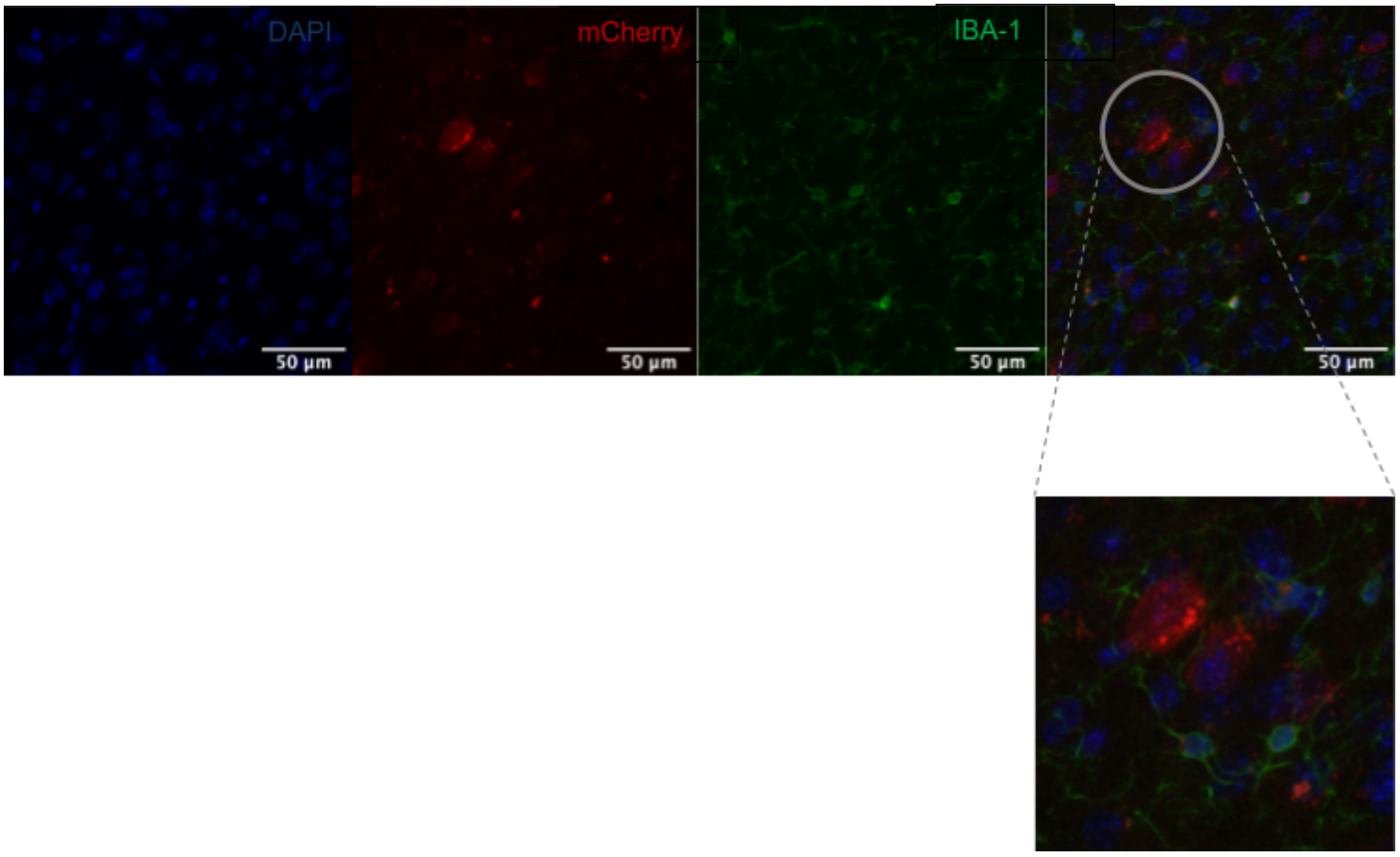

b)

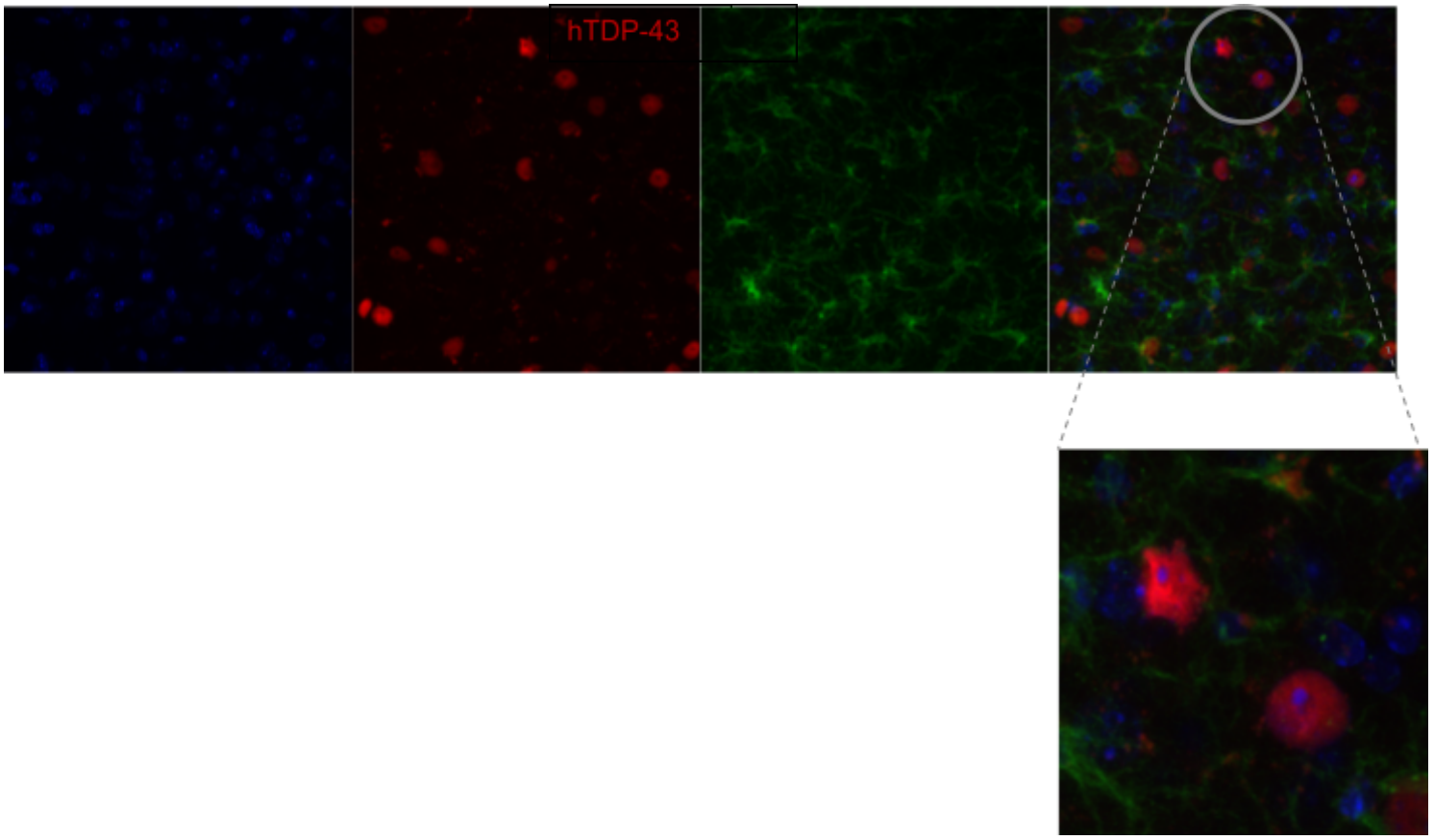

c)

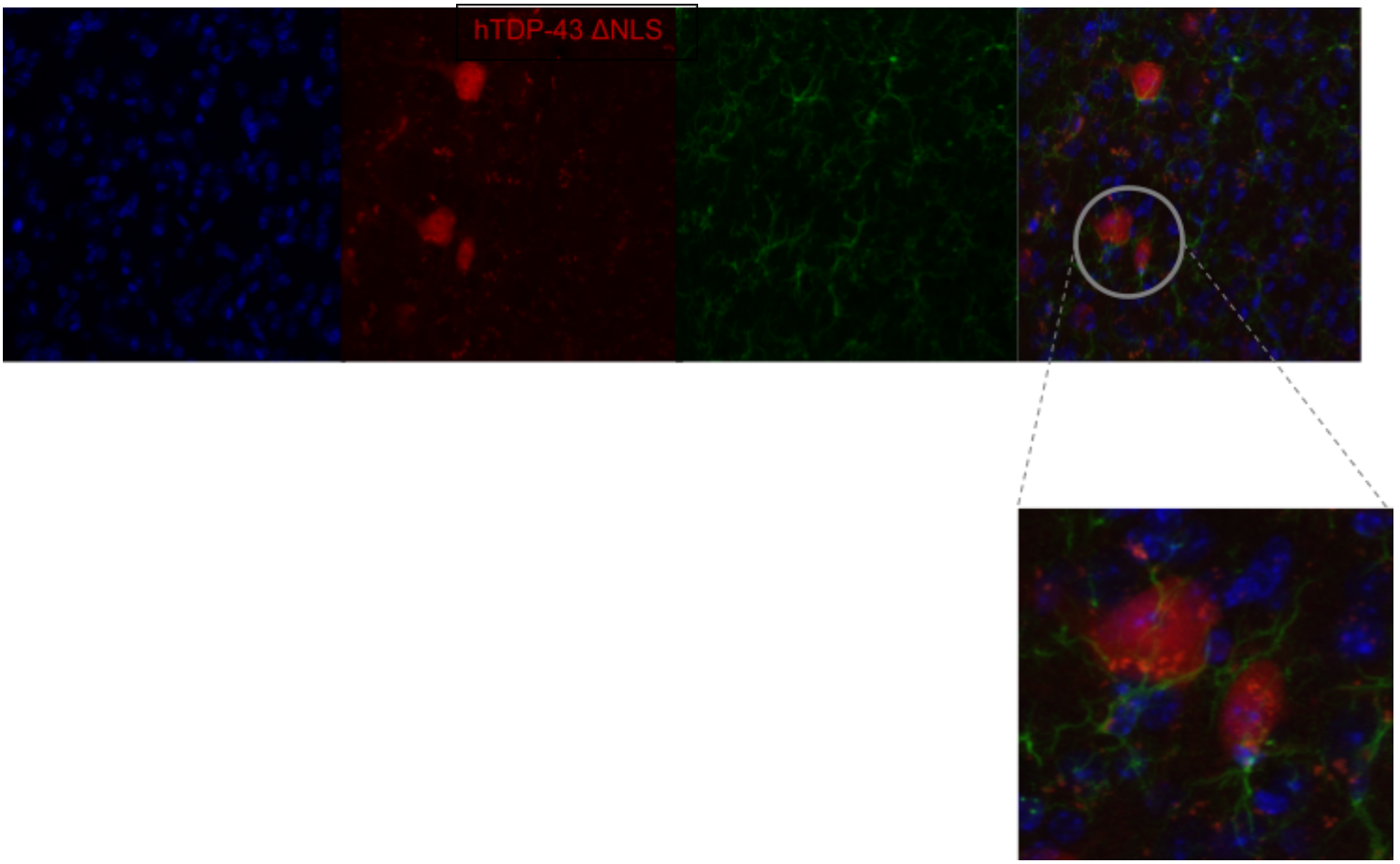

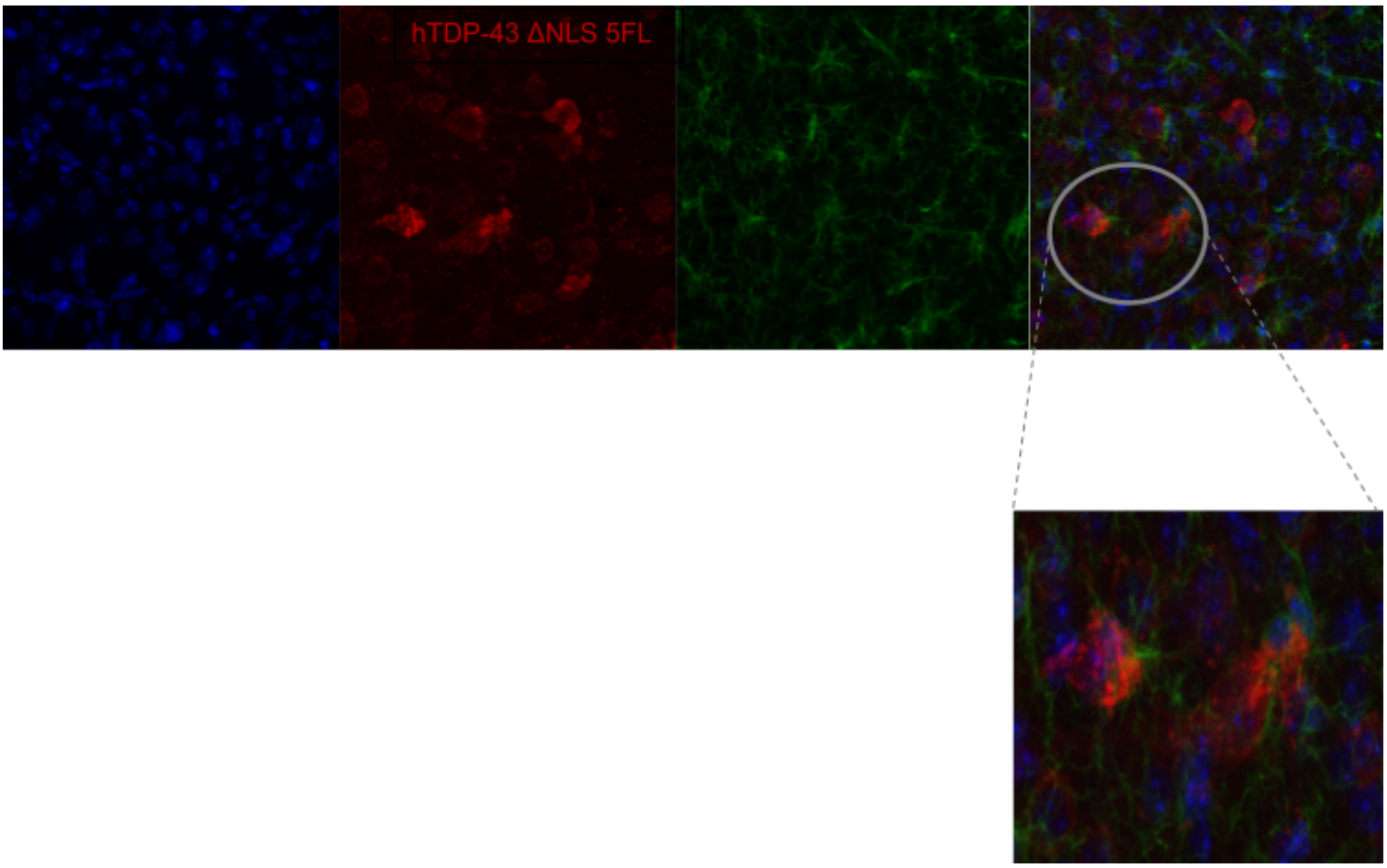

Figure 13. AAV-mediated TDP-43 neuropathology triggers microglia (re)activity. a) Confocal images displaying neuronal mCherry expression and microglia morphology (Iba1) in mouse injected with AAV-mCherry. b) Confocal images displaying neuronal mCherry expression and microglia morphology (Iba1) in mouse injected with AAV-hTDP-43. c) Confocal images displaying neuronal mCherry expression and microglia morphology (Iba1) in mouse injected with AAV-hTDP-43 ΔNLS d) Confocal images displaying neuronal mCherry expression and microglia morphology (Iba1) in mouse injected with AAV-hTDP-43 ΔNLS 5FL.

Cytoplasmic mislocalization of TDP-43 is seen in AAV-hTDP-43 ΔNLS and AAV-hTDP-43 ΔNLS 5FL injected mice (Fig. 13c and 13d). Nuclear TDP-43 overexpression is observed in AAV-hTDP-43 injected mice (Fig. 13b).

4.2 Microglia morphology

The assessment of alterations in microglia morphology is widely utilized as a proxy to quantify microglial activation and for examining the role of microglia in neurological and neurodegenerative disorders. The shift of microglia from a resting to a (re)activated state can be assessed by its morphological transformation from a highly ramified cell to an amoeboid cell body with fewer processes (Heindl et al., 2018). In the following section, the morphological analysis of the sphericity, process lengths and ramification is detailed.

4.2.1 Sphericity

The sphericity can be defined as a function of surface area and volume of a 3-dimensional object. It is used as a measure of compactness. A 3D item that is the most compact and has a score of one and represents a sphere (Heindl et al., 2018).

Sphericity is calculated as follows:

$$sphericity = \frac{\pi^{\frac{1}{3}} (6V)^{\frac{2}{3}}}{A}$$

where, V represents volume and A represents surface area

After 4 weeks of expression, I found that the sphericity is significantly higher for microglia in mice injected with AAV-hTDP-43 ΔNLS-5FL and AAV-hTDP-43 compared to AAV-mCherry control and AAV-hTDP-43 ΔNLS. However, there is no significant difference between AAV-hTDP43-ΔNLS and mCherry. After 8 weeks of expression, the sphericity of microglia in mice injected with AAV-hTDP-43 ΔNLS-5FL is significantly higher compared to AAV-hTDP-43, AAV-hTDP-43 ΔNLS and AAV-mCherry. The sphericity for microglia in mice injected with AAV-hTDP-43 ΔNLS is significantly lower compared to AAV-hTDP-43, AAV-mCherry and AAV-hTDP-43 ΔNLS-5FL. However, there is no significant difference between the sphericity of AAV-hTDP-43 and AAV-mCherry.

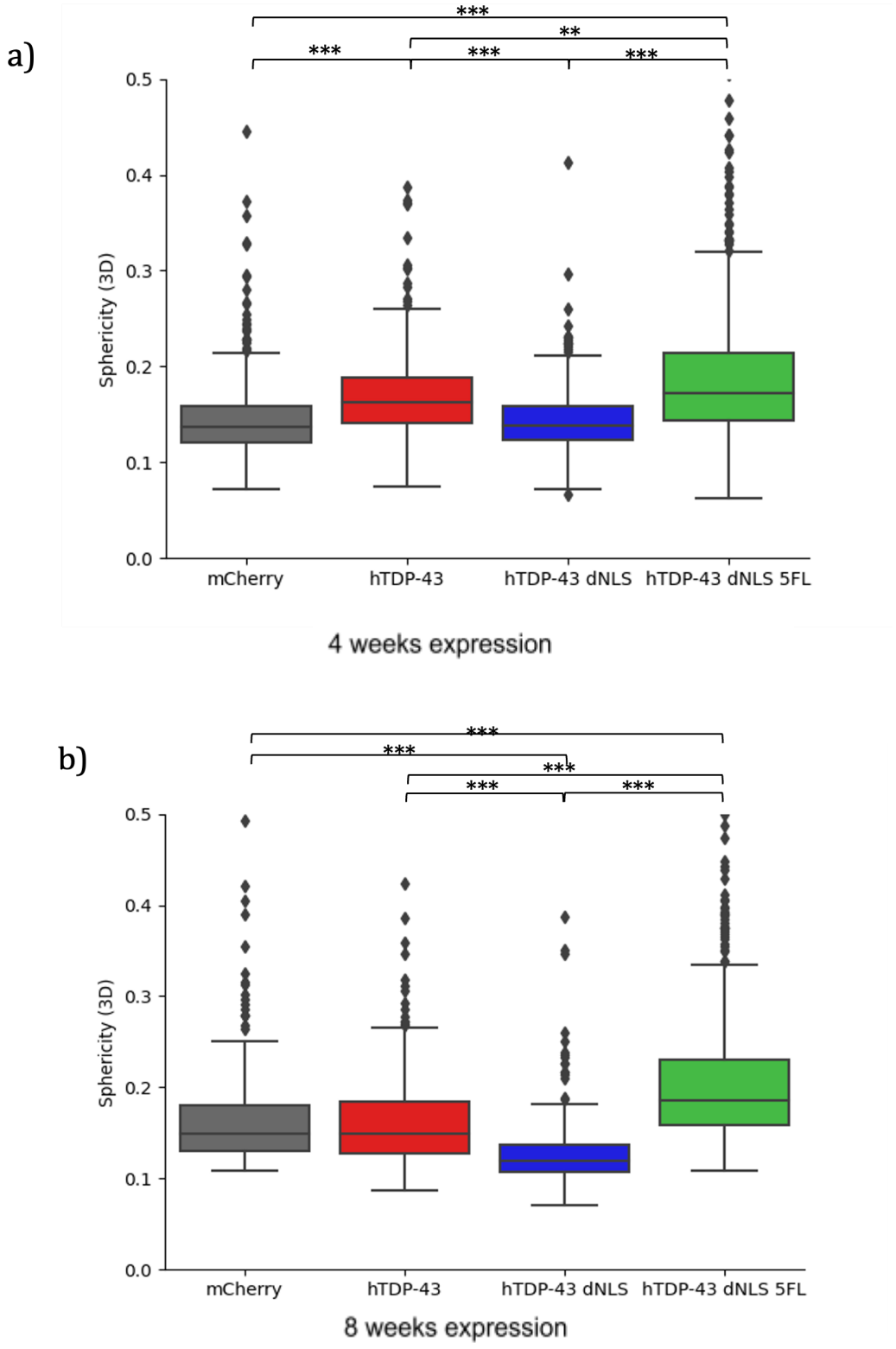

Figure 14. Sphericity of microglia. A) 4 weeks expression. Sphericity of microglia upon 4 weeks of neuronal expression of mCherry, hTDP-43, hTDP-43 ΔNLS and hTDP-43 ΔNLS 5FL (mCherry vs hTDP-43 p = 1.514e-13, mCherry vs hTDP-43 ΔNLS p = 7.86e-01, mCherry vs hTDP-43 ΔNLS-5FL p = 4.777e-38, hTDP-43 vs hTDP-43 ΔNLS p = 1.33e-11, hTDP-43 vs

hTDP-43 ΔNLS-5FL p = 1.38e-03, hTDP-43 ΔNLS vs hTDP-43 ΔNLS-5FL p = 3.837e-31, Kruskal Wallis with Dunn's post-hoc, mCherry: n = 305 (pooled), 3 mice ; hTDP-43: n = 259 (pooled), 2 mice, hTDP-43 ΔNLS: n = 287 (pooled), 3 mice, hTDP-43 ΔNLS-5FL: n = 720 (pooled), n = 3). B) 8 weeks expression. Sphericity of microglia upon 8 weeks of neuronal expression of mCherry, hTDP-43, hTDP-43 ΔNLS and hTDP-43 ΔNLS 5FL (mCherry vs hTDP-43 p = 3.95e-01; mCherry vs hTDP-43 ΔNLS p = 2.87e-22; mCherry vs hTDP-43 ΔNLS-5FL p = 2.132e-18; hTDP-43 vs hTDP-43 ΔNLS p = 1.687e-17; hTDP-43 vs hTDP-43 ΔNLS-5FL p = 5.368e-20; hTDP-43 ΔNLS vs hTDP-43 ΔNLS-5FL p = 3.374e-87, Kruskal Wallis with Dunn's post-hoc, mCherry: n = 278 (pooled), 3 mice; hTDP-43: n = 236 (pooled), 3 mice; hTDP-43 ΔNLS: n = 261 (pooled), 3 mice; hTDP-43 ΔNLS-5FL: n = 537 (pooled), 3 mice). Data is plotted as mean +/- SEM.

4.2.2 Branch length

In the automated analysis, Iba1 positive structures are considered as microglia. The fundamental structural elements of the microglial cells and their arrangement were documented using a skeleton. This consisted of three steps. Based on the binary mask of the microglial cells, a distance map was created, showing the shortest path from each voxel inside a cell to the cell surface. Then, using a watershed segmentation, this distance map was divided into segments. The skeleton was then created in a third stage by connecting the centroids of the generated segments with straight lines. Mathematically, this skeleton can be defined and analysed as a r=graph consisting of nodes and edges. The centroids of the watershed segments serve as the nodes and the connecting lines serve as the edges. The longest pathway of nodes and edges between any end node of a branch and the first node outside of the soma is referred to as "Branch length skeleton" (Heindl et al., 2018). In biological terms, this is the length of major processes of individual microglia.

My data demonstrate that the neuronal expression of hTDP-43 ΔNLS-5FL and hTDP-43 for 4 weeks leads to lower length of processes of microglia compared to mCherry and hTDP-43 ΔNLS. The length of processes is also lower for mice injected with AAV-hTDP-43 ΔNLS compared to mCherry control. After 8 weeks of expression, the length of process is again lower for hTDP-43 ΔNLS-5FL and hTDP-43 compared to mCherry. However, mice injected with hTDP-43 ΔNLS have higher length of process of microglia compared to mCherry.

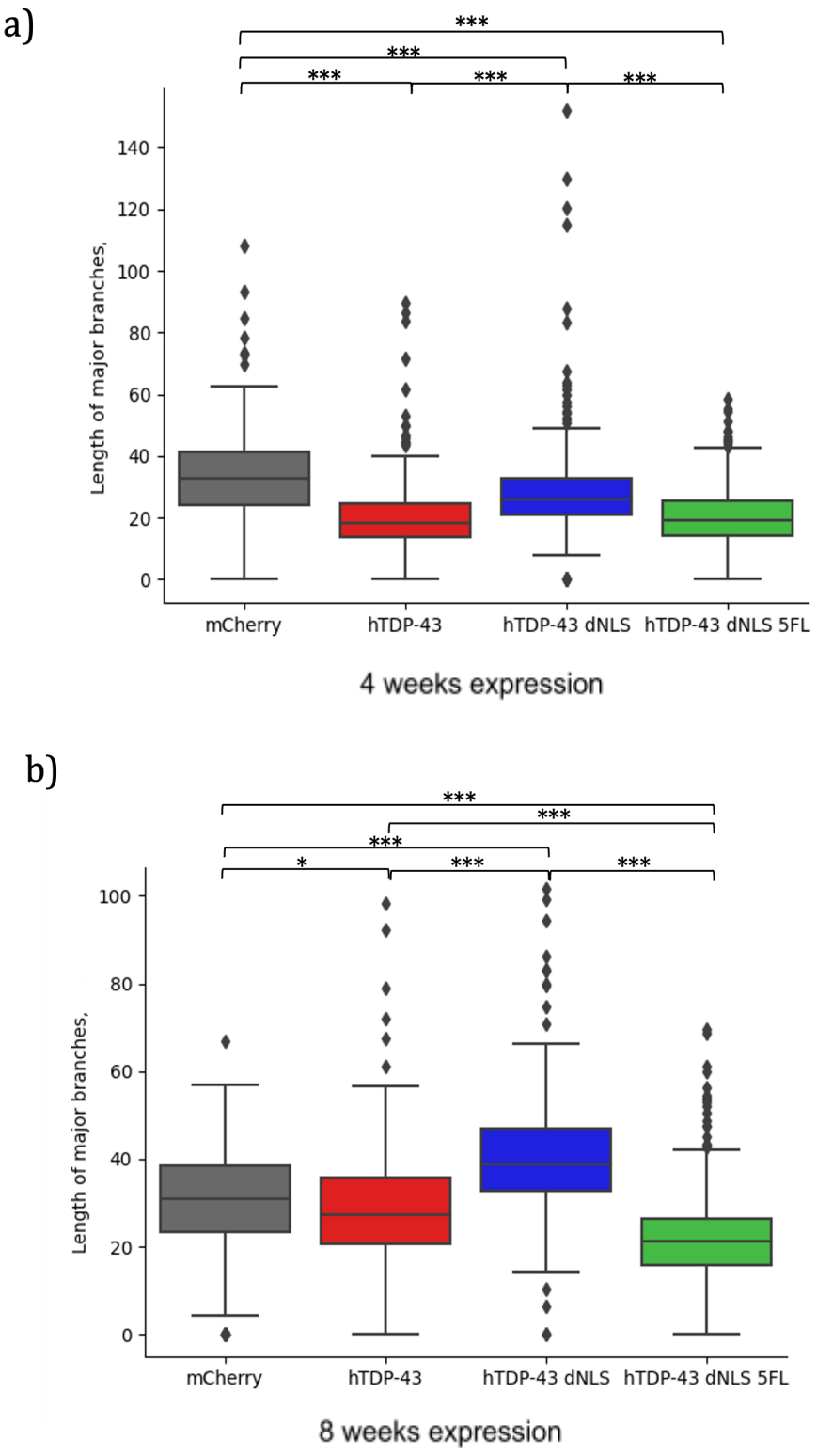

Figure 15. Branch length. A) The branch length of microglia upon 4 weeks of neuronal expression of mCherry, hTDP-43, hTDP-43 ΔNLS and hTDP-43 ΔNLS 5FL (mCherry vs hTDP-43 p = 4.1e-41, mCherry vs hTDP-43 ΔNLS p = 2.303e-05, mCherry vs hTDP-43 ΔNLS-5FL p = 1.375e-53, hTDP-43 vs hTDP-43 ΔNLS p = 8.815e-18, hTDP-43 vs hTDP-43 ΔNLS-5FL p = 2.773e-01, hTDP-43 ΔNLS vs hTDP-43 ΔNLS-5FL p = 2.564e-20, Kruskal

Wallis with Dunn's post-hoc, mCherry: n = 305 (pooled), 3 mice ; hTDP-43: n = 259 (pooled), 2 mice, hTDP-43 ΔNLS: n = 287 (pooled), 3 mice, hTDP-43 ΔNLS-5FL: n = 720 (pooled), n = 3). B) The branch length of microglia upon 8 weeks of neuronal expression of mCherry, hTDP-43, hTDP-43 ΔNLS and hTDP-43 ΔNLS 5FL (mCherry vs hTDP-43 p = 3.087e-02, mCherry vs hTDP-43 ΔNLS p = 4.223e-14, mCherry vs hTDP-43 ΔNLS-5FL p = 1.377e-24, hTDP-43 vs hTDP-43 ΔNLS p = 1.109e-20, hTDP-43 vs hTDP-43 ΔNLS-5FL p = 4.662e-13, hTDP-43 ΔNLS vs hTDP-43 ΔNLS-5FL p = 9.19e-79, Kruskal Wallis with Dunn's post-hoc, mCherry: n = 278 (pooled), 3 mice; hTDP-43: n = 236 (pooled), 3 mice; hTDP-43 ΔNLS: n = 261 (pooled), 3 mice; hTDP-43 ΔNLS-5FL: n = 537 (pooled), 3 mice). Data is plotted as mean +/- SEM.

4.2.3 Branch segments

Another parameter determining the complexity and ramification of microglia is the number of branch segments. Branch segments can be described as all alternative pathways for the primary branches of a single microglia that have exactly two nodes connected by an unequal number of edges. In biological terms, this represents the ramifications of major processes of microglia.

After 4 weeks of expression, I found that the ramifications of major processes of microglia were lower for mice injected with AAV-hTDP-43 ΔNLS-5FL and AAV-hTDP-43 compared to AAV-mCherry control and AAV-hTDP-43 ΔNLS. There is no significant difference between AAV-mCherry control and AAV-hTDP-43 ΔNLS injected mice. After 8 weeks of expression, I found that the ramifications of major processes of microglia were lower for mice injected with AAV-hTDP-43 ΔNLS-5FL compared to AAV-mCherry control, AAV-hTDP-43 and AAV-hTDP-43 ΔNLS. There was no significant difference between hTDP-43 and mCherry. However, the ramifications of major processes of microglia were higher for mouse injected with AAV-hTDP-43 ΔNLS compare to mCherry.

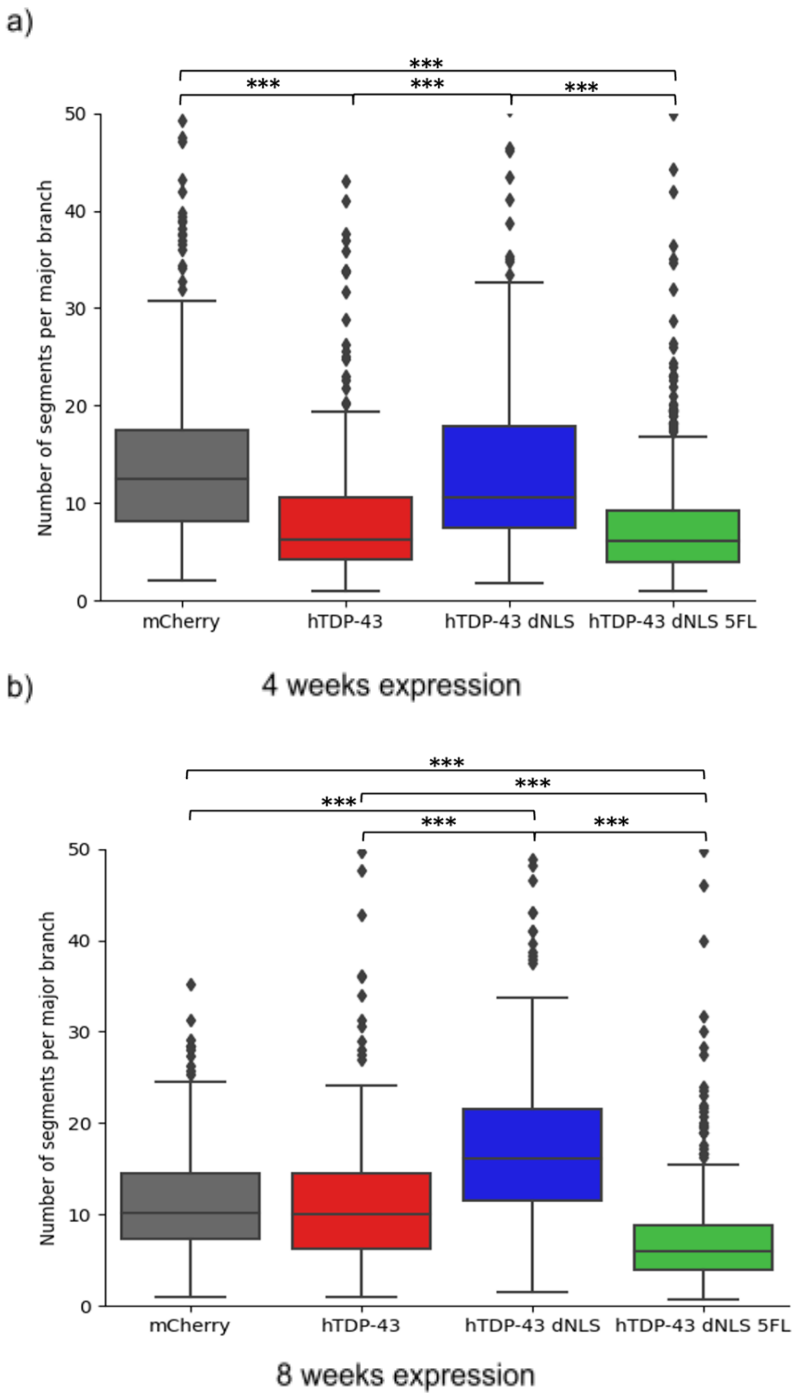

Figure 16. Branch segments. A) The branch segments of microglia upon 4 weeks of neuronal expression of mCherry, hTDP-43, hTDP-43 ΔNLS and hTDP-43 ΔNLS 5FL (mCherry vs hTDP-43 p = 3.06e-26, mCherry vs hTDP-43 ΔNLS p = 3.1e-01, mCherry vs hTDP-43 ΔNLS-5FL p = 2.586e-50, hTDP-43 vs hTDP-43 ΔNLS p = 1.202e-19, hTDP-43 vs hTDP-43 ΔNLS-5FL p = 1.921e-01, hTDP-43 ΔNLS vs hTDP-43 ΔNLS-5FL p = 3.026e-36, Kruskal Wallis with Dunn's post-hoc, mCherry: n = 305 (pooled), 3 mice ; hTDP-43: n = 259 (pooled), 2 mice, hTDP-43 ΔNLS: n = 287 (pooled), 3 mice, hTDP-43 ΔNLS-5FL: n = 720 (pooled), n = 3). B) The branch segments of microglia upon 8 weeks of neuronal expression of mCherry, hTDP-43, hTDP-43 ΔNLS and hTDP-43 ΔNLS 5FL (mCherry vs hTDP-43 p = 3.368e-01,

mCherry vs hTDP-43 ΔNLS p = 1.047e-13, mCherry vs hTDP-43 ΔNLS-5FL p = 8.29e-24, hTDP-43 vs hTDP-43 ΔNLS p = 6.67e-16, hTDP-43 vs hTDP-43 ΔNLS-5FL p = 2.238e-17, hTDP-43 ΔNLS vs hTDP-43 ΔNLS-5FL p = 2.807e-77, Kruskal Wallis with Dunn's post-hoc, mCherry: n = 278 (pooled), 3 mice; hTDP-43: n = 236 (pooled), 3 mice; hTDP-43 ΔNLS: n = 261 (pooled), 3 mice; hTDP-43 ΔNLS-5FL: n = 537 (pooled), 3 mice). Data is plotted as mean +/- SEM.

4.3 Microglia process motility

Microglia process motility describes the retraction and extension of processes of individual microglia within the local microenvironment without the cell body migrating during a given timeframe (Franco-Bocanegra et al., 2019).

Microglia process motility was tracked across three timepoints with 10 minutes interval. The experiments were performed approximately 3 weeks post-injection surgery using *in vivo* 2-photon imaging. Three parameters were assessed for the quantification of microglia process motility – the image area stably populated by microglial processes (stable area), the area were processes are retracted (area lost) and the image area newly populated by extending processes (area gained).

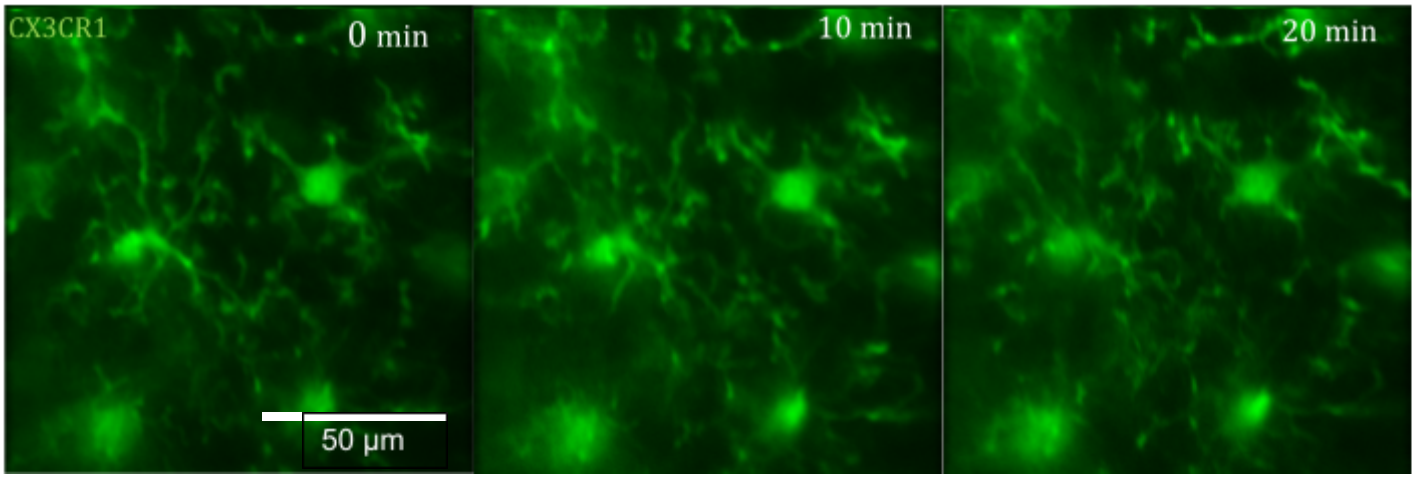

Figure 17. Time series of microglia process motility. Image captured using *in vivo* 2 photon microscopy displaying microglial processes in CX3CR1-GFP mouse across three time points with 10 minutes interval.

This analysis was performed in mice injected with either AAV-mCherry or AAV-hTDP-43 ΔNLS 5FL. In my investigations, I observed that the microglia in mice injected with

AAV-hTDP-43 ΔNLS 5FL have a more stable area compared to AAV-mCherry. These mice also have higher area gained and lost compared to mice injected with AAV-mCherry.

a)

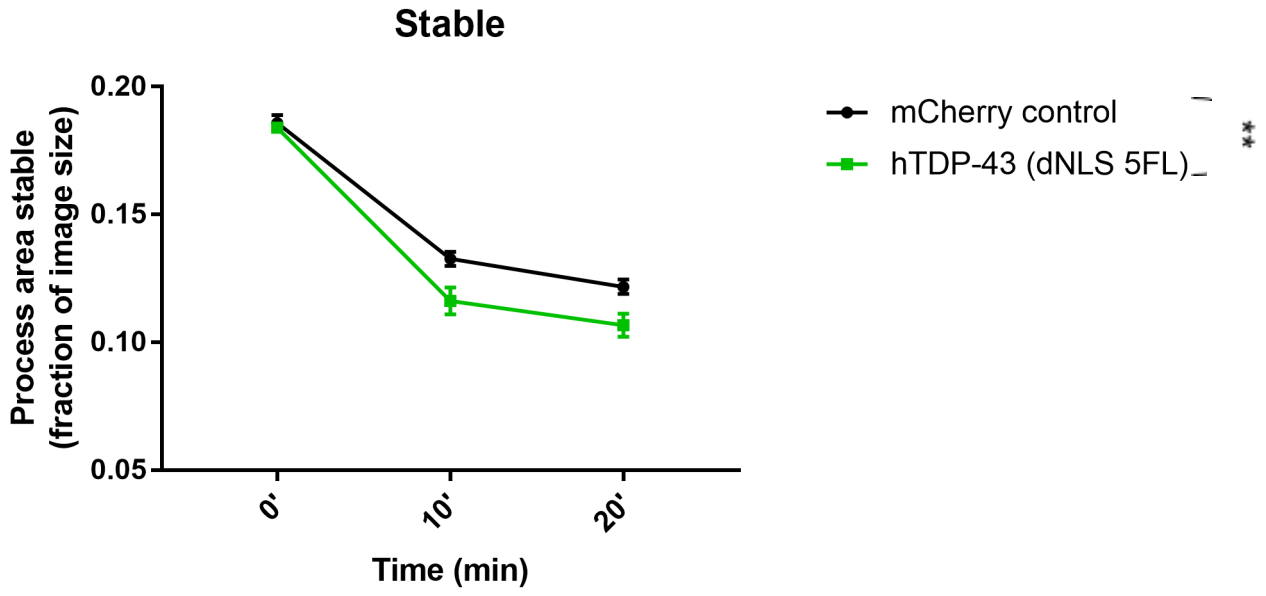

b)

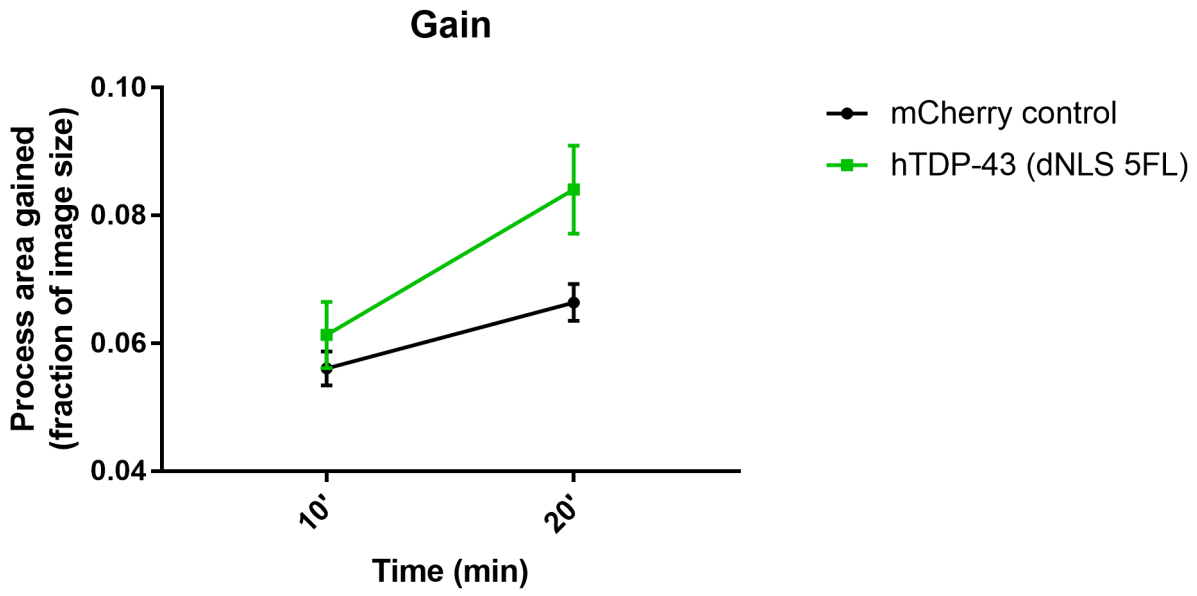

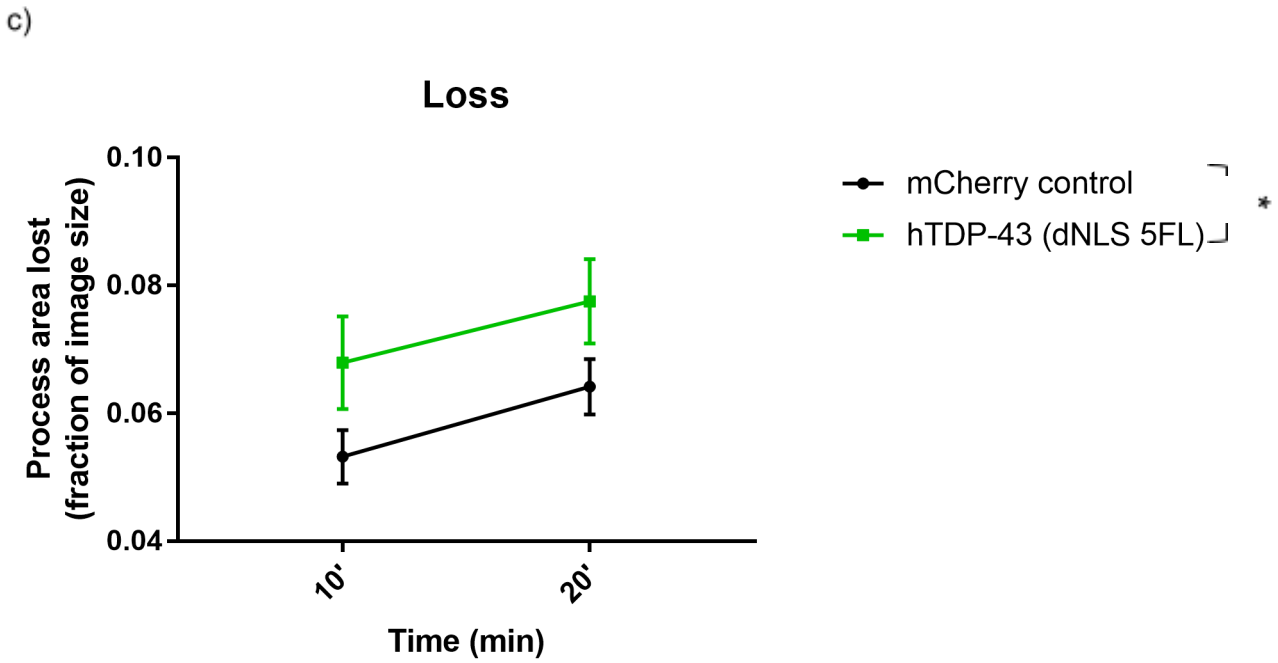

Figure 17. Microglia process motility. a) The fraction of the image area continuously covered by microglial processes (stable area) upon neuronal expression of mCherry and hTDP-43 ΔNLS 5FL across three timepoints (mCherry vs hTDP-43 ΔNLS-5FL p = 0.0068, 2 way repeated measures with Sidak's post-hoc, mCherry: field of view (FOV) = 85 μmx 85 μm, 4 mice; hTDP-43 ΔNLS 5FL: FOV = 85μm x 85μm, 2 mice) b) The fraction of the image area lost by microglial processes (stable area) upon neuronal expression of mCherry and hTDP-43 ΔNLS 5FL across three timepoints (mCherry vs hTDP-43 ΔNLS-5FL p = 0.088, 2 way repeated measures with Sidak's post-hoc, mCherry: FOV = 85μm x 85μm, 4 mice; hTDP-43 ΔNLS 5FL: FOV = 85μm x 85μm, 2 mice) c) The fraction of the image area lost by microglial processes (stable area) upon neuronal expression of mCherry and hTDP-43 ΔNLS 5FL across three timepoints (mCherry vs hTDP-43 ΔNLS-5FL p = 0.048, 2 way repeated measures with Sidak's post-hoc, mCherry: FOV = 85μm x 85μm 4 mice; hTDP-43 ΔNLS 5FL: FOV = 85μm x 85μm, 2 mice). Data is plotted as mean +/- SEM.

4.4 Effect of injected viral vectors on motor skills

4.4.1 Cylinder test

Cylinder test was used to assess the effect of single hemisphere-injected viral vectors on the motor skills of mice. I found no difference the proportional use of the left limb (the limb innervated by the injected hemisphere) between mice injected with the control AAV-mCherry and AAV-hTDP-43 ΔNLS 5FL (Fig. 18).

This experiment included 2 wild-type mice for 4 weeks post-injection, 4 wild-type mice for 6 weeks post-injection and 6 wild-type mice for 8 weeks post-injection for the mCherry-injected cohort. For the hTDP-43 ΔNLS 5FL-injected cohort, 4 wild-type mice were included for 4 weeks post-injection, 3 wild-type mice for 6 weeks post-injection and 5 wild-type mice for 8 weeks post-injection. There is not significant difference between the two viral vectors injected (P=0.3629). There is also no significant difference among the different time points of weeks post-injection surgery (P=0.9868) and the interaction between these two factors (P=0.0560) is also not significant. Ordinary two-way ANOVA was used for statistical analysis.

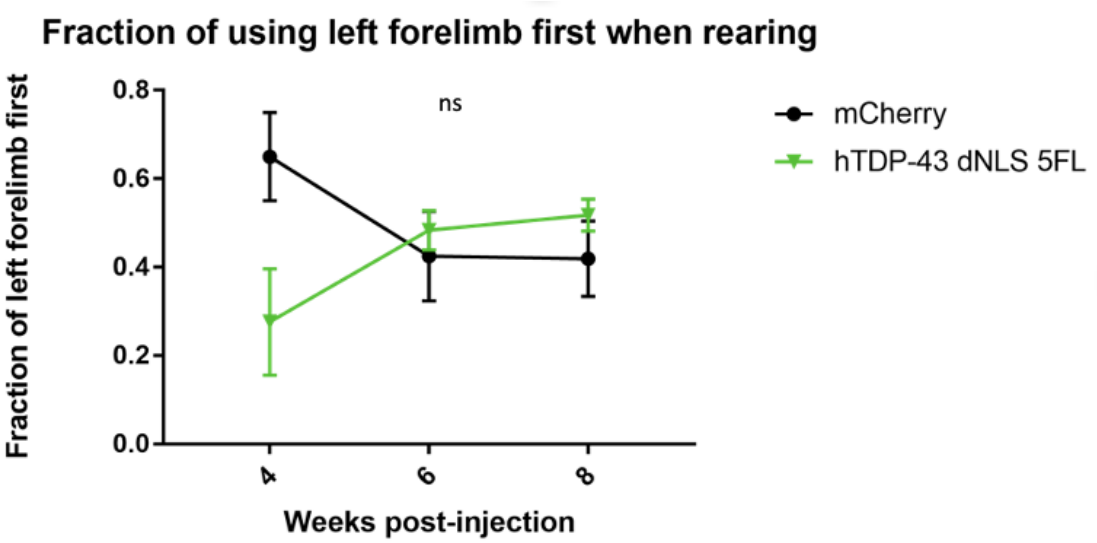

Figure 18. Cylinder test. Fraction of using left forelimb first while rearing for mice injected with mCherry and hTDP-43 ΔNLS 5FL 4, 6 and 8 weeks post-injection (mCherry vs hTDP-43 ΔNLS-5FL p = 0.3629, ordinary 2 way ANOVA, for 4 weeks - mCherry: n = 2, hTDP-43 ΔNLS-5FL: n = 4, for 6 weeks - mCherry: n = 4, hTDP-43 ΔNLS-5FL: n = 3, for 8 weeks - mCherry: n = 5, hTDP-43 ΔNLS-5FL: n = 5). Data is plotted as mean +/- SEM.

4.4.2 Pole test

The pole test was used to assess the effect of both hemisphere-injected viral injections on the motor skills of the mice.

Kruskal-Wallis test was used for statistical analysis and the result was significant (P = 0.0268). For post-hoc analysis, Dunn's multiple comparisons test was performed. There is no significant difference for mCherry vs. hTDP-43 (adjusted P value = 0.7762)

and mCherry vs. hTDP-43 ΔNLS (adjusted P value = 0.4898). There is significant difference for hTDP-43 vs. hTDP-43 ΔNLS (adjusted P value = 0.0441).

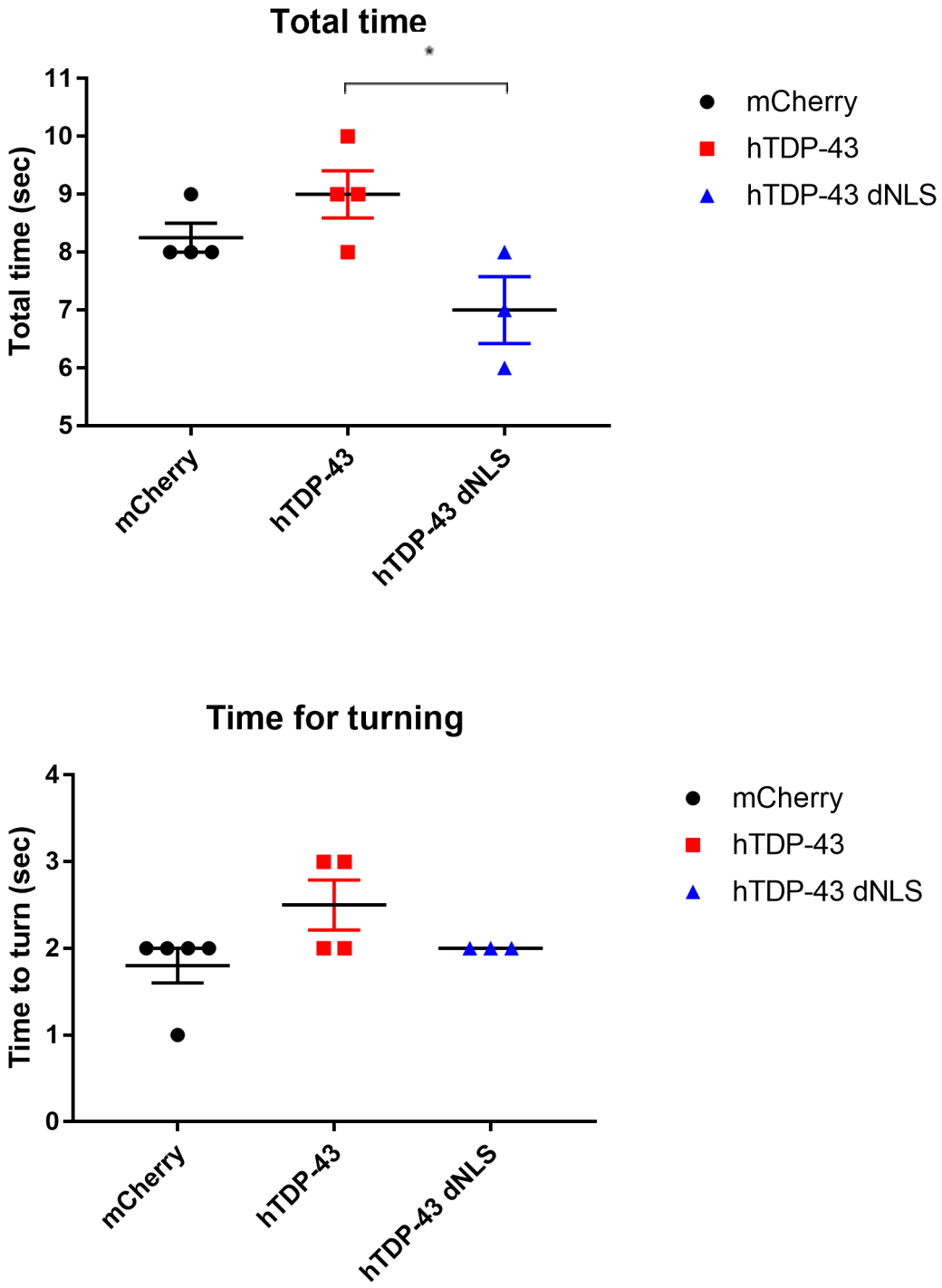

Figure 19. Pole test. A)The total time needed to descend on the pole in mice injected with mCherry, hTDP-43 and hTDP-43 ΔNLS upon 4 weeks of neuronal expression (mCherry vs hTDP-43 p = 0.7762, mCherry vs hTDP-43 ΔNLS p = 0.4898, hTDP-43 vs hTDP-43 ΔNLS p =

0.0441, Kruskal Wallis with Dunn's post-hoc, mCherry: n = 4, hTDP-43: n = 4, hTDP-43 ΔNLS: n = 3). B) The time taken by mice injected with mCherry, hTDP-43 and hTDP-43 ΔNLS to turn and face downwards upon 4 weeks of neuronal expression (p = 0.1136, Kruskal Wallis, mCherry: n = 4, hTDP-43: n = 4, hTDP-43 ΔNLS: n = 3). Data is plotted as mean +/- SEM.

5. Discussion

Several studies have shown different microglial responses like morphology transformation, motility changes and altered microglial migration towards injury, in neurodegenerative disorders like PD and AD (Huang et al., 2018, Colonna et al., 2017, Davalos et al., 2005, Tremblay et al., 2011, Nimmerjahn et al., 2005, Bolmont et al., 2008, Gyoneva et al., 2014, Hefendehl et al., 2014, Kettenmann et al., 2011, Carbonell et al., 2005).

In this study, we addressed the microglial response to various forms of neuronal TDP-43 pathology in the primary motor cortex of mice *in vivo* and *in vitro*. We showed that there is morphological transformation of microglia in terms of increased sphericity and decreased length of process and branching of processes when neurons express RNA binding deficient mutatant TDP-43 (hTDP-43 ΔNLS-5FL) which results in the formation of cytoplasmic TDP-43 aggregates and when full length hTDP43 is overexpressed. We also show that there is a significant difference in the motility of microglial processes for mice upon the neuronal expression of RNA binding deficient mutation TDP-43. Furthermore, we also investigated the effect of the different forms of neuronal TDP-43 pathology on the motor skills of mice.

We investigated the microglia morphological changes using confocal imaging of brain sections. These brain sections were taken from mice injected with AAV-hTDP-43, AAV-hTDP-43 ΔNLS and AAV-hTDP-43 ΔNLS-5FL and they were perfused 4 weeks and 8 weeks post-injection. This gave us several interesting findings. To summarise our results briefly, upon 4 weeks of injection, we found clear morphological changes demonstrating the activation of microglia in response to neuronal TDP-43. As such I found that the sphericity of microglia for mice injected with AAV-hTDP-43 and AAV-hTDP-43 ΔNLS-5FL was significantly higher compared to mice injected with

AAV-mCherry and AAV-hTDP-43 ΔNLS mice, but it was not altered in mice injected with AAV-hTDP-43 ΔNLS mice compared to AAV-mCherry. Upon 8 weeks of expression, the sphericity of microglia was significantly higher for mice injected with AAV-hTDP-43 ΔNLS-5FL compared to mice injected with AAV-mCherry and AAV-hTDP-43 ΔNLS mice. For mice injected with hTDP-43, the sphericity is significantly higher compared to hTDP-43 ΔNLS mice but it's not significantly higher compared to mCherry control injected mice. Furthermore, the length of processes is significantly less for AAV-hTDP-43 and AAV-hTDP-43 ΔNLS-5FL compared to mice injected with AAV-mCherry and AAV-hTDP-43 ΔNLS mice for both timepoints. The length of processes is significantly less for hTDP-43 ΔNLS compared to mCherry for 4 weeks timepoint and high for 8 weeks timepoint. Another important finding from morphological study of microglia are the changes in number of segments per branch i.e. the ramifications of individual microglial processes are significantly reduced for hTDP-43 and hTDP-43 ΔNLS-5FL compared to mice injected with mCherry and hTDP-43 ΔNLS mice. For 8 weeks timepoint, it is significantly less for hTDP-43 compared to mCherry control mice. For hTDP-43 ΔNLS injected mice, there is no significant difference with mCherry control for 4 weeks timepoint and it has higher processes compared to mCherry control for 8 weeks timepoint.

The amoeboid (activated) microglia has small and thicker cell body, thus resulting in higher sphericity and it also has retracted processes (Doorn et al., 2014). During resting state, microglial morphology consists of very fine and highly ramified processes (Tremblay et al., 2011, Nimmerjahn et al., 2012). During active state, the amoeboid cell has fewer processes (Damani et al., 2011, Lee et al., 2008). Upon activation, there is rapid morphological change in microglia characterized by retraction of numerous fine and ramified process and gradual conversion of cell body into a small, thicker amoeboid-like cell body (Anttila et al., 2016). Microglia in the ischemic brain are particularly known for their morphological variety; various morphologies were discovered at various distances from the ischemic lesion, demonstrating that microglia close to the lesion are amoeboid, whereas microglia in the contralateral hemisphere distant from the lesion retain the highly ramified shape (Fumagalli et al., 2013; Butovsky et al., 2014; Anttila et al., 2016; Krasemann et al., 2017). This change in microglia morphology has also been observed in several neurodegenerative disorders. For instance, in mice carrying the human amyloid precursor protein gene mutation

CRND8, microglia close to A plaques were less ramified than microglia further away from A plaques, as well as compared to microglia from mice carrying the wild-type gene (Plescher et al. 2018). Evidence from two human studies with 7 and 8 AD individuals each suggests that the microglia in AD undergo morphological alterations (Paasila et al. 2019, Davies et al. 2017). A microglia morphology assessment study conducted in a larger cohort of AD cases also showed that reactive/amoeboid microglia are the most prevalent population in the ageing human brain (Franco – Bocanegra et al. 2021). Thus, taking this into account, based on our microglial morphology analysis we can conclude that microglia in AAV-hTDP-43 ΔNLS-5FL and AAV-hTDP43 injected mice shows more activated microglia like features in terms of increased sphericity and decreased length of processes and branching. However, the mice injected with hTDP-43 ΔNLS doesn't show these features of activated microglia.

Using 2-photon *in vivo* imaging we also looked at the effect on microglial process motility upon injecting AAV-mCherry and AAV-hTDP-43 ΔNLS-5FL in primary motor cortex of mice. The stable process area of microglial processes was significantly higher for microglia in the mice injected with mCherry compared to AAV-hTDP-43 ΔNLS-5FL. Both, the microglial area lost and gained was higher for microglia in the mice injected with AAV-hTDP-43 ΔNLS-5FL compared to mCherry. This suggests that the microglial processes for mice injected with AAV-hTDP-43 ΔNLS-5FL are more motile compared to microglial processes for mice injected with mCherry.

Several studies suggests that microglial motility changes during neurodegenerative disorders and aging conditions and during systemic inflammation (Bolmont et al., 2008, Gyoneva et al., 2014, Hefendehl et al., 2014). There are studies which assess the microglia motility under isofluorane anesthesia. It has been seen that there is decreased microglia motility in this case both in acute slice preparations and in vivo (Nebeling et al., 2023, Madry et al., 2018). Recent studies also point towards the positive correlation between microglia motility and neuronal active in cortex in vivo (Hristovska et al., 2022). Thus, based on this we can conclude that the difference in microglial process motility between mice injected with AAV-hTDP-43 ΔNLS-5FL and AAV-mCherry point towards the difference in neuronal activity in both of these conditions.

Based on the above results, we can conclude that microglia respond to AAV-hTDP-43 ΔNLS-5FL like activated microglia by morphologically transforming into a less ramified cell and by becoming more motile. This TDP-43 construct has mutations in the RRM, thus resulting in the formation of cytoplasmic aggregates of TDP-43. This suggests that RRM of TDP-43 can play an important role in aberrant self-assembly of the protein. Several studies have shown that the C-terminal domain (CTD) is the aggregation prone-domain and it contains the majority of ALS-related mutations, thus the accumulation of the C-terminal fragments (CTF) are the primary hallmark of ALS (Jiang et al., 2017, Lee et al., 2014, Afroz et al., 2017, Wang et al., 2013, Tavella et al., 2018, Prasad et al., 2019). The RRM2 fragment in the CTFs is crucial for this type of aggregation, since it has been noted that while the CTD is necessary for cytoplasmic aggregation and toxicity, it is insufficient because an intact RRM is also required (Johnson et al., 2008). Due to a cluster of twelve interconnected hydrophobic residues in its core, RRM2 is a very stable domain under physiological conditions (Tavella et al., 2008). In the presence of a cleavage, the RRM2 is prevented from interacting with RRM1 to stabilize it. It has been shown that these mutually stabilizing interactions between RRM1 and RRM2 decreases the number of intermediate RRM2, which are associated with pathological misfolding (Mackness et al., 2014). This state of RRM2 may facilitate access to the NES within its sequence, thus increasing transport to the cytoplasm and acting as molecular hazard as a result of linking pathological aggregation and misfolding with physiological folding (Grassman et al., 2021).

Another effect of RRM cleavage is that, the RRM2 cleavage's aggregation-prone -strands are exposed to the solvent (Wang et al 2013, Kumar et al., 2019). Although generally hidden in the native state, it has been discovered that these strands can form fibrils in vitro, thus validating the function of the RRM2 fragment in the aggregation-related CTFs (Kumar et al., 2019). The β-strands in particular may be at the center of the aggregation as they can create steric zippers, which follow a common atomic model for the creation of amyloid fibril structures (Lee et al., 2014). Packed β -sheets that interact with one another through side chains make up amyloid fibrils. The so-called steric zipper is created when side chains from adjacent sheets that are projected nearly perpendicular to the fibril axis interdigitate (Lee et al., 2014). It has been proposed that, specifically, the β3 and β5 strands create the steric zippers that give rise to the aggregation of CTFs (Lee et al., 2014). Some studies have also shown

that the specific areas of RRM2 can form various types of steric zipper structures (Prasad et al., 2019, Guenther et al., 2018) at the core of the creation of these amyloid fibrils (Nelson et al., 2006), supporting the notion that this type of structure is at the base of the CTFs aggregation. Thus, this proves that the RRM has an important role in TDP-43 aggregation as found in ALS and FTD. Our results shows that the activated state of microglial response towards cytoplasmic TDP43 with RRM mutation provides evidence for the above *in vivo* and *in vitro*.

Our results also suggests that overexpression of wild-type human TDP-43 is toxic to neurons thus explaining the activated microglia cell type. During pathological conditions, there is an increase in overall TDP-43 levels in these cells (Bilican et al., 2012, Kasai et al., 2009, Ling et al., 2010, Neumann et al., 2006). The adverse effects of abnormally high TDP-43 levels include reduced RNA synthesis, which is crucial for neuronal development and synaptic function (Polymenidou et al., 2011, Arnold et al., 2013). Several studies have also shown that the overexpression of wild-type TDP-43 can also result in ALS- or FTLD-TDP-like pathogenesis in transgenic mice (Arnold et al., 2013, D'Alton et al., 2014, Igaz et al., 2011, Wu et al., 2012). Thus, our results showing a activated microglial response in mice overexpressing full length human TDP-43 in neurons supports this hypothesis.

Our microglia morphology analysis also suggests that microglia in mice expressing AAV-hTDP-43 ΔNLS are less activated compared to hTDP-43 and hTDP-43 ΔNLS-5FL expressing mice for both the 4 weeks and 8 weeks timepoint. Compared to mCherry controls, there is either no difference or microglia are more activated for the 4 weeks timepoint and less activated at the 8 weeks timepoint compared to mCherry expressing controls. hTDP-43 ΔNLS lacks the NLS sequence thus resulting in cytoplasmic mislocalization of TDP-43. Several studies have shown that TDP-43 mislocalizes and aggregates within the cytoplasm when the nuclear localization signal (NLS) sequence in the N-terminal domain (NTD) is deleted or altered (Winton et al., 2008a, Barmada et al., 2010). A recent study also reveal that a dynamic solenoid-like structure that spatially isolates the aggregation-prone C-terminal region of the TDP-43 NTD and likely lessens pathogenic aggregation was found in the structure of the 1-80 residues of the TDP-43 NTD at 2.1 resolution (Winton et al., 2008b). Thus, our results show that

although mutation in NTD results in cytoplasmic TDP-43 but unlike mutations in CTD and overexpression of TDP-43, it's seems less detrimental to neuronal health.

It was also observed that at the 8 weeks timepoint, the microglia in mCherry injected mice become more activated compared to hTDP-43 ΔNLS based on microglia morphology analysis of length of processes and ramifications. It was also observed that there is no significant difference in the sphericity of microglia at 8 weeks timepoint between mice injected with hTDP-43 and mCherry. This suggests that mCherry aggregates might become slightly toxic over time. This has been shown in some other studies as well (Ning et al., 2022).

Although these results point towards the neurotoxicity of hTDP-43 and hTDP-43 ΔNLS 5FL construct, it will be useful to look at other microglia features like migration as well to get a more conclusive picture. Apart from this, in this study we did not quantify the neuronal death. This is one of the caveats of our present study and quantifying this can also give us a more conclusive picture on toxicity of these constructs. Another caveat of this study can be the low sample size for microglia motility. This is still a very limited dataset to draw conclusions.

The effect of AAV-mCherry, AAV-hTDP-43, AAV-hTDP-43 ΔNLS and AAV-hTDP-43 ΔNLS-5FL on the motor skills of the mice was also assessed as the TDP-43 pathology is one of the main aggregates found in ALS patients, which has effect on motor skills. Cylinder test was used to find the effect of these different injections on motor skills for one hemisphere (right hemisphere) injection. Since the injections were in the right hemisphere, the frequency of using left paw first for rearing was calculated. No significant difference was found for using left paw first for the mice injected with AAV-mCherry and AAV-hTDP-43 ΔNLS-5FL. Since a total of 4 injections, each with 300 ul of virus vectors was done on motor cortex, the result seems plausible. These four injections might have lead to TDP-43 pathology in local area near the injection site instead of in the entirety of motor cortex, thus leading to unimpaired motor skills.

Another behaviour test that was used to assess the effect of neuronal mCherry, hTDP-43 and hTDP-43 ΔNLS expression on motor skills was pole test. In this case, the mice received injections on both hemisphere. The time taken to turn and to climb

down the pole was assessed. There was significant difference observed for the total time taken to climb down pole for hTDP-43 injected mice compared to hTDP-43 ΔNLS injected mice. This suggests that hTDP-43 has toxic effects on mouse motor cortex which in turn affects the motor skills of mice. In other experiments, we have observed a rapid neuronal loss in primary motor cortex when injected with hTDP-43, thus this is plausible. From this, we can conclude that nuclear overexpression of TDP-43 is highly toxic and it also leads to motor skill impairment. However, it is important to note that these results come from 4 mice injected with hTDP-43 and 3 mice injected with hTDP-43 ΔNLS. So, further tests with higher sample size are required to conclusively prove the effect of overexpression of TDP-43 on impairment of motor skills.

To summarise the results obtained from this study, we found that mutations in RRM of CTD are very toxic to neuronal health and overexpression of TDP-43 is also toxic to neuronal health. Thus, this shows that RRM has important role in TDP-43 aggregation as found in ALS and FTD. Although, mutations in the NLS results in cytoplasmic TDP-43, they are not as toxic to neuronal health. This suggests that in the future, it will be also interesting to look at the 2 weeks timepoint for microglia morphology for all the four virus vectors. This will help us compare what is happening to microglia and these aberrant TDP-43 expressed by these viral vectors over time. It will be also interesting to look at the migration of microglia in the brain of mice injected with these different viral constructs. Overall, these results provide us insights into the impact of various pathological forms of TDP43 found in ALS and various neurodegenerative disorder through the microglial response to them.

References

1. Afroz, T., Hock, E. M., Ernst, P., Foglieni, C., Jambeau, M., Gilhespy, L. A. B., Laferriere, F., Maniecka, Z., Plückthun, A., Mittl, P., Paganetti, P., Allain, F. H. T., & Polymenidou, M. (2017). Functional and dynamic polymerization of the ALS-linked protein TDP-43 antagonizes its pathologic aggregation. *Nature communications*, *8*(1), 45. https://doi.org/10.1038/s41467-017-00062-0
2. Ajroud-Driss, S., & Siddique, T. (2015). Sporadic and hereditary amyotrophic lateral sclerosis (ALS). *Biochimica et biophysica acta*, *1852*(4), 679–684. https://doi.org/10.1016/j.bbadis.2014.08.010
3. Alami, N. H., Smith, R. B., Carrasco, M. A., Williams, L. A., Winborn, C. S., Han, S. S. W., Kiskinis, E., Winborn, B., Freibaum, B. D., Kanagaraj, A., Clare, A. J., Badders, N. M., Bilican, B., Chaum, E., Chandran, S., Shaw, C. E., Eggan, K. C., Maniatis, T., & Taylor, J. P. (2014). Axonal transport of TDP-43 mRNA granules is impaired by ALS-causing mutations. *Neuron*, *81*(3), 536–543. https://doi.org/10.1016/j.neuron.2013.12.018
4. Alsultan, A. A., Waller, R., Heath, P. R., & Kirby, J. (2016). The genetics of amyotrophic lateral sclerosis: current insights. *Degenerative neurological and neuromuscular disease*, *6*, 49–64. https://doi.org/10.2147/DNND.S84956
5. Andersen P. M. (2006). Amyotrophic lateral sclerosis associated with mutations in the CuZn superoxide dismutase gene. *Current neurology and neuroscience reports*, *6*(1), 37–46. https://doi.org/10.1007/s11910-996-0008-9
6. Anttila, J. E., Whitaker, K. W., Wires, E. S., Harvey, B. K., & Airavaara, M. (2017). Role of microglia in ischemic focal stroke and recovery: focus on Toll-like receptors. *Progress in neuro-psychopharmacology & biological psychiatry*, *79*(Pt A), 3–14. https://doi.org/10.1016/j.pnpbp.2016.07.003
7. Arai, T., Hasegawa, M., Akiyama, H., Ikeda, K., Nonaka, T., Mori, H., Mann, D., Tsuchiya, K., Yoshida, M., Hashizume, Y., & Oda, T. (2006). TDP-43 is a component of ubiquitin-positive tau-negative inclusions in frontotemporal lobar degeneration and amyotrophic lateral sclerosis. *Biochemical and biophysical research communications*, *351*(3), 602–611. https://doi.org/10.1016/j.bbrc.2006.10.093
8. Arnold, E. S., Ling, S. C., Huelga, S. C., Lagier-Tourenne, C., Polymenidou, M., Ditsworth, D., Kordasiewicz, H. B., McAlonis-Downes, M., Platoshyn, O.,

Parone, P. A., Da Cruz, S., Clutario, K. M., Swing, D., Tessarollo, L., Marsala, M., Shaw, C. E., Yeo, G. W., & Cleveland, D. W. (2013). ALS-linked TDP-43 mutations produce aberrant RNA splicing and adult-onset motor neuron disease without aggregation or loss of nuclear TDP-43. *Proceedings of the National Academy of Sciences of the United States of America*, *110*(8), E736–E745. https://doi.org/10.1073/pnas.1222809110

9. Arthur, K. C., Calvo, A., Price, T. R., Geiger, J. T., Chiò, A., & Traynor, B. J. (2016). Projected increase in amyotrophic lateral sclerosis from 2015 to 2040. *Nature communications*, *7*, 12408. https://doi.org/10.1038/ncomms12408
10. Aulas, Anaïs et al., “G3BP1 promotes stress-induced RNA granule interactions to preserve polyadenylated mRNA.” *The Journal of cell biology* vol. 209,1 (2015): 73-84. doi:10.1083/jcb.201408092
11. Ayala, Y. M., De Conti, L., Avendaño-Vázquez, S. E., Dhir, A., Romano, M., D'Ambrogio, A., Tollervey, J., Ule, J., Baralle, M., Buratti, E., & Baralle, F. E. (2011). TDP-43 regulates its mRNA levels through a negative feedback loop. *The EMBO journal*, *30*(2), 277–288. https://doi.org/10.1038/emboj.2010.310
12. Badimon, A., Strasburger, H. J., Ayata, P., Chen, X., Nair, A., Ikegami, A., Hwang, P., Chan, A. T., Graves, S. M., Uweru, J. O., Ledderose, C., Kutlu, M. G., Wheeler, M. A., Kahan, A., Ishikawa, M., Wang, Y. C., Loh, Y. E., Jiang, J. X., Surmeier, D. J., Robson, S. C., … Schaefer, A. (2020). Negative feedback control of neuronal activity by microglia. *Nature*, *586*(7829), 417–423. https://doi.org/10.1038/s41586-020-2777-8
13. Barmada, S. J., Serio, A., Arjun, A., Bilican, B., Daub, A., Ando, D. M., Tsvetkov, A., Pleiss, M., Li, X., Peisach, D., Shaw, C., Chandran, S., & Finkbeiner, S. (2014). Autophagy induction enhances TDP43 turnover and survival in neuronal ALS models. *Nature chemical biology*, *10*(8), 677–685. https://doi.org/10.1038/nchembio.1563
14. Barmada, S. J., Serio, A., Arjun, A., Bilican, B., Daub, A., Ando, D. M., Tsvetkov, A., Pleiss, M., Li, X., Peisach, D., Shaw, C., Chandran, S., & Finkbeiner, S. (2014). Autophagy induction enhances TDP43 turnover and survival in neuronal ALS models. *Nature chemical biology*, *10*(8), 677–685. https://doi.org/10.1038/nchembio.1563

15. Barmada, S. J., Skibinski, G., Korb, E., Rao, E. J., Wu, J. Y., & Finkbeiner, S. (2010). Cytoplasmic mislocalization of TDP-43 is toxic to neurons and enhanced by a mutation associated with familial amyotrophic lateral sclerosis. *The Journal of neuroscience : the official journal of the Society for Neuroscience*, *30*(2), 639–649. https://doi.org/10.1523/JNEUROSCI.4988-09.2010
16. Barmada, S. J., Skibinski, G., Korb, E., Rao, E. J., Wu, J. Y., & Finkbeiner, S. (2010). Cytoplasmic mislocalization of TDP-43 is toxic to neurons and enhanced by a mutation associated with familial amyotrophic lateral sclerosis. *The Journal of neuroscience : the official journal of the Society for Neuroscience*, *30*(2), 639–649. https://doi.org/10.1523/JNEUROSCI.4988-09.2010
17. Bilican, B., Serio, A., Barmada, S. J., Nishimura, A. L., Sullivan, G. J., Carrasco, M., Phatnani, H. P., Puddifoot, C. A., Story, D., Fletcher, J., Park, I. H., Friedman, B. A., Daley, G. Q., Wyllie, D. J., Hardingham, G. E., Wilmut, I., Finkbeiner, S., Maniatis, T., Shaw, C. E., & Chandran, S. (2012). Mutant induced pluripotent stem cell lines recapitulate aspects of TDP-43 proteinopathies and reveal cell-specific vulnerability. *Proceedings of the National Academy of Sciences of the United States of America*, *109*(15), 5803–5808. https://doi.org/10.1073/pnas.1202922109
18. Boillée, S., Yamanaka, K., Lobsiger, C. S., Copeland, N. G., Jenkins, N. A., Kassiotis, G., Kollias, G., & Cleveland, D. W. (2006). Onset and progression in inherited ALS determined by motor neurons and microglia. *Science (New York, N.Y.)*, *312*(5778), 1389–1392. https://doi.org/10.1126/science.1123511
19. Bolmont, T., Haiss, F., Eicke, D., Radde, R., Mathis, C. A., Klunk, W. E., Kohsaka, S., Jucker, M., & Calhoun, M. E. (2008). Dynamics of the microglial/amyloid interaction indicate a role in plaque maintenance. *The Journal of neuroscience : the official journal of the Society for Neuroscience*, *28*(16), 4283–4292. https://doi.org/10.1523/JNEUROSCI.4814-07.2008
20. Braak, H., Brettschneider, J., Ludolph, A. C., Lee, V. M., Trojanowski, J. Q., & Del Tredici, K. (2013). Amyotrophic lateral sclerosis--a model of corticofugal axonal spread. *Nature reviews. Neurology*, *9*(12), 708–714. https://doi.org/10.1038/nrneurol.2013.221
21. Brettschneider, J., Del Tredici, K., Toledo, J. B., Robinson, J. L., Irwin, D. J., Grossman, M., Suh, E., Van Deerlin, V. M., Wood, E. M., Baek, Y., Kwong, L., Lee, E. B., Elman, L., McCluskey, L., Fang, L., Feldengut, S., Ludolph, A. C.,

Lee, V. M., Braak, H., & Trojanowski, J. Q. (2013). Stages of pTDP-43 pathology in amyotrophic lateral sclerosis. *Annals of neurology*, *74*(1), 20–38. https://doi.org/10.1002/ana.23937

22. Brooks, B. R., Berry, J. D., Ciepielewska, M., Liu, Y., Zambrano, G. S., Zhang, J., & Hagan, M. (2022). Intravenous edaravone treatment in ALS and survival: An exploratory, retrospective, administrative claims analysis. *EClinicalMedicine*, *52*, 101590. https://doi.org/10.1016/j.eclinm.2022.101590
23. Buratti, E., & Baralle, F. E. (2001). Characterization and functional implications of the RNA binding properties of nuclear factor TDP-43, a novel splicing regulator of CFTR exon 9. *The Journal of biological chemistry*, *276*(39), 36337–36343. https://doi.org/10.1074/jbc.M104236200
24. Buratti, E., Brindisi, A., Giombi, M., Tisminetzky, S., Ayala, Y. M., & Baralle, F. E. (2005). TDP-43 binds heterogeneous nuclear ribonucleoprotein A/B through its C-terminal tail: an important region for the inhibition of cystic fibrosis transmembrane conductance regulator exon 9 splicing. *The Journal of biological chemistry*, *280*(45), 37572–37584. https://doi.org/10.1074/jbc.M505557200
25. Butovsky, O., Jedrychowski, M. P., Moore, C. S., Cialic, R., Lanser, A. J., Gabriely, G., Koeglsperger, T., Dake, B., Wu, P. M., Doykan, C. E., Fanek, Z., Liu, L., Chen, Z., Rothstein, J. D., Ransohoff, R. M., Gygi, S. P., Antel, J. P., & Weiner, H. L. (2014). Identification of a unique TGF-β-dependent molecular and functional signature in microglia. *Nature neuroscience*, *17*(1), 131–143. https://doi.org/10.1038/nn.3599
26. Cairns, N. J., Bigio, E. H., Mackenzie, I. R., Neumann, M., Lee, V. M., Hatanpaa, K. J., White, C. L., 3rd, Schneider, J. A., Grinberg, L. T., Halliday, G., Duyckaerts, C., Lowe, J. S., Holm, I. E., Tolnay, M., Okamoto, K., Yokoo, H., Murayama, S., Woulfe, J., Munoz, D. G., Dickson, D. W., … Consortium for Frontotemporal Lobar Degeneration (2007). Neuropathologic diagnostic and nosologic criteria for frontotemporal lobar degeneration: consensus of the Consortium for Frontotemporal Lobar Degeneration. *Acta neuropathologica*, *114*(1), 5–22. https://doi.org/10.1007/s00401-007-0237-2
27. Carbonell, W. S., Murase, S., Horwitz, A. F., & Mandell, J. W. (2005). Migration of perilesional microglia after focal brain injury and modulation by CC chemokine receptor 5: an in situ time-lapse confocal imaging study. *The Journal of*

neuroscience : the official journal of the Society for Neuroscience, *25*(30), 7040–7047. https://doi.org/10.1523/JNEUROSCI.5171-04.2005

28. Cervenakova, L., Protas, I. I., Hirano, A., Votiakov, V. I., Nedzved, M. K., Kolomiets, N. D., Taller, I., Park, K. Y., Sambuughin, N., Gajdusek, D. C., Brown, P., & Goldfarb, L. G. (2000). Progressive muscular atrophy variant of familial amyotrophic lateral sclerosis (PMA/ALS). *Journal of the neurological sciences*, *177*(2), 124–130. https://doi.org/10.1016/s0022-510x(00)00350-6
29. Chang, C. K., Wu, T. H., Wu, C. Y., Chiang, M. H., Toh, E. K., Hsu, Y. C., Lin, K. F., Liao, Y. H., Huang, T. H., & Huang, J. J. (2012). The N-terminus of TDP-43 promotes its oligomerization and enhances DNA binding affinity. *Biochemical and biophysical research communications*, *425*(2), 219–224. https://doi.org/10.1016/j.bbrc.2012.07.071
30. Chiò, A., Logroscino, G., Hardiman, O., Swingler, R., Mitchell, D., Beghi, E., Traynor, B. G., & Eurals Consortium (2009). Prognostic factors in ALS: A critical review. *Amyotrophic lateral sclerosis : official publication of the World Federation of Neurology Research Group on Motor Neuron Diseases*, *10*(5-6), 310–323. https://doi.org/10.3109/17482960802566824
31. Chou, C. C., Zhang, Y., umoh, M. E., Vaughan, S. W., Lorenzini, I., Liu, F., Sayegh, M., Donlin-Asp, P. G., Chen, Y. H., Duong, D. M., Seyfried, N. T., Powers, M. A., Kukar, T., Hales, C. M., Gearing, M., Cairns, N. J., Boylan, K. B., Dickson, D. W., Rademakers, R., Zhang, Y. J., … Rossoll, W. (2018). TDP-43 pathology disrupts nuclear pore complexes and nucleocytoplasmic transport in ALS/FTD. *Nature neuroscience*, *21*(2), 228–239. https://doi.org/10.1038/s41593-017-0047-3
32. Colombrita, C., Zennaro, E., Fallini, C., Weber, M., Sommacal, A., Buratti, E., Silani, V., & Ratti, A. (2009). TDP-43 is recruited to stress granules in conditions of oxidative insult. *Journal of neurochemistry*, *111*(4), 1051–1061. https://doi.org/10.1111/j.1471-4159.2009.06383.x
33. Colonna, M., & Butovsky, O. (2017). Microglia Function in the Central Nervous System During Health and Neurodegeneration. *Annual review of immunology*, *35*, 441–468. https://doi.org/10.1146/annurev-immunol-051116-052358

34. Cronin, S., Hardiman, O., & Traynor, B. J. (2007). Ethnic variation in the incidence of ALS: a systematic review. *Neurology*, *68*(13), 1002–1007. https://doi.org/10.1212/01.wnl.0000258551.96893.6f
35. D'Alton, S., Altshuler, M., Cannon, A., Dickson, D. W., Petrucelli, L., & Lewis, J. (2014). Divergent phenotypes in mutant TDP-43 transgenic mice highlight potential confounds in TDP-43 transgenic modeling. *PloS one*, *9*(1), e86513. https://doi.org/10.1371/journal.pone.0086513
36. Davalos, D., Grutzendler, J., Yang, G., Kim, J. V., Zuo, Y., Jung, S., Littman, D. R., Dustin, M. L., & Gan, W. B. (2005). ATP mediates rapid microglial response to local brain injury in vivo. *Nature neuroscience*, *8*(6), 752–758. https://doi.org/10.1038/nn1472
37. Davies, D. S., Ma, J., Jegathees, T., & Goldsbury, C. (2017). Microglia show altered morphology and reduced arborization in human brain during aging and Alzheimer's disease. *Brain pathology (Zurich, Switzerland)*, *27*(6), 795–808. https://doi.org/10.1111/bpa.12456
38. de Boer, E. M. J., Orie, V. K., Williams, T., Baker, M. R., De Oliveira, H. M., Polvikoski, T., Silsby, M., Menon, P., van den Bos, M., Halliday, G. M., van den Berg, L. H., Van Den Bosch, L., van Damme, P., Kiernan, M. C., van Es, M. A., & Vucic, S. (2020). TDP-43 proteinopathies: a new wave of neurodegenerative diseases. *Journal of neurology, neurosurgery, and psychiatry*, *92*(1), 86–95. Advance online publication. https://doi.org/10.1136/jnnp-2020-322983
39. DeJesus-Hernandez, M., Mackenzie, I. R., Boeve, B. F., Boxer, A. L., Baker, M., Rutherford, N. J., Nicholson, A. M., Finch, N. A., Flynn, H., Adamson, J., Kouri, N., Wojtas, A., Sengdy, P., Hsiung, G. Y., Karydas, A., Seeley, W. W., Josephs, K. A., Coppola, G., Geschwind, D. H., Wszolek, Z. K., … Rademakers, R. (2011). Expanded GGGGCC hexanucleotide repeat in noncoding region of C9ORF72 causes chromosome 9p-linked FTD and ALS. *Neuron*, *72*(2), 245–256. https://doi.org/10.1016/j.neuron.2011.09.011
40. Deng, H., Gao, K., & Jankovic, J. (2014). The role of FUS gene variants in neurodegenerative diseases. *Nature reviews. Neurology*, *10*(6), 337–348. https://doi.org/10.1038/nrneurol.2014.78
41. Dewey, C. M., Cenik, B., Sephton, C. F., Dries, D. R., Mayer, P., 3rd, Good, S. K., Johnson, B. A., Herz, J., & Yu, G. (2011). TDP-43 is directed to stress granules by sorbitol, a novel physiological osmotic and oxidative

stressor. *Molecular and cellular biology*, *31*(5), 1098–1108. https://doi.org/10.1128/MCB.01279-10

42. Diaper, D. C., Adachi, Y., Sutcliffe, B., Humphrey, D. M., Elliott, C. J., Stepto, A., Ludlow, Z. N., Vanden Broeck, L., Callaerts, P., Dermaut, B., Al-Chalabi, A., Shaw, C. E., Robinson, I. M., & Hirth, F. (2013). Loss and gain of Drosophila TDP-43 impair synaptic efficacy and motor control leading to age-related neurodegeneration by loss-of-function phenotypes. *Human molecular genetics*, *22*(8), 1539–1557. https://doi.org/10.1093/hmg/ddt005
43. Dols-Icardo, O., Montal, V., Sirisi, S., López-Pernas, G., Cervera-Carles, L., Querol-Vilaseca, M., Muñoz, L., Belbin, O., Alcolea, D., Molina-Porcel, L., Pegueroles, J., Turón-Sans, J., Blesa, R., Lleó, A., Fortea, J., Rojas-García, R., & Clarimón, J. (2020). Motor cortex transcriptome reveals microglial key events in amyotrophic lateral sclerosis. *Neurology(R) neuroimmunology & neuroinflammation*, *7*(5), e829. https://doi.org/10.1212/NXI.0000000000000829
44. Doorn, K. J., Goudriaan, A., Blits-Huizinga, C., Bol, J. G., Rozemuller, A. J., Hoogland, P. V., Lucassen, P. J., Drukarch, B., van de Berg, W. D., & van Dam, A. M. (2014). Increased amoeboid microglial density in the olfactory bulb of Parkinson's and Alzheimer's patients. *Brain pathology (Zurich, Switzerland)*, *24*(2), 152–165. https://doi.org/10.1111/bpa.12088
45. Fellner, L., Irschick, R., Schanda, K., Reindl, M., Klimaschewski, L., Poewe, W., Wenning, G. K., & Stefanova, N. (2013). Toll-like receptor 4 is required for α-synuclein dependent activation of microglia and astroglia. *Glia*, *61*(3), 349–360. https://doi.org/10.1002/glia.22437
46. Franco-Bocanegra, D. K., George, B., Lau, L. C., Holmes, C., Nicoll, J. A. R., & Boche, D. (2019). Microglial motility in Alzheimer's disease and after Aβ42 immunotherapy: a human post-mortem study. *Acta neuropathologica communications*, *7*(1), 174. https://doi.org/10.1186/s40478-019-0828-x
47. Franco-Bocanegra, D. K., Gourari, Y., McAuley, C., Chatelet, D. S., Johnston, D. A., Nicoll, J. A. R., & Boche, D. (2021). Microglial morphology in Alzheimer's disease and after Aβ immunotherapy. *Scientific reports*, *11*(1), 15955. https://doi.org/10.1038/s41598-021-95535-0
48. Fu, H., Hardy, J., & Duff, K. E. (2018). Selective vulnerability in neurodegenerative diseases. *Nature neuroscience*, *21*(10), 1350–1358. https://doi.org/10.1038/s41593-018-0221-

49. Fumagalli, S., Perego, C., Ortolano, F., & De Simoni, M. G. (2013). CX3CR1 deficiency induces an early protective inflammatory environment in ischemic mice. *Glia*, *61*(6), 827–842. https://doi.org/10.1002/glia.22474
50. Gasset-Rosa, F., Lu, S., Yu, H., Chen, C., Melamed, Z., Guo, L., Shorter, J., Da Cruz, S., & Cleveland, D. W. (2019). Cytoplasmic TDP-43 De-mixing Independent of Stress Granules Drives Inhibition of Nuclear Import, Loss of Nuclear TDP-43, and Cell Death. *Neuron*, *102*(2), 339–357.e7. https://doi.org/10.1016/j.neuron.2019.02.038
51. Gerrits, E., Brouwer, N., Kooistra, S. M., Woodbury, M. E., Vermeiren, Y., Lambourne, M., Mulder, J., Kummer, M., Möller, T., Biber, K., Dunnen, W. F. A. D., De Deyn, P. P., Eggen, B. J. L., & Boddeke, E. W. G. M. (2021). Distinct amyloid-β and tau-associated microglia profiles in Alzheimer's disease. *Acta neuropathologica*, *141*(5), 681–696. https://doi.org/10.1007/s00401-021-02263-w
52. Geser, F., Martinez-Lage, M., Robinson, J., Uryu, K., Neumann, M., Brandmeir, N. J., Xie, S. X., Kwong, L. K., Elman, L., McCluskey, L., Clark, C. M., Malunda, J., Miller, B. L., Zimmerman, E. A., Qian, J., Van Deerlin, V., Grossman, M., Lee, V. M., & Trojanowski, J. Q. (2009). Clinical and pathological continuum of multisystem TDP-43 proteinopathies. *Archives of neurology*, *66*(2), 180–189. https://doi.org/10.1001/archneurol.2008.558
53. Ghasemi, M., & Brown, R. H., Jr (2018). Genetics of Amyotrophic Lateral Sclerosis. *Cold Spring Harbor perspectives in medicine*, *8*(5), a024125. https://doi.org/10.1101/cshperspect.a024125
54. Grassmann, G., Miotto, M., Di Rienzo, L., Salaris, F., Silvestri, B., Zacco, E., Rosa, A., Tartaglia, G. G., Ruocco, G., & Milanetti, E. (2021). A Computational Approach to Investigate TDP-43 RNA-Recognition Motif 2 C-Terminal Fragments Aggregation in Amyotrophic Lateral Sclerosis. *Biomolecules*, *11*(12), 1905. https://doi.org/10.3390/biom11121905
55. Guerreiro, R., Wojtas, A., Bras, J., Carrasquillo, M., Rogaeva, E., Majounie, E., Cruchaga, C., Sassi, C., Kauwe, J. S., Younkin, S., Hazrati, L., Collinge, J., Pocock, J., Lashley, T., Williams, J., Lambert, J. C., Amouyel, P., Goate, A., Rademakers, R., Morgan, K., … Alzheimer Genetic Analysis Group (2013). TREM2 variants in Alzheimer's disease. *The New England journal of medicine*, *368*(2), 117–127. https://doi.org/10.1056/NEJMoa1211851

56. Guo, W., Chen, Y., Zhou, X., Kar, A., Ray, P., Chen, X., Rao, E. J., Yang, M., Ye, H., Zhu, L., Liu, J., Xu, M., Yang, Y., Wang, C., Zhang, D., Bigio, E. H., Mesulam, M., Shen, Y., Xu, Q., Fushimi, K., … Wu, J. Y. (2011). An ALS-associated mutation affecting TDP-43 enhances protein aggregation, fibril formation and neurotoxicity. *Nature structural & molecular biology*, *18*(7), 822–830. https://doi.org/10.1038/nsmb.2053
57. Gyoneva, S., Davalos, D., Biswas, D., Swanger, S. A., Garnier-Amblard, E., Loth, F., Akassoglou, K., & Traynelis, S. F. (2014). Systemic inflammation regulates microglial responses to tissue damage in vivo. *Glia*, *62*(8), 1345–1360. https://doi.org/10.1002/glia.22686
58. Hampel, H., Mesulam, M. M., Cuello, A. C., Khachaturian, A. S., Vergallo, A., Farlow, M. R., Snyder, P. J., Giacobini, E., & Khachaturian, Z. S. (2019). Revisiting the Cholinergic Hypothesis in Alzheimer's Disease: Emerging Evidence from Translational and Clinical Research. *The journal of prevention of Alzheimer's disease*, *6*(1), 2–15. https://doi.org/10.14283/jpad.2018.43
59. Hardiman, O., & van den Berg, L. H. (2017). Edaravone: a new treatment for ALS on the horizon?. *The Lancet. Neurology*, *16*(7), 490–491. https://doi.org/10.1016/S1474-4422(17)30163-1
60. Hardiman, O., Al-Chalabi, A., Chio, A., Corr, E. M., Logroscino, G., Robberecht, W., Shaw, P. J., Simmons, Z., & van den Berg, L. H. (2017). Amyotrophic lateral sclerosis. *Nature reviews. Disease primers*, *3*, 17071. https://doi.org/10.1038/nrdp.2017.71
61. Hartley, A., Davies, M., & Rice-Evans, C. (1990). Desferrioxamine as a lipid chain-breaking antioxidant in sickle erythrocyte membranes. *FEBS letters*, *264*(1), 145–148. https://doi.org/10.1016/0014-5793(90)80786-i
62. Hasegawa, M., Arai, T., Nonaka, T., Kametani, F., Yoshida, M., Hashizume, Y., Beach, T. G., Buratti, E., Baralle, F., Morita, M., Nakano, I., Oda, T., Tsuchiya, K., & Akiyama, H. (2008). Phosphorylated TDP-43 in frontotemporal lobar degeneration and amyotrophic lateral sclerosis. *Annals of neurology*, *64*(1), 60–70. https://doi.org/10.1002/ana.21425
63. Hefendehl, J. K., Neher, J. J., Sühs, R. B., Kohsaka, S., Skodras, A., & Jucker, M. (2014). Homeostatic and injury-induced microglia behavior in the aging brain. *Aging cell*, *13*(1), 60–69. https://doi.org/10.1111/acel.12149

64. Heindl, S., Gesierich, B., Benakis, C., Llovera, G., Duering, M., & Liesz, A. (2018). Automated Morphological Analysis of Microglia After Stroke. *Frontiers in cellular neuroscience*, *12*, 106. https://doi.org/10.3389/fncel.2018.00106
65. Herzog, J. J., Deshpande, M., Shapiro, L., Rodal, A. A., & Paradis, S. (2017). TDP-43 misexpression causes defects in dendritic growth. *Scientific reports*, *7*(1), 15656. https://doi.org/10.1038/s41598-017-15914-4
66. Hong, S., Beja-Glasser, V. F., Nfonoyim, B. M., Frouin, A., Li, S., Ramakrishnan, S., Merry, K. M., Shi, Q., Rosenthal, A., Barres, B. A., Lemere, C. A., Selkoe, D. J., & Stevens, B. (2016). Complement and microglia mediate early synapse loss in Alzheimer mouse models. *Science (New York, N.Y.)*, *352*(6286), 712–716. https://doi.org/10.1126/science.aad8373
67. Hristovska, I., Robert, M., Combet, K., Honnorat, J., Comte, J. C., & Pascual, O. (2022). Sleep decreases neuronal activity control of microglial dynamics in mice. *Nature communications*, *13*(1), 6273. https://doi.org/10.1038/s41467-022-34035-9
68. Huang, Y., Xu, Z., Xiong, S., Sun, F., Qin, G., Hu, G., Wang, J., Zhao, L., Liang, Y. X., Wu, T., Lu, Z., Humayun, M. S., So, K. F., Pan, Y., Li, N., Yuan, T. F., Rao, Y., & Peng, B. (2018). Repopulated microglia are solely derived from the proliferation of residual microglia after acute depletion. *Nature neuroscience*, *21*(4), 530–540. https://doi.org/10.1038/s41593-018-0090-8
69. Igaz, L. M., Kwong, L. K., Lee, E. B., Chen-Plotkin, A., Swanson, E., Unger, T., Malunda, J., Xu, Y., Winton, M. J., Trojanowski, J. Q., & Lee, V. M. (2011). Dysregulation of the ALS-associated gene TDP-43 leads to neuronal death and degeneration in mice. *The Journal of clinical investigation*, *121*(2), 726–738. https://doi.org/10.1172/JCI44867
70. Ingre, C., Roos, P. M., Piehl, F., Kamel, F., & Fang, F. (2015). Risk factors for amyotrophic lateral sclerosis. *Clinical epidemiology*, *7*, 181–193. https://doi.org/10.2147/CLEP.S37505
71. Ishigaki, S., Masuda, A., Fujioka, Y., Iguchi, Y., Katsuno, M., Shibata, A., Urano, F., Sobue, G., & Ohno, K. (2012). Position-dependent FUS-RNA interactions regulate alternative splicing events and transcriptions. *Scientific reports*, *2*, 529. https://doi.org/10.1038/srep00529

72. Ishigaki, Shinsuke, and Gen Sobue. “Importance of Functional Loss of FUS in FTLD/ALS.” *Frontiers in molecular biosciences* vol. 5 44. 3 May. 2018, doi:10.3389/fmolb.2018.00044
73. Jaiswal M. K. (2019). Riluzole and edaravone: A tale of two amyotrophic lateral sclerosis drugs. *Medicinal research reviews*, *39*(2), 733–748. https://doi.org/10.1002/med.21528
74. Jiang, L. L., Xue, W., Hong, J. Y., Zhang, J. T., Li, M. J., Yu, S. N., He, J. H., & Hu, H. Y. (2017). The N-terminal dimerization is required for TDP-43 splicing activity. *Scientific reports*, *7*(1), 6196. https://doi.org/10.1038/s41598-017-06263-3
75. Jo, M., Lee, S., Jeon, Y. M., Kim, S., Kwon, Y., & Kim, H. J. (2020). The role of TDP-43 propagation in neurodegenerative diseases: integrating insights from clinical and experimental studies. *Experimental & molecular medicine*, *52*(10), 1652–1662. https://doi.org/10.1038/s12276-020-00513-7
76. Johnson, B. S., McCaffery, J. M., Lindquist, S., & Gitler, A. D. (2008). A yeast TDP-43 proteinopathy model: Exploring the molecular determinants of TDP-43 aggregation and cellular toxicity. *Proceedings of the National Academy of Sciences of the United States of America*, *105*(17), 6439–6444. https://doi.org/10.1073/pnas.0802082105
77. Johnson, B. S., Snead, D., Lee, J. J., McCaffery, J. M., Shorter, J., & Gitler, A. D. (2009). TDP-43 is intrinsically aggregation-prone, and amyotrophic lateral sclerosis-linked mutations accelerate aggregation and increase toxicity. *The Journal of biological chemistry*, *284*(30), 20329–20339. https://doi.org/10.1074/jbc.M109.010264
78. Jonsson, T., Stefansson, H., Steinberg, S., Jonsdottir, I., Jonsson, P. V., Snaedal, J., Bjornsson, S., Huttenlocher, J., Levey, A. I., Lah, J. J., Rujescu, D., Hampel, H., Giegling, I., Andreassen, O. A., Engedal, K., Ulstein, I., Djurovic, S., Ibrahim-Verbaas, C., Hofman, A., Ikram, M. A., … Stefansson, K. (2013). Variant of TREM2 associated with the risk of Alzheimer's disease. *The New England journal of medicine*, *368*(2), 107–116. https://doi.org/10.1056/NEJMoa1211103
79. Kasai, T., Tokuda, T., Ishigami, N., Sasayama, H., Foulds, P., Mitchell, D. J., Mann, D. M., Allsop, D., & Nakagawa, M. (2009). Increased TDP-43 protein in cerebrospinal fluid of patients with amyotrophic lateral sclerosis. *Acta neuropathologica*, *117*(1), 55–62. https://doi.org/10.1007/s00401-008-0456-1

80. Kawahara, Y., & Mieda-Sato, A. (2012). TDP-43 promotes microRNA biogenesis as a component of the Drosha and Dicer complexes. *Proceedings of the National Academy of Sciences of the United States of America*, *109*(9), 3347–3352. https://doi.org/10.1073/pnas.1112427109
81. Keating, S. S., San Gil, R., Swanson, M. E. V., Scotter, E. L., & Walker, A. K. (2022). TDP-43 pathology: From noxious assembly to therapeutic removal. *Progress in neurobiology*, *211*, 102229. https://doi.org/10.1016/j.pneurobio.2022.102229
82. Kettenmann, H., Hanisch, U. K., Noda, M., & Verkhratsky, A. (2011). Physiology of microglia. *Physiological reviews*, *91*(2), 461–553. https://doi.org/10.1152/physrev.00011.2010
83. Kiernan, M. C., Vucic, S., Cheah, B. C., Turner, M. R., Eisen, A., Hardiman, O., Burrell, J. R., & Zoing, M. C. (2011). Amyotrophic lateral sclerosis. *Lancet (London, England)*, *377*(9769), 942–955. https://doi.org/10.1016/S0140-6736(10)61156-7
84. Kraemer, B. C., Schuck, T., Wheeler, J. M., Robinson, L. C., Trojanowski, J. Q., Lee, V. M., & Schellenberg, G. D. (2010). Loss of murine TDP-43 disrupts motor function and plays an essential role in embryogenesis. *Acta neuropathologica*, *119*(4), 409–419. https://doi.org/10.1007/s00401-010-0659-0
85. Krasemann, S., Madore, C., Cialic, R., Baufeld, C., Calcagno, N., El Fatimy, R., Beckers, L., O'Loughlin, E., Xu, Y., Fanek, Z., Greco, D. J., Smith, S. T., Tweet, G., Humulock, Z., Zrzavy, T., Conde-Sanroman, P., Gacias, M., Weng, Z., Chen, H., Tjon, E., … Butovsky, O. (2017). The TREM2-APOE Pathway Drives the Transcriptional Phenotype of Dysfunctional Microglia in Neurodegenerative Diseases. *Immunity*, *47*(3), 566–581.e9. https://doi.org/10.1016/j.immuni.2017.08.008
86. Kumar, V., Wahiduzzaman, Prakash, A., Tomar, A. K., Srivastava, A., Kundu, B., Lynn, A. M., & Imtaiyaz Hassan, M. (2019). Exploring the aggregation-prone regions from structural domains of human TDP-43. *Biochimica et biophysica acta. Proteins and proteomics*, *1867*(3), 286–296. https://doi.org/10.1016/j.bbapap.2018.10.008
87. Lannes, N., Eppler, E., Etemad, S., Yotovski, P., & Filgueira, L. (2017). Microglia at center stage: a comprehensive review about the versatile and unique

residential macrophages of the central nervous system. *Oncotarget*, *8*(69), 114393–114413. https://doi.org/10.18632/oncotarget.23106

88. Lannes, N., Eppler, E., Etemad, S., Yotovski, P., & Filgueira, L. (2017). Microglia at center stage: a comprehensive review about the versatile and unique residential macrophages of the central nervous system. *Oncotarget*, *8*(69), 114393–114413. https://doi.org/10.18632/oncotarget.23106
89. Lee, C. Y., & Landreth, G. E. (2010). The role of microglia in amyloid clearance from the AD brain. *Journal of neural transmission (Vienna, Austria : 1996)*, *117*(8), 949–960. https://doi.org/10.1007/s00702-010-0433-4
90. Lee, D. Y., & McMurray, C. T. (2014). Trinucleotide expansion in disease: why is there a length threshold?. *Current opinion in genetics & development*, *26*, 131–140. https://doi.org/10.1016/j.gde.2014.07.003
91. Liebman, Susan W, and Yury O Chernoff. “Prions in yeast.” *Genetics* vol. 191,4 (2012): 1041-72. doi:10.1534/genetics.111.137760
92. Ling, S. C., Albuquerque, C. P., Han, J. S., Lagier-Tourenne, C., Tokunaga, S., Zhou, H., & Cleveland, D. W. (2010). ALS-associated mutations in TDP-43 increase its stability and promote TDP-43 complexes with FUS/TLS. *Proceedings of the National Academy of Sciences of the United States of America*, *107*(30), 13318–13323. https://doi.org/10.1073/pnas.1008227107
93. Liu-Yesucevitz, L., Lin, A. Y., Ebata, A., Boon, J. Y., Reid, W., Xu, Y. F., Kobrin, K., Murphy, G. J., Petrucelli, L., & Wolozin, B. (2014). ALS-linked mutations enlarge TDP-43-enriched neuronal RNA granules in the dendritic arbor. *The Journal of neuroscience : the official journal of the Society for Neuroscience*, *34*(12), 4167–4174. https://doi.org/10.1523/JNEUROSCI.2350-13.2014
94. Liu, H., Wang, X., Chen, L., Chen, L., Tsirka, S. E., Ge, S., & Xiong, Q. (2021). Microglia modulate stable wakefulness via the thalamic reticular nucleus in mice. *Nature communications*, *12*(1), 4646. https://doi.org/10.1038/s41467-021-24915-x
95. Liu, Y. C., Chiang, P. M., & Tsai, K. J. (2013). Disease animal models of TDP-43 proteinopathy and their pre-clinical applications. *International journal of molecular sciences*, *14*(10), 20079–20111. https://doi.org/10.3390/ijms141020079

96. Mackenzie, I. R., Rademakers, R., & Neumann, M. (2010). TDP-43 and FUS in amyotrophic lateral sclerosis and frontotemporal dementia. *The Lancet. Neurology*, *9*(10), 995–1007. https://doi.org/10.1016/S1474-4422(10)70195-2
97. Mackness, B. C., Tran, M. T., McClain, S. P., Matthews, C. R., & Zitzewitz, J. A. (2014). Folding of the RNA recognition motif (RRM) domains of the amyotrophic lateral sclerosis (ALS)-linked protein TDP-43 reveals an intermediate state. *The Journal of biological chemistry*, *289*(12), 8264–8276. https://doi.org/10.1074/jbc.M113.542779
98. Madry, C., Kyrargyri, V., Arancibia-Cárcamo, I. L., Jolivet, R., Kohsaka, S., Bryan, R. M., & Attwell, D. (2018). Microglial Ramification, Surveillance, and Interleukin-1β Release Are Regulated by the Two-Pore Domain K^+ Channel THIK-1. *Neuron*, *97*(2), 299–312.e6. https://doi.org/10.1016/j.neuron.2017.12.002
99. Maharana, S., Wang, J., Papadopoulos, D. K., Richter, D., Pozniakovsky, A., Poser, I., Bickle, M., Rizk, S., Guillén-Boixet, J., Franzmann, T. M., Jahnel, M., Marrone, L., Chang, Y. T., Sterneckert, J., Tomancak, P., Hyman, A. A., & Alberti, S. (2018). RNA buffers the phase separation behavior of prion-like RNA binding proteins. *Science (New York, N.Y.)*, *360*(6391), 918–921. https://doi.org/10.1126/science.aar7366
100. Marin, B., Logroscino, G., Boumédiene, F., Labrunie, A., Couratier, P., Babron, M. C., Leutenegger, A. L., Preux, P. M., & Beghi, E. (2016). Clinical and demographic factors and outcome of amyotrophic lateral sclerosis in relation to population ancestral origin. *European journal of epidemiology*, *31*(3), 229–245. https://doi.org/10.1007/s10654-015-0090-x
101. Masuda, A., Takeda, J., Okuno, T., Okamoto, T., Ohkawara, B., Ito, M., Ishigaki, S., Sobue, G., & Ohno, K. (2015). Position-specific binding of FUS to nascent RNA regulates mRNA length. *Genes & development*, *29*(10), 1045–1057. https://doi.org/10.1101/gad.255737.114
102. McAlary, L., Plotkin, S. S., Yerbury, J. J., & Cashman, N. R. (2019). Prion-Like Propagation of Protein Misfolding and Aggregation in Amyotrophic Lateral Sclerosis. *Frontiers in molecular neuroscience*, *12*, 262. https://doi.org/10.3389/fnmol.2019.00262
103. McKhann, G. M., Albert, M. S., Grossman, M., Miller, B., Dickson, D., Trojanowski, J. Q., & Work Group on Frontotemporal Dementia and Pick's

Disease (2001). Clinical and pathological diagnosis of frontotemporal dementia: report of the Work Group on Frontotemporal Dementia and Pick's Disease. *Archives of neurology*, *58*(11), 1803–1809. https://doi.org/10.1001/archneur.58.11.1803

104. Mioshi, E., Hsieh, S., Savage, S., Hornberger, M., & Hodges, J. R. (2010). Clinical staging and disease progression in frontotemporal dementia. *Neurology*, *74*(20), 1591–1597. https://doi.org/10.1212/WNL.0b013e3181e04070

105. Mitsuzawa, S., Akiyama, T., Nishiyama, A., Suzuki, N., Kato, M., Warita, H., Izumi, R., Osana, S., Koyama, S., Kato, T., Suzuki, Y., & Aoki, M. (2018). *TARDBP* p.G376D mutation, found in rapid progressive familial ALS, induces mislocalization of TDP-43. *eNeurologicalSci*, *11*, 20–22. https://doi.org/10.1016/j.ensci.2018.04.001

106. Miyamoto, A., Wake, H., Ishikawa, A. W., Eto, K., Shibata, K., Murakoshi, H., Koizumi, S., Moorhouse, A. J., Yoshimura, Y., & Nabekura, J. (2016). Microglia contact induces synapse formation in developing somatosensory cortex. *Nature communications*, *7*, 12540. https://doi.org/10.1038/ncomms12540

107. Mompeán, M., Romano, V., Pantoja-Uceda, D., Stuani, C., Baralle, F. E., Buratti, E., & Laurents, D. V. (2016). The TDP-43 N-terminal domain structure at high resolution. *The FEBS journal*, *283*(7), 1242–1260. https://doi.org/10.1111/febs.13651

108. Morlando, Mariangela et al., “FUS stimulates microRNA biogenesis by facilitating co-transcriptional Drosha recruitment.” *The EMBO journal* vol. 31,24 (2012): 4502-10. doi:10.1038/emboj.2012.319

109. Muzio, L., Viotti, A., & Martino, G. (2021). Microglia in Neuroinflammation and Neurodegeneration: From Understanding to Therapy. *Frontiers in neuroscience*, *15*, 742065. https://doi.org/10.3389/fnins.2021.742065

110. Nagai, M., Re, D. B., Nagata, T., Chalazonitis, A., Jessell, T. M., Wichterle, H., & Przedborski, S. (2007). Astrocytes expressing ALS-linked mutated SOD1 release factors selectively toxic to motor neurons. *Nature neuroscience*, *10*(5), 615–622. https://doi.org/10.1038/nn1876

111. Nebeling, F. C., Poll, S., Justus, L. C., Steffen, J., Keppler, K., Mittag, M., & Fuhrmann, M. (2023). Microglial motility is modulated by neuronal activity and

correlates with dendritic spine plasticity in the hippocampus of awake mice. *eLife*, *12*, e83176. https://doi.org/10.7554/eLife.83176

112. Nelson, R., & Eisenberg, D. (2006). Recent atomic models of amyloid fibril structure. *Current opinion in structural biology*, *16*(2), 260–265. https://doi.org/10.1016/j.sbi.2006.03.007

113. Neumann, M., Sampathu, D. M., Kwong, L. K., Truax, A. C., Micsenyi, M. C., Chou, T. T., Bruce, J., Schuck, T., Grossman, M., Clark, C. M., McCluskey, L. F., Miller, B. L., Masliah, E., Mackenzie, I. R., Feldman, H., Feiden, W., Kretzschmar, H. A., Trojanowski, J. Q., & Lee, V. M. (2006). Ubiquitinated TDP-43 in frontotemporal lobar degeneration and amyotrophic lateral sclerosis. *Science (New York, N.Y.)*, *314*(5796), 130–133. https://doi.org/10.1126/science.1134108

114. Nguyen, H. P., Van Broeckhoven, C., & van der Zee, J. (2018). ALS Genes in the Genomic Era and their Implications for FTD. *Trends in genetics : TIG*, *34*(6), 404–423. https://doi.org/10.1016/j.tig.2018.03.001

115. Nimmerjahn, A., Kirchhoff, F., & Helmchen, F. (2005). Resting microglial cells are highly dynamic surveillants of brain parenchyma in vivo. *Science (New York, N.Y.)*, *308*(5726), 1314–1318. https://doi.org/10.1126/science.1110647

116. Ning, L., Geng, Y., Lovett-Barron, M., Niu, X., Deng, M., Wang, L., Ataie, N., Sens, A., Ng, H. L., Chen, S., Deisseroth, K., Lin, M. Z., & Chu, J. (2022). A Bright, Nontoxic, and Non-aggregating red Fluorescent Protein for Long-Term Labeling of Fine Structures in Neurons. *Frontiers in cell and developmental biology*, *10*, 893468. https://doi.org/10.3389/fcell.2022.893468

117. Nishimura, A. L., Zupunski, V., Troakes, C., Kathe, C., Fratta, P., Howell, M., Gallo, J. M., Hortobágyi, T., Shaw, C. E., & Rogelj, B. (2010). Nuclear import impairment causes cytoplasmic trans-activation response DNA-binding protein accumulation and is associated with frontotemporal lobar degeneration. *Brain : a journal of neurology*, *133*(Pt 6), 1763–1771. https://doi.org/10.1093/brain/awq111

118. Nonaka, T., Kametani, F., Arai, T., Akiyama, H., & Hasegawa, M. (2009). Truncation and pathogenic mutations facilitate the formation of intracellular aggregates of TDP-43. *Human molecular genetics*, *18*(18), 3353–3364. https://doi.org/10.1093/hmg/ddp275

119. Ogawa, N., Hirose, Y., Ohara, S., Ono, T., & Watanabe, Y. (1985). A simple quantitative bradykinesia test in MPTP-treated mice. *Research communications in chemical pathology and pharmacology*, *50*(3), 435–441.

120. Ou, S. H., Wu, F., Harrich, D., García-Martínez, L. F., & Gaynor, R. B. (1995). Cloning and characterization of a novel cellular protein, TDP-43, that binds to human immunodeficiency virus type 1 TAR DNA sequence motifs. *Journal of virology*, *69*(6), 3584–3596. https://doi.org/10.1128/JVI.69.6.3584-3596.1995

121. Paasila, P. J., Davies, D. S., Kril, J. J., Goldsbury, C., & Sutherland, G. T. (2019). The relationship between the morphological subtypes of microglia and Alzheimer's disease neuropathology. *Brain pathology (Zurich, Switzerland)*, *29*(6), 726–740. https://doi.org/10.1111/bpa.12717

122. Peng, C., Trojanowski, J. Q., & Lee, V. M. (2020). Protein transmission in neurodegenerative disease. *Nature reviews. Neurology*, *16*(4), 199–212. https://doi.org/10.1038/s41582-020-0333-7

123. Plescher, M., Seifert, G., Hansen, J. N., Bedner, P., Steinhäuser, C., & Halle, A. (2018). Plaque-dependent morphological and electrophysiological heterogeneity of microglia in an Alzheimer's disease mouse model. *Glia*, *66*(7), 1464–1480. https://doi.org/10.1002/glia.23318

124. Polymenidou, M., Lagier-Tourenne, C., Hutt, K. R., Huelga, S. C., Moran, J., Liang, T. Y., Ling, S. C., Sun, E., Wancewicz, E., Mazur, C., Kordasiewicz, H., Sedaghat, Y., Donohue, J. P., Shiue, L., Bennett, C. F., Yeo, G. W., & Cleveland, D. W. (2011). Long pre-mRNA depletion and RNA missplicing contribute to neuronal vulnerability from loss of TDP-43. *Nature neuroscience*, *14*(4), 459–468. https://doi.org/10.1038/nn.2779

125. Prasad, A., Bharathi, V., Sivalingam, V., Girdhar, A., & Patel, B. K. (2019). Molecular Mechanisms of TDP-43 Misfolding and Pathology in Amyotrophic Lateral Sclerosis. *Frontiers in molecular neuroscience*, *12*, 25. https://doi.org/10.3389/fnmol.2019.00025

126. Przedborski, S., Vila, M., & Jackson-Lewis, V. (2003). Neurodegeneration: what is it and where are we?. *The Journal of clinical investigation*, *111*(1), 3–10. https://doi.org/10.1172/JCI17522

127. Quek, H., Cuní-López, C., Stewart, R., Colletti, T., Notaro, A., Nguyen, T. H., Sun, Y., Guo, C. C., Lupton, M. K., Roberts, T. L., Lim, Y. C., Oikari, L. E., La Bella, V., & White, A. R. (2022). ALS monocyte-derived microglia-like cells

reveal cytoplasmic TDP-43 accumulation, DNA damage, and cell-specific impairment of phagocytosis associated with disease progression. *Journal of neuroinflammation*, *19*(1), 58. https://doi.org/10.1186/s12974-022-02421-1

128. Ravits, J. M., & La Spada, A. R. (2009). ALS motor phenotype heterogeneity, focality, and spread: deconstructing motor neuron degeneration. *Neurology*, *73*(10), 805–811. https://doi.org/10.1212/WNL.0b013e3181b6bbbd

129. Renton, A. E., Majounie, E., Waite, A., Simón-Sánchez, J., Rollinson, S., Gibbs, J. R., Schymick, J. C., Laaksovirta, H., van Swieten, J. C., Myllykangas, L., Kalimo, H., Paetau, A., Abramzon, Y., Remes, A. M., Kaganovich, A., Scholz, S. W., Duckworth, J., Ding, J., Harmer, D. W., Hernandez, D. G., … Traynor, B. J. (2011). A hexanucleotide repeat expansion in C9ORF72 is the cause of chromosome 9p21-linked ALS-FTD. *Neuron*, *72*(2), 257–268. https://doi.org/10.1016/j.neuron.2011.09.010

130. Rosen, D. R., Siddique, T., Patterson, D., Figlewicz, D. A., Sapp, P., Hentati, A., Donaldson, D., Goto, J., O'Regan, J. P., & Deng, H. X. (1993). Mutations in Cu/Zn superoxide dismutase gene are associated with familial amyotrophic lateral sclerosis. *Nature*, *362*(6415), 59–62. https://doi.org/10.1038/362059a0

131. Rothstein J. D. (2017). Edaravone: A new drug approved for ALS. *Cell*, *171*(4), 725. https://doi.org/10.1016/j.cell.2017.10.011

132. Rothstein J. D. (2017). Edaravone: A new drug approved for ALS. *Cell*, *171*(4), 725. https://doi.org/10.1016/j.cell.2017.10.011

133. Rubinsztein D. C. (2006). The roles of intracellular protein-degradation pathways in neurodegeneration. *Nature*, *443*(7113), 780–786. https://doi.org/10.1038/nature05291

134. Scheiblich, H., Dansokho, C., Mercan, D., Schmidt, S. V., Bousset, L., Wischhof, L., Eikens, F., Odainic, A., Spitzer, J., Griep, A., Schwartz, S., Bano, D., Latz, E., Melki, R., & Heneka, M. T. (2021). Microglia jointly degrade fibrillar alpha-synuclein cargo by distribution through tunneling nanotubes. *Cell*, *184*(20), 5089–5106.e21. https://doi.org/10.1016/j.cell.2021.09.007

135. Scheiblich, H., Dansokho, C., Mercan, D., Schmidt, S. V., Bousset, L., Wischhof, L., Eikens, F., Odainic, A., Spitzer, J., Griep, A., Schwartz, S., Bano, D., Latz, E., Melki, R., & Heneka, M. T. (2021). Microglia jointly degrade fibrillar

alpha-synuclein cargo by distribution through tunneling nanotubes. *Cell*, *184*(20), 5089–5106.e21. https://doi.org/10.1016/j.cell.2021.09.007

136. Schmid, B., Hruscha, A., Hogl, S., Banzhaf-Strathmann, J., Strecker, K., van der Zee, J., Teucke, M., Eimer, S., Hegermann, J., Kittelmann, M., Kremmer, E., Cruts, M., Solchenberger, B., Hasenkamp, L., van Bebber, F., Van Broeckhoven, C., Edbauer, D., Lichtenthaler, S. F., & Haass, C. (2013). Loss of ALS-associated TDP-43 in zebrafish causes muscle degeneration, vascular dysfunction, and reduced motor neuron axon outgrowth. *Proceedings of the National Academy of Sciences of the United States of America*, *110*(13), 4986–4991. https://doi.org/10.1073/pnas.1218311110

137. Schwartz, G., & Fehlings, M. G. (2002). Secondary injury mechanisms of spinal cord trauma: a novel therapeutic approach for the management of secondary pathophysiology with the sodium channel blocker riluzole. *Progress in brain research*, *137*, 177–190. https://doi.org/10.1016/s0079-6123(02)37016-x

138. Sephton, C. F., Good, S. K., Atkin, S., Dewey, C. M., Mayer, P., 3rd, Herz, J., & Yu, G. (2010). TDP-43 is a developmentally regulated protein essential for early embryonic development. *The Journal of biological chemistry*, *285*(9), 6826–6834. https://doi.org/10.1074/jbc.M109.061846

139. Shibata, M., & Suzuki, N. (2017). Exploring the role of microglia in cortical spreading depression in neurological disease. *Journal of cerebral blood flow and metabolism : official journal of the International Society of Cerebral Blood Flow and Metabolism*, *37*(4), 1182–1191. https://doi.org/10.1177/0271678X17690537

140. Shin, Y., & Brangwynne, C. P. (2017). Liquid phase condensation in cell physiology and disease. *Science (New York, N.Y.)*, *357*(6357), eaaf4382. https://doi.org/10.1126/science.aaf4382

141. Soreq, L., UK Brain Expression Consortium, North American Brain Expression Consortium, Rose, J., Soreq, E., Hardy, J., Trabzuni, D., Cookson, M. R., Smith, C., Ryten, M., Patani, R., & Ule, J. (2017). Major Shifts in Glial Regional Identity Are a Transcriptional Hallmark of Human Brain Aging. *Cell reports*, *18*(2), 557–570. https://doi.org/10.1016/j.celrep.2016.12.011

142. Soulet, D., & Rivest, S. (2008). Bone-marrow-derived microglia: myth or reality?. *Current opinion in pharmacology*, *8*(4), 508–518. https://doi.org/10.1016/j.coph.2008.04.002

143. Spiller, K. J., Restrepo, C. R., Khan, T., Dominique, M. A., Fang, T. C., Canter, R. G., Roberts, C. J., Miller, K. R., Ransohoff, R. M., Trojanowski, J. Q., & Lee, V. M. (2018). Microglia-mediated recovery from ALS-relevant motor neuron degeneration in a mouse model of TDP-43 proteinopathy. *Nature neuroscience*, *21*(3), 329–340. https://doi.org/10.1038/s41593-018-0083-7

144. Starr, A., & Sattler, R. (2018). Synaptic dysfunction and altered excitability in C9ORF72 ALS/FTD. *Brain research*, *1693*(Pt A), 98–108. https://doi.org/10.1016/j.brainres.2018.02.011

145. Sugai, Akihiro et al., “Robustness and Vulnerability of the Autoregulatory System That Maintains Nuclear TDP-43 Levels: A Trade-off Hypothesis for ALS Pathology Based on *in Silico* Data.” *Frontiers in neuroscience* vol. 12 28. 1 Feb. 2018, doi:10.3389/fnins.2018.00028

146. Suk, T. R., & Rousseaux, M. W. C. (2020). The role of TDP-43 mislocalization in amyotrophic lateral sclerosis. *Molecular neurodegeneration*, *15*(1), 45. https://doi.org/10.1186/s13024-020-00397-1

147. Sun, C. S., Wang, C. Y., Chen, B. P., He, R. Y., Liu, G. C., Wang, C. H., Chen, W., Chern, Y., & Huang, J. J. (2014). The influence of pathological mutations and proline substitutions in TDP-43 glycine-rich peptides on its amyloid properties and cellular toxicity. *PloS one*, *9*(8), e103644. https://doi.org/10.1371/journal.pone.0103644

148. Tavella, D., Zitzewitz, J. A., & Massi, F. (2018). Characterization of TDP-43 RRM2 Partially Folded States and Their Significance to ALS Pathogenesis. *Biophysical journal*, *115*(9), 1673–1680. https://doi.org/10.1016/j.bpj.2018.09.011

149. Taylor, J. P., Brown, R. H., Jr, & Cleveland, D. W. (2016). Decoding ALS: from genes to mechanism. *Nature*, *539*(7628), 197–206. https://doi.org/10.1038/nature20413

150. Tremblay, M. È., Stevens, B., Sierra, A., Wake, H., Bessis, A., & Nimmerjahn, A. (2011). The role of microglia in the healthy brain. *The Journal of neuroscience: the official journal of the Society for Neuroscience*, *31*(45), 16064–16069. https://doi.org/10.1523/JNEUROSCI.4158-11.2011

151. Turner, M. R., Cagnin, A., Turkheimer, F. E., Miller, C. C., Shaw, C. E., Brooks, D. J., Leigh, P. N., & Banati, R. B. (2004). Evidence of widespread cerebral microglial activation in amyotrophic lateral sclerosis: an

[11C](R)-PK11195 positron emission tomography study. *Neurobiology of disease*, *15*(3), 601–609. https://doi.org/10.1016/j.nbd.2003.12.012

152. Udan-Johns, M., Bengoechea, R., Bell, S., Shao, J., Diamond, M. I., True, H. L., Weihl, C. C., & Baloh, R. H. (2014). Prion-like nuclear aggregation of TDP-43 during heat shock is regulated by HSP40/70 chaperones. *Human molecular genetics*, *23*(1), 157–170. https://doi.org/10.1093/hmg/ddt408

153. Urushitani, M., Sik, A., Sakurai, T., Nukina, N., Takahashi, R., & Julien, J. P. (2006). Chromogranin-mediated secretion of mutant superoxide dismutase proteins linked to amyotrophic lateral sclerosis. *Nature neuroscience*, *9*(1), 108–118. https://doi.org/10.1038/nn1603

154. Walling A. D. (1999). Amyotrophic lateral sclerosis: Lou Gehrig's disease. *American family physician*, *59*(6), 1489–1496.

155. Wang, A., Conicella, A. E., Schmidt, H. B., Martin, E. W., Rhoads, S. N., Reeb, A. N., Nourse, A., Ramirez Montero, D., Ryan, V. H., Rohatgi, R., Shewmaker, F., Naik, M. T., Mittag, T., Ayala, Y. M., & Fawzi, N. L. (2018). A single N-terminal phosphomimic disrupts TDP-43 polymerization, phase separation, and RNA splicing. *The EMBO journal*, *37*(5), e97452. https://doi.org/10.15252/embj.201797452

156. Wang, J., Choi, J. M., Holehouse, A. S., Lee, H. O., Zhang, X., Jahnel, M., Maharana, S., Lemaitre, R., Pozniakovsky, A., Drechsel, D., Poser, I., Pappu, R. V., Alberti, S., & Hyman, A. A. (2018). A Molecular Grammar Governing the Driving Forces for Phase Separation of Prion-like RNA Binding Proteins. *Cell*, *174*(3), 688–699.e16. https://doi.org/10.1016/j.cell.2018.06.006

157. Wang, Y. T., Kuo, P. H., Chiang, C. H., Liang, J. R., Chen, Y. R., Wang, S., Shen, J. C., & Yuan, H. S. (2013). The truncated C-terminal RNA recognition motif of TDP-43 protein plays a key role in forming proteinaceous aggregates. *The Journal of biological chemistry*, *288*(13), 9049–9057. https://doi.org/10.1074/jbc.M112.438564

158. Ward, M. E., Taubes, A., Chen, R., Miller, B. L., Sephton, C. F., Gelfand, J. M., Minami, S., Boscardin, J., Martens, L. H., Seeley, W. W., Yu, G., Herz, J., Filiano, A. J., Arrant, A. E., Roberson, E. D., Kraft, T. W., Farese, R. V., Jr, Green, A., & Gan, L. (2014). Early retinal neurodegeneration and impaired Ran-mediated nuclear import of TDP-43 in progranulin-deficient FTLD. *The*

Journal of experimental medicine, *211*(10), 1937–1945. https://doi.org/10.1084/jem.20140214

159. Weihl, C. C., Temiz, P., Miller, S. E., Watts, G., Smith, C., Forman, M., Hanson, P. I., Kimonis, V., & Pestronk, A. (2008). TDP-43 accumulation in inclusion body myopathy muscle suggests a common pathogenic mechanism with frontotemporal dementia. *Journal of neurology, neurosurgery, and psychiatry*, *79*(10), 1186–1189. https://doi.org/10.1136/jnnp.2007.131334

160. White, M. A., Kim, E., Duffy, A., Adalbert, R., Phillips, B. U., Peters, O. M., Stephenson, J., Yang, S., Massenzio, F., Lin, Z., Andrews, S., Segonds-Pichon, A., Metterville, J., Saksida, L. M., Mead, R., Ribchester, R. R., Barhomi, Y., Serre, T., Coleman, M. P., Fallon, J. R., … Sreedharan, J. (2018). TDP-43 gains function due to perturbed autoregulation in a Tardbp knock-in mouse model of ALS-FTD. *Nature neuroscience*, *21*(4), 552–563. https://doi.org/10.1038/s41593-018-0113-5

161. Winton, M. J., Igaz, L. M., Wong, M. M., Kwong, L. K., Trojanowski, J. Q., & Lee, V. M. (2008). Disturbance of nuclear and cytoplasmic TAR DNA-binding protein (TDP-43) induces disease-like redistribution, sequestration, and aggregate formation. *The Journal of biological chemistry*, *283*(19), 13302–13309. https://doi.org/10.1074/jbc.M800342200

162. Winton, M. J., Igaz, L. M., Wong, M. M., Kwong, L. K., Trojanowski, J. Q., & Lee, V. M. (2008a). Disturbance of nuclear and cytoplasmic TAR DNA-binding protein (TDP-43) induces disease-like redistribution, sequestration, and aggregate formation. *The Journal of biological chemistry*, *283*(19), 13302–13309. https://doi.org/10.1074/jbc.M800342200

163. Winton, M. J., Van Deerlin, V. M., Kwong, L. K., Yuan, W., Wood, E. M., Yu, C. E., Schellenberg, G. D., Rademakers, R., Caselli, R., Karydas, A., Trojanowski, J. Q., Miller, B. L., & Lee, V. M. (2008b). A90V TDP-43 variant results in the aberrant localization of TDP-43 in vitro. *FEBS letters*, *582*(15), 2252–2256. https://doi.org/10.1016/j.febslet.2008.05.024

164. World Population prospects 2017 – Volume 1: Comprehensive Tables (2021)

165. Wright-Jin, E. C., & Gutmann, D. H. (2019). Microglia as Dynamic Cellular Mediators of Brain Function. *Trends in molecular medicine*, *25*(11), 967–979. https://doi.org/10.1016/j.molmed.2019.08.013

166. Wu, L. S., Cheng, W. C., & Shen, C. K. (2012). Targeted depletion of TDP-43 expression in the spinal cord motor neurons leads to the development of amyotrophic lateral sclerosis-like phenotypes in mice. *The Journal of biological chemistry*, *287*(33), 27335–27344. https://doi.org/10.1074/jbc.M112.359000

167. Xie, M., Liu, Y. U., Zhao, S., Zhang, L., Bosco, D. B., Pang, Y. P., Zhong, J., Sheth, U., Martens, Y. A., Zhao, N., Liu, C. C., Zhuang, Y., Wang, L., Dickson, D. W., Mattson, M. P., Bu, G., & Wu, L. J. (2022). TREM2 interacts with TDP-43 and mediates microglial neuroprotection against TDP-43-related neurodegeneration. *Nature neuroscience*, *25*(1), 26–38. https://doi.org/10.1038/s41593-021-00975-6

168. Xie, M., Liu, Y. U., Zhao, S., Zhang, L., Bosco, D. B., Pang, Y. P., Zhong, J., Sheth, U., Martens, Y. A., Zhao, N., Liu, C. C., Zhuang, Y., Wang, L., Dickson, D. W., Mattson, M. P., Bu, G., & Wu, L. J. (2022). TREM2 interacts with TDP-43 and mediates microglial neuroprotection against TDP-43-related neurodegeneration. *Nature neuroscience*, *25*(1), 26–38. https://doi.org/10.1038/s41593-021-00975-6

169. Yang, C., Wang, H., Qiao, T., Yang, B., Aliaga, L., Qiu, L., Tan, W., Salameh, J., McKenna-Yasek, D. M., Smith, T., Peng, L., Moore, M. J., Brown, R. H., Jr, Cai, H., & Xu, Z. (2014). Partial loss of TDP-43 function causes phenotypes of amyotrophic lateral sclerosis. *Proceedings of the National Academy of Sciences of the United States of America*, *111*(12), E1121–E1129. https://doi.org/10.1073/pnas.1322641111

170. Yun, Y., & Ha, Y. (2020). CRISPR/Cas9-Mediated Gene Correction to Understand ALS. *International journal of molecular sciences*, *21*(11), 3801. https://doi.org/10.3390/ijms21113801

171. Zhang, Y. J., Xu, Y. F., Cook, C., Gendron, T. F., Roettges, P., Link, C. D., Lin, W. L., Tong, J., Castanedes-Casey, M., Ash, P., Gass, J., Rangachari, V., Buratti, E., Baralle, F., Golde, T. E., Dickson, D. W., & Petrucelli, L. (2009). Aberrant cleavage of TDP-43 enhances aggregation and cellular toxicity. *Proceedings of the National Academy of Sciences of the United States of America*, *106*(18), 7607–7612. https://doi.org/10.1073/pnas.0900688106

172. Zhao, W., Beers, D. R., Henkel, J. S., Zhang, W., Urushitani, M., Julien, J. P., & Appel, S. H. (2010). Extracellular mutant SOD1 induces microglial-mediated motoneuron injury. *Glia*, *58*(2), 231–243. https://doi.org/10.1002/glia.20919

173. Zhao, X., Liao, Y., Morgan, S., Mathur, R., Feustel, P., Mazurkiewicz, J., Qian, J., Chang, J., Mathern, G. W., Adamo, M. A., Ritaccio, A. L., Gruenthal, M., Zhu, X., & Huang, Y. (2018). Noninflammatory Changes of Microglia Are Sufficient to Cause Epilepsy. *Cell reports*, *22*(8), 2080–2093. https://doi.org/10.1016/j.celrep.2018.02.004

174. Zheng J. (2022). Hippocampal neurogenesis and pro-neurogenic therapies for Alzheimer's disease. *Animal models and experimental medicine*, *5*(1), 3–14. https://doi.org/10.1002/ame2.12212

175. Zou, Z. Y., Zhou, Z. R., Che, C. H., Liu, C. Y., He, R. L., & Huang, H. P. (2017). Genetic epidemiology of amyotrophic lateral sclerosis: a systematic review and meta-analysis. *Journal of neurology, neurosurgery, and psychiatry*, *88*(7), 540–549. https://doi.org/10.1136/jnnp-2016-315018